การวิเคราะห์ภูมิลักษณ์การแปรสัณฐานของเขตรอยเลื่อนแม่ปิงใน

จังหวัดตากและจังหวัดกำแพงเพชร บริเวณตะวันตกเฉียงเหนือ ประเทศไทย

ว่าที่ร้อยตรี ภูริวัจน์ จิราตันติพัฒน์

MORPHOTECTONIC ANALYSIS OF MAE PING FAULT ZONE IN CHANGWAT TAK

AND CHANGWAT KAMPHAENG PHET, NORTHWESTERN THAILAND

Acting Sub Lt. Phuriwat Jiratantipat

A Thesis Submitted in Partial Fulfillment of the Requirements

for the Degree of Master of Science Program in Earth Sciences

Department of Geology

Faculty of Science

Chulalongkorn University

Academic Year 2012

Thesis Title   MORPHOTECTONIC ANALYSIS OF MAE PING FAULT ZONE

           IN CHANGWAT TAK AND CHANGWAT KAMPHAENG PHET,

           NORTHWESTERN THAILAND

By   Acting Sub Lt. Phuriwat Jiratantipat

Field of Study   Earth Sciences

Thesis Advisor   Pitsanupong Kanjanapayont, Dr.rer.nat.

Accepted by the Faculty of Science, Chulalongkorn University in Partial Fulfillment of the Requirements for the Master's Degree

………………………………………… Dean of the Faculty of Science

(Professor Supot Hannongbua, Dr.rer.nat.)

THESIS COMMITTEE

………………………………………… Chairman

(Assistant Professor Sombat Yumuang, Ph.D.)

………………………………………..… Thesis Advisor

(Pitsanupong Kanjanapayont, Dr.rer.nat.)

……………………………………….. Examiner

(Santi Pailoplee, Ph.D.)

……………………………………….. External Examiner

(Krit Won-In, Ph.D.)

ภูริวัจน์ จิราตันติพัฒน์: การวิเคราะห์ภูมิลักษณ์การแปรสัณฐานของเขตรอยเลื่อนแม่ปิงใน จังหวัดตาก และจังหวัดกำแพงเพชร บริเวณตะวันตกเฉียงเหนือ ประเทศไทย. (MORPHOTECTONIC ANALYSIS OF MAE PING FAULT ZONE IN CHANGWAT TAK AND CHANGWAT KAMPHAENG PHET, NORTHWESTERN THAILAND) อ.ที่ปรึกษาวิทยานิพนธ์หลัก :ดร. พิษณุพงศ์ กาญจนพยนต์, 113 หน้า.

การวิจัยฉบับนี้เป็นการสำรวจภูมิลักษณ์การแปรสัณฐานของเขตรอยเลื่อนแม่ปิงในพื้นที่จังหวัดตาก และจังหวัดกำแพงเพชร โดยการประยุกต์ใช้ข้อมูลโทรสัมผัสในการประเมินการแปรสัณฐานของเขตรอยเลื่อน แม่ปิง จังหวัดตาก และจังหวัดกำแพงเพชร มีวัตถุประสงค์เพื่อศึกษาภูมิลักษณ์การแปรสัณฐานและแปล ความหมายการแปรสัณฐานของเขตรอยเลื่อนแม่ปิง

ในการศึกษาได้ใช้ข้อมูลแบบจำลองระดับสูงเชิงเลข และภาพถ่ายดาวเทียมLANDSAT-7 ระบบ ETM+ และเลือกช่วงคลื่นที่จะมาวิเคราะห์จำนวน 3 ช่วงคลื่น คือ 7 4 และ 5 เพื่อทำภาพผสมสีเท็จ แปลตีความลักษณะ ภูมิประเทศด้วยสายตาบนจอภาพ ร่วมกับการใช้วิธีการหาค่าดัชนีธรณีสัณฐาน จากนั้นจึงนำข้อมูลที่ได้มา จัดสร้างเป็นฐานข้อมูลสารสนเทศภูมิศาสตร์ และทำการตรวจสอบความถูกต้องของการวิเคราะห์ภูมิลักษณ์การ แปรสัณฐานด้วยการสุ่มสำรวจในภาคสนาม

ผลการศึกษาวิจัยพบว่าลักษณะการวางตัวของแนวเขาวางตัวในแนวทิศตะวันตกเฉียงเหนือ-ตะวันออก เฉียงใต้ มีความยาวทั้งสิ้นประมาณ 230 กิโลเมตร ค่าดัชนีความคดโค้งเชิงเขาในพื้นที่ศึกษามีค่าตั้งแต่ 1.04 ถึง 1.77 อัตราส่วนของความกว้างพื้นต่อความสูงของหุบเขามีค่าตั้งแต่ 0.30 ถึง 2.66 และดัชนีความลาดชันของทาง น้ำมีค่าสูงมาก ผลการสำรวจภาคสนามพบลักษณะธรณีสัณฐานคือผาสามเหลี่ยม ทางน้ำเบี่ยงแนว และสัน ขวางกั้น จากการวิเคราะห์ค่าดัชนีธรณีสัณฐานและข้อมูลสำรวจภาคสนามแสดงว่าเขตรอยเลื่อนแม่ปิงที่ถูก ควบคุมโดยรอยเลื่อนปกติและรอยเลื่อนเหลื่อมข้างมีกระบวนการแปรสัณฐานมากที่สุดในบริเวณตอนใต้ของ พื้นที่ศึกษา

ข้อมูลและผลวิเคราะห์ที่ได้จากการศึกษาในครั้งนี้ สามารถนำไปใช้เป็นข้อมูลในการศึกษากลุ่มรอยเลื่อน แม่ปิงในบริเวณที่ยากแก่การเข้าถึง รวมไปถึงข้อมูลเชิงพื้นที่สำหรับสนับสนุนการป้องกันธรณีพิบัติภัยและการ วางผังเมืองในพื้นที่ดังกล่าวในอนาคต

ภาควิชา	ธรณีวิทยา	ลายมือชื่อนิสิต	
สาขาวิชา	โลกศาสตร์	ลายมือชื่อ อ.ที่ปรึกษาวิทยานิพนธ์หลัก	

5272413023   : MAJOR EARTH SCIENCES

KEYWORDS : MORPHOTECTONIC ANALYSIS/ GEOMORPHIC INDICES/ MAE PING FAULT ZONE/ ACTIVE FAULTS

PHURIWAT JIRATANTIPAT : MORPHOTECTONIC ANALYSIS OF MAE PING FAULT ZONE IN CHANGWAT TAK AND CHANGWAT KAMPHAENG PHET, NORTHWESTERN THAILAND. ADVISOR : PITSANUPONG KANJANAPAYONT, Dr.rer.nat., 113 pp.

The Mae Ping fault zone in Changwat Tak and Changwat Kamphaeng phet was selected for analysis of morphotectonic and tectonic interpretation. The application of remote-sensing data was conducted toward the present study. Morphotectonic analysis and tectonic interpretation of the Mae Ping fault zone are the main task of this study.

In this study, Digital elevation model and Landsat-7 ETM+ bands 4-5-7 were chosen to create the false color composite. The visual images interpretation combined with geomorphic indices was conducted to analyze the morphotectonic that were created in GIS database. Field investigations were also used to test for accuracy of the lineament interpretation and values of geomorphic indices.

The analysis found that lineament patterns are mainly trend in NW-SE azimuth direction with a total length of about 230 kilometers. From the calculated data reveal that mountain front sinuosity index represent low values from 1.04 to 1.77, Valley floor width to height ratio show very low values from 0.30 to 2.66, and Stream length gradient index display very high values. Geomorphological features like offset streams, triangular facets, and shutter ridges show that the tectonic controls in the area. Morphotectonic evidences such as straight mountain front, V-shape valley and narrow valley floor, and abruptly change slope of several streams and result of geomorphic indices indicate that tectonic activities are highest in zone 3 of the study areas which are control by strike-slip fault and normal fault.

The final results from this research can be used as a spatial data for supporting active faults study in Thailand including geological hazard warning and city planning for much better efficient management in the future.

Department : ____Geology_____   Student's Signature _____

Field of Study : ____Earth Sciences_____   Advisor's Signature _____

ACKNOWLEDGEMENTS

CONTENTS

LIST OF TABLES

LIST OF FIGURES

CHAPTER I

INTRODUCTION

1.1 Rationale

Remote sensing data is the acquisition of information about an object or incident, without making physical contact with the object that possible to collected data in regional scale once a time. There are two main types of remote sensing: passive remote sensing and active remote sensing (Campbell, 2002). Passive sensors detect natural radiation that is emitted or reflected by the object or surrounding area being observed. Reflected sunlight is the most common source of radiation measured by passive sensors. For example, passive remote sensors include film photography, infrared, and radiometers. Active collection, on the other side, emits energy in order to scan objects and areas whereupon a sensor then detects and measures the radiation that is reflected or backscattered from the target. Such as, RADAR and LiDAR where the time delay between emission and return is measured, establishing the location, height, speed and direction of an object (Jian-Guo and Mason, 2009)

Active faults have been known as the faults that have adequately recent movement to displace the ground surface are commonly determine active by geologists because the ground surface is very young and fleeting feature. If triangular facets, stream offsets, and alluvium are the criteria of fault motion, then the phrase "active" mean that the events dating back into about 100,000 years (Allen et al., 1965). Active faults in these settings can originate earthquakes which make extensive damage cause of the low reduction of seismic energy and local constructions are not prepared to cope with them (Hanks and Johnston, 1992).

Earthquakes, as a part of environmental hazard of human concern, can be considered as natural disasters causing extreme and energetic destruction. Fault movements are major causes of earthquakes on land. Many approaches have been applied for detecting fault activities, the most generally and approximately approach for fault studies perhaps is a remote-sensing approach together with a ground-truth field survey. Because of them there are several, good supporting lines of evidence for explaining those earthquake activities within the landforms being produced by Fault movements (Songmuang et al., 2007).

Geomorphic indices are utility tools in evaluating tectonic activity. Beneficial geomorphic indices are the mountain front sinuosity (Smf index) and the ratio of valley-floor width to valley height (Vf index), both developed by Bull and McFadden (1977). Rapid uplift along mountain boundary faults generates a straight front and narrow valley floors due to down cutting of the streams. Until tectonic activities sluggish or stops, mountain front sinuosity increases with time as the front retreats depend on erosional processes, at the same time streams cut laterally producing wide valley floors. These indices have been applied to mountain range in different countries to determine the relative tectonic activity (Keller, 1977; Keller and Rockwell, 1984; Keller and Pinter, 1996; Silva, 2003; Verrios and Alii, 2004).

Plate tectonics is a scientific theory that describes the large-scale motions of Earth's lithosphere. The theory builds on the concepts of continental drift, developed during the first decades of the 20th century. The lithosphere is broken up into tectonic plates. When the plate movement, their relative motion defines the type of boundary: convergent, divergent, or transform. Earthquakes, volcanoes, mountain, and oceanic trench construction occur along these plate boundaries. The lateral movement of the plates typically varies from 0 to 100 mm annually (Read et al., 1975).

One of the major active faults in Thailand is the Mae Ping fault zone (also known as the Wang Chao fault zone). The Mae Ping fault zone is 500 km long; its continuation to the SE is uncertain. Some interpretations extend the Mae Ping fault zone over 1000 km further to the SE, to reach the Mekong Delta of southern Vietnam (Lacassin et al., 1997). The Mae Ping fault zone trends predominantly NW–SE, but displays important north–south-trending segments (Morley, 2004). These fault zones has characteristic and dating data in some of part that is not sufficiency to explain tectonic activities in this area. Morphotectonic analysis by use geomorphic indices can reach to regional area and some of part that cannot reach by field surveys. The results of this research could be fulfilled data and interpretation of tectonic activities in an area.

1.2 Objectives

The objectives of this present thesis are

- To study morphotectonic of the Mae Ping fault zone in Changwat Tak and Changwat Kamphaeng Phet, northwestern Thailand and
- To interpret tectonic activities of the Mae Ping fault zone in Changwat Tak and Changwat Kamphaeng Phet, northwestern Thailand.

1.3 Scope and limitation

The scope of this research is limited to investigation and study tectonic activities of the Mae Ping fault zone in Changwat Tak and Changwat Kamphaeng Phet, northwestern Thailand by three geomorphic indices, i.e. mountain front sinuosity index, valley floor width to height ratio, and stream length gradient index which are selected from geomorphological features in the study area.

1.4 Location of the study area

The study area selected for the present research was situated in Changwat Tak and Kamphaeng phet that is in the northwestern Thailand. It locates between 16° and 18° N latitude and between 97° 30' and 99° 30' E longitude. The total study area is approximately 12,000 square kilometers, covering path row 130-131/48-49 of LANDSAT-7 ETM+. The geomorphological features of the study area consist of high mountains, valleys and narrow plain areas (Figure 1-1).

1.5 Expected outcomes

The expected outcomes of this study are

- Geomorphic indices of the Mae Ping fault zone and
- Tectonic activities of the Mae Ping fault zone.

These results should fulfill data and determination with sufficiency and understandable information for a more effective explaining with appropriate strategies for interpretation tectonic activities and related events in a long term risk that may be repeatedly occurred in the study area as well as in other areas of similar topography and tectonic settings.

1.6 Research methodology

To achievement the proposes of this thesis, the research consist of four consecutively steps. Each of them is described as follows:

1.6.1 Preparation

This step includes:

- Literature review of the associated researches in the study area, northwestern Thailand, and other countries.

- Acquisition and study of the previous basic data acquisition, i.e. Digital elevation data, topographic map, and geologic map to understand the topography and rock pattern of the study area as general background information.

- Intensive perception on the conceptual framework of morphotectonic analysis and especially the criteria to interpretation tectonic activities.

1.6.2 Morphotectonic Analysis

The morphotectonic analysis is contained as follows:

- Thematic (GIS and remote sensing) data preparation. These inventory data consist of Digital elevation data (DEM), contour line and stream line. Software of geographic information system (GIS) and remote sensing (ArcGIS 9.3, Global mapper 11.0, and Google earth) are applied in developing, manipulating, and analyzing the digital data.

- Interpretation of Digital elevation data which is resolution 30 meter that were acquired from http://gdem.aster.ersdac.or.jp. Then overlay contour line and stream line over DEM to calculate geomorphic indices (e.g. mountain front sinuosity). These geomorphic indices were also checked from ground-truth information to examine accuracy in the intermediate field investigation.

- Calculated geomorphic indices from index equations by using GIS techniques and GIS software. Geomorphic indices are based on the topographic data, in order to estimate the relative rate at which constructive and destructive processes are operating in the landscape.

1.6.3 Field investigation

The field investigation and data collection includes:

- Reconnaissance to recognize the Mae Ping fault zone orientation and morphology in the study area for preparing the data to verified geomorphic indices.

- Intermediate field survey to conduct ground-truth to inspect the correctness of the analyzed results from the remote sensing data analysis and interpretation.

1.6.4 Evaluate, discussion and conclusions

This step includes:

- Evaluating, discussing and concluding tectonic activities of the Mae Ping fault zone in the northwestern, Thailand.

In order to accomplish the aims of this thesis, the schematic diagram illustrating the present methodology system was designed as shown in figure 1-2.
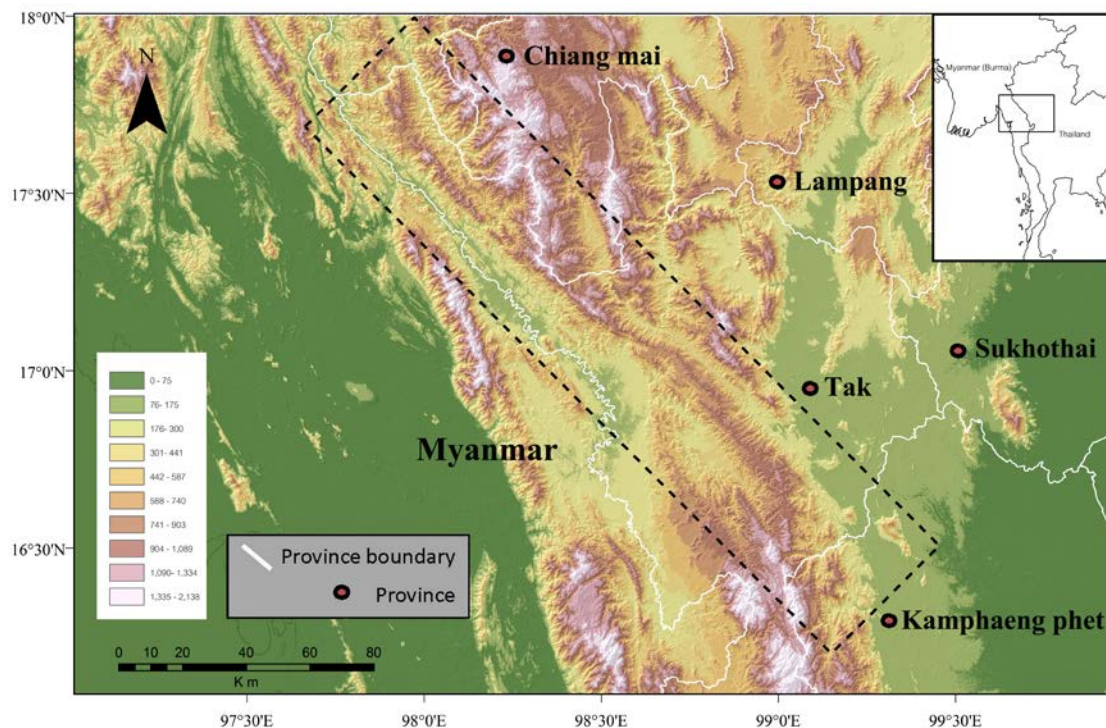
Figure 1-1 Location map of the study area

PREPARATION:

- Literature review,

- Acquisition and study the previous basic data,

- Intensive perception on the conceptual framework

Thematic data preparation and interpretation using GIS and remote sensing

Morphotectonic analysis

- Remote sensing image analysis

- Calculated geomorphic indices

Field investigation

- Reconnaissance

- Intermediate field survey

Analysis and Evaluate

Tectonic activities of the Mae Ping fault zone

Discussion and Conclusion

Figure 1-2 Schematic diagrams illustrating the research methodology system.

1.7 General information

1.7.1 Plate tectonics

The theory of plate tectonics report that the Earth's crust separated into eight major crust and approximately twenty smaller tectonic plates which shift over the surface of the earth (Figure 1-3). These tectonic plates are huge, irregular shaped thick of solid rocks. The smaller plates are about few hundred kilometers in diameter, as the major plates are thousands kilometer in diameter. Plate thickness is range from 15 kilometer at the ocean ridges to 200 kilometer at highly mountains. Some of plates are consist of oceanic, continental crust, and upper mantle part. Such as, the North American plate comprise of the North American continental crust and oceanic crust spreading out from the eastern edge of the North American continent to the extending ridge of the Mid-Atlantic oceanic ridge.

Plate tectonics is investigated of the structure of the Earth, and how the Earth's surfaces transform depending to the movement of tectonic plates. The most natural features are result of plate tectonics, for example volcanoes, hot springs, mountain belts, rift valleys, and mid-oceanic ridge. Earth is divided in three layers: the crust, mantle and the core. The core contains two layers which are the inner core and the outer core. The inner core mainly comprises of iron and nickel, this layer also is the densest layer of the earth. The outer core surrounds the inner core. Actually, the inner core has the same composition as the inner core does but the lower pressure which makes the components exist in the liquid status. Temperature in this core is around 4700 Celsius. Furthermore, there is convection current in the core result from the heat, which created from the radioactive decay inside the earth and drives plate tectonics.
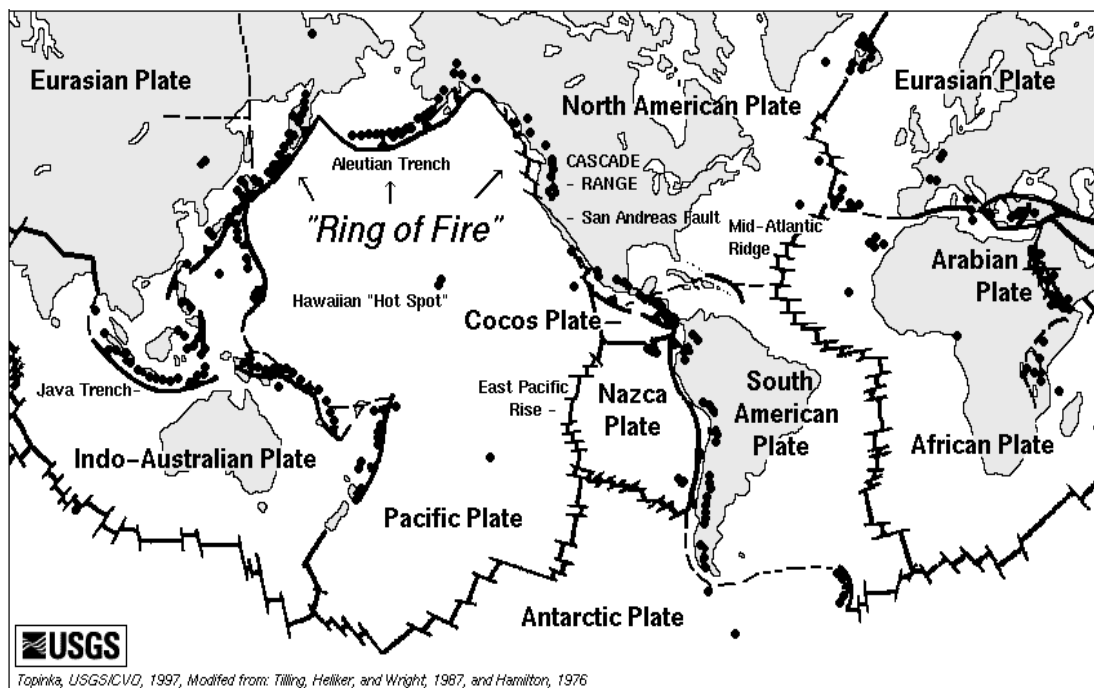
Figure 1-3 Map of the major tectonic plates (USGSICVO, 1997)
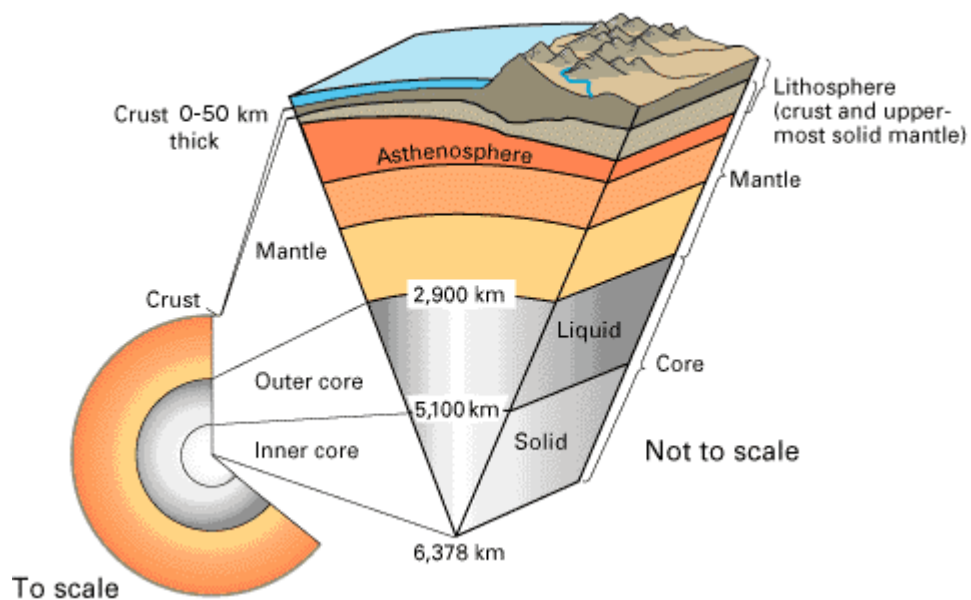
Figure 1-4 Layers of earth interior (http://www.oceansjsu.com)

The core is surrounded by the mantle. The mantle is consisted of dense rocks which range from being practically solid near the lower boundary with the core, to more scrawl toward the boundary with overlying layer, the crust. Addition, the crust is denser than the crust but less than the core (Figure 1-4).

The surface of the earth is known as lithosphere which is the outermost part. It covers the earth's surface, the top part of the mantle and all of the crust. Lithosphere means sphere of rocks which is more solid than the asthenosphere is. According to the material differences, thick crust will act as ice on the lake or loaf of fresh bread. However the crust is not one whole piece but it breaks in many pieces, because of the difference of convection current. There are two types of the crust: continental crust and oceanic crust. They are differ in variance way but the main parts are thickness and composition.

The Plate Tectonics Theory refers to the slow movement plate and large segment of both crusts which boundaries are connected; divergent, convergent and transform are three types of plates. Two plates move away each other are the divergent plate, which always has mantle well fill up the gap by bring the deep mantle rock to uppermost mantle and then to the crust. This plate occurs in the Mid Atlantic Ridge, Iceland, East Africa and Gulf of California. Most of these boundaries appear underwater, the oceanic creates. Moreover, the volcanic and the earthquake commonly happen here. Convergent boundaries are one plate moves toward another and avoid overlapping on the surface; the one must dive into deep mantle which occurs in the subduction zone. The incident has never be avoid is the earthquake, which will often happen around this plate boundaries. The surface rocks will be drown into upper mantle and finally, deep mantle. The last types, transform boundaries, which are one crust slide one another.

1.7.2 Active Faults

1.7.2.1 Definition of Active Faults

The present status of the study of active faults program in Thailand was reviewed by Hinthong (1995) and Hinthong (1997). Apart from the knowledge of the importance of understanding of active faults, the various basic concepts, principles or even the implications have been laid out for refining. Approaches towards refining their definitions and classifications, as well as their criteria for recognition of active faults have been compiled from various sources.

The significant of active fault evaluation to society is that it provides the basis for design, sitting, zoning, communication, and response to earthquake hazards. It is necessary for all types of major engineering structures in for reducing potential loss of life, injuries, or damage.

According to various authors and researchers, active faults can be defined in three approaches, which would be distinguished and applies. These three definitions are characterized as general technical definition, engineering definition, and regulatory definition. Those three applications of definitions were discussed, based primarily on its original definition which was proposed in the context of a two-fold classification of "dead" and "alive" or "active" fault, and with respect to their potential for future renewal or recurrence of displacement or offset.

In determination that based upon available data, fault activity can be classified as three classes: active, potentially active, and tentatively active. Basically, there are three major criteria for recognition of active faults; they are geologic, historic, and seismologic criteria.

In order to cope with the problem of the study of active faults in Thailand, the adoption of active fault classifications, especially for the benefit of the utilization only in Thailand, four classes have been proposed, namely, potentially active, historically and seismologically active, neotectonically active, and tentatively active faults and fault zones.

Consequently, with the restriction, deficiency of necessary data, and the lack of various seismological, geodetic, geophysical and other subsurface methods of analysis, but only supported by thermoluminescence age dating, the inventory of twenty-two preliminary active faults in Thailand have been outlined. The related purpose was to lay out major faults/ fault zones for the preparation of preliminary active faults map of Thailand, scale 1:1,000,000 (Figure 1-5).

Charusiri et al (2001), therefore, ranked the active faults, based upon historic, geologic, and seismological data. Since Thailand is not the main site for present day-large earthquakes as compared with those of the nearby countries, the best definition used herein is from the combination and modification of those above-mentioned definitions. Additionally, the age of the fault is also essentially in their justification, it is proposed that the fault becomes "active" if it displays a slip movement in the ground at least once in the past 35,000 years or a series of quakes within 100,000 years. If the fault shows only one movement within 100,000 years, it would be defined as "potentially active". Furthermore, if only once in the past 500,000 years, it would be become "tentatively active". All of those faults are expected to occur within a future time span of concern to society. The fault becomes "neotectonic" if it occurred in Pleiocene or Late Tertiary, and as it regarded" Paleo- tectonic" or "inactive" if it occurred before Pleiocene.

Hinthong (1997) studies active faults in Thailand and classified most of the faults in the Northern Thailand as potentially active faults. There is hot springs, which can be observed along the trend of these faults. These comprise five fault zones in the northern and the western highlands geologic provinces, namely:

1) The N-S trending, Mae Sariang Fault Zones located in the west, which close to Thai-Myanmar border, having activity between 0.32 to 0.89 Ma;

2) The sigmoidal-shape, Mae Tha Fault Zone, which bounds the east part of Chiang Mai basin, having activity between from 0.19 to 0.77 Ma.

3) The NE-trending Theon Fault Zone, which lies on the middle part of northern Thailand as a part of sigmoidal shape and occurred about 0.16 Ma.

4) The NE-trending Phrae Fault Zone, which bounds the eastern flank of Phrae Basin and has the shape similar to Theon Fault, shows fault activity of about 0.19 to 0.10 Ma; and

5) The NW-trending Three Pagodas Fault Zone, which has the activity range from 0.012 to >1.0 Ma.

Some thermoluminescence dating mostly determined by Isao Takashima, Akita University supported the age dating (Hinthong, 1997).
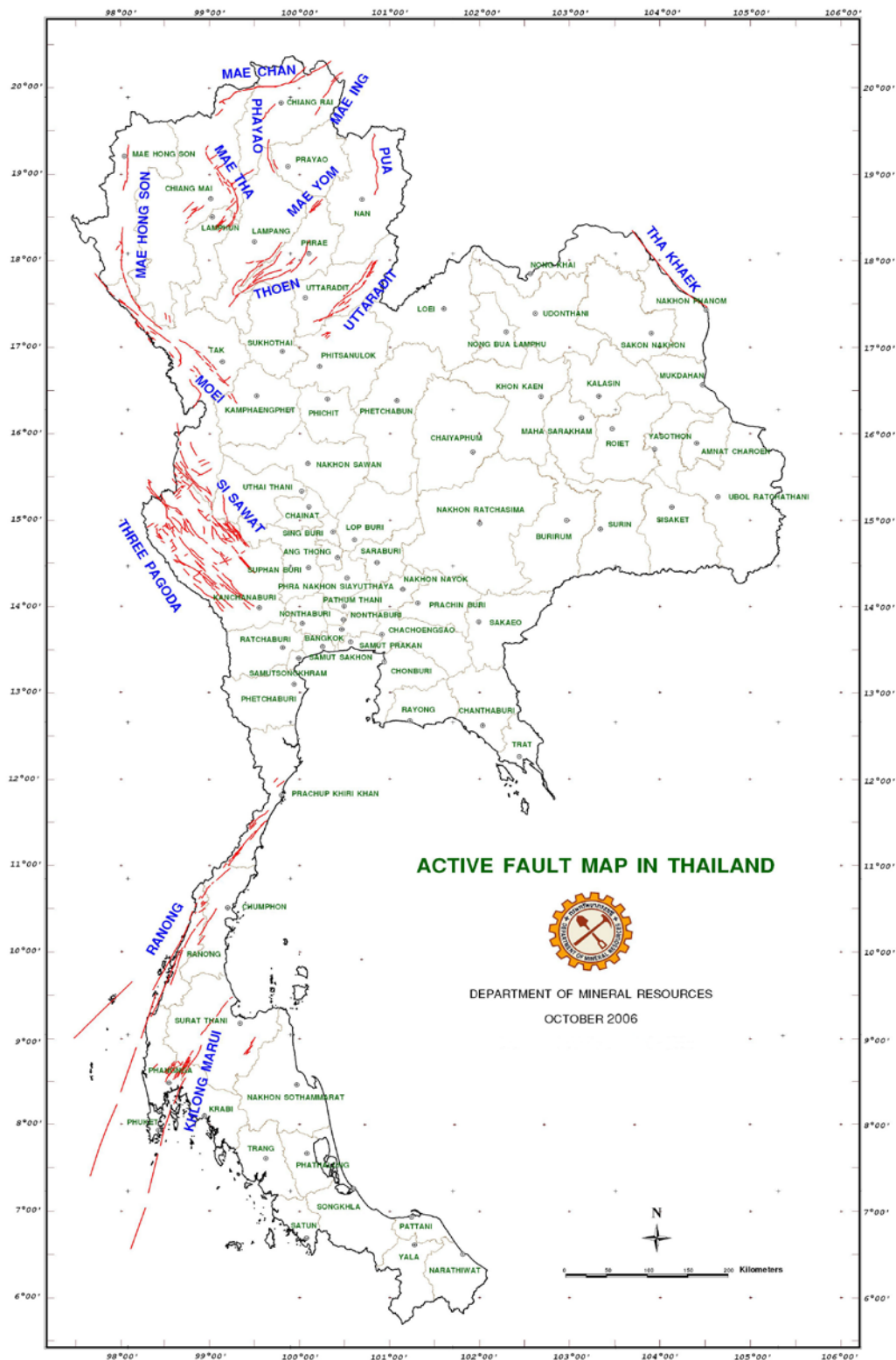
Figure 1-5 Map of Thailand showing of major active faults

(Department of Mineral Resources 2006)

CHAPTER II

LITERATURE REVIEW

2.1 Geo-informatics

Remote sensing (RS), geographic information system (GIS), and global positioning system (GPS) are parts of the geo-informatics. We can use them to measuring, recording, processing, analyzing, representation, and visualizing geo-spatial data because they are defined as multi-disciplinary science of geo-informatics.

2.1.1 Remote sensing

2.1.1.1 Definition

Techniques and methods to observe the Earth's surface at a distance are not much; remote sensing is the useful one to work on that. Remote Sensing can be described as the instrumentation, which interprets the pictures or numerical values obtained to acquire meaningful data of regularly materials on the earth. Remote sensing can be divides in three definitions, they are given below:

"Instrument-based techniques employed in the acquisition and measurement of spatially organized data/information on some properties of an array of target points (pixels) within the sensed scene that correspond to features, objects, and materials, doing this by applying one or more recording devices not in physical, intimate contact with the item(s) under surveillance; techniques involve amassing knowledge pertinent to the sensed scene (target) by utilizing electromagnetic radiation, force fields, or acoustic energy sensed by recording cameras, radiometers and scanners, lasers, radio frequency receivers, radar systems, sonar, thermal devices, sound detectors, seismographs, magnetometers, gravimeters, scintillometers, and other instruments" is the definition of Remote Sensing (NASA, 2010).

Lillesand et al. (2008) supported that remote sensing combines the science and art through obtaining information about an object, region, or phenomenon under investigation. "This method, remote sensing, is similar to mathematics. Through, making sensors to measure the quantity of electromagnetic radiation (EMR) exiting an object or geographic region from a distance and then extracting valuable information from the data using mathematically and statistically based algorithms is a scientific activity" (Figure 2-1). It functionally works in harmony with other spatial data-collection techniques or equipments of the mapping sciences, including cartography and geographic information systems (GIS) (Clarke, 2001; Jensen et. al., 2007).
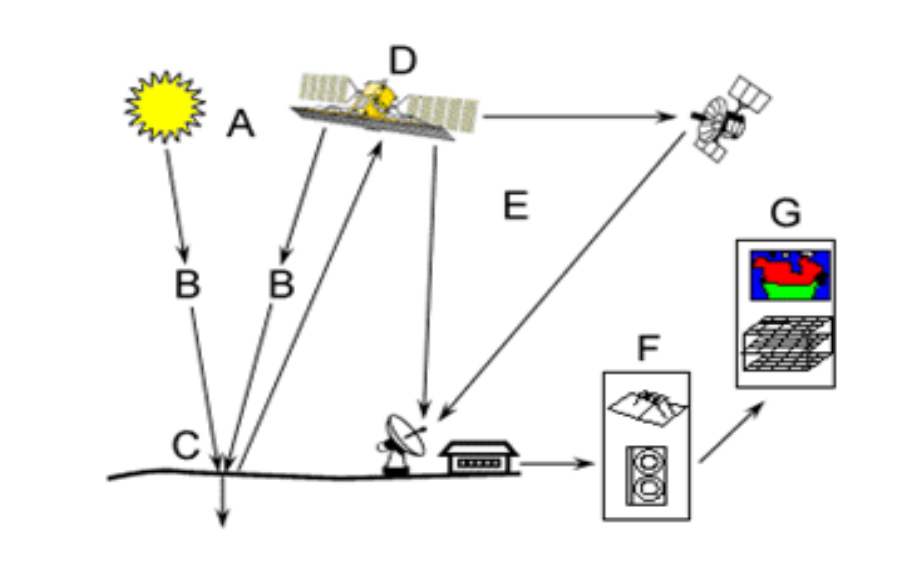
Figure 2-1 Process of Remote Sensing (Canada Centre for Remote Sensing, 2008). Note: A) Energy source to illuminate the target; B) Interaction of the radiation with the earth's atmosphere; C) Radiation-target interactions; D) Data reception; E) Data transmission; F) Data processing; G) Data application

2.1.1.2 Remote sensing techniques

Basically, the concept of remote sensing concentrates on the truths that anything on the Earth is not below 0 Kelvin creates electromagnetic energy. An object reflection one absorbs sunlight or emits its own internal energy, because of its atomic and molecular vibration. Remote sensing are refined tools to record invisible light such as infrared, thermal infrared and microwave radiation.

Passive remote sensing and active remote sensing are classified into two systems in remote sensing. (Jensen and Kiefer, 2007)

Passive remote sensing is the object or surrounding area emits or reflects natural radiation, which received and being observed by sensors. Source of radiation generally is reflected sunlight that is the most detected by passive sensors. For instant, passive remote sensing, film photography, infrared, charge-coupled devices, and radiometers.

Active remote sensing scan objects and areas by mean of emitting energy at which a sensor then ascertains and measures the reflected or backscattered radiation from the target. An example of active remote sensing is RADAR where it measures the time postponement between emission and coming back, instituting the location, height, speeding and direction of material.

Normally, remote sensing operates on theory of the inverse question. When the object or incident of interest (the state) may be implicitly measured, moreover, there display some other inconstant that can be detected and measured (the observation), which may be corresponded to the material of interest in virtue of the use of a data-derived computer model. The ordinarily similarity given to express this is trying to considering the type of animal from its footprints. For example, while it is not possible to measure temperatures straight in the upper atmosphere, but it is possible to measure the spectral emissions from a known chemical functions; such as carbon dioxide in that area. The frequency of the radiation may then be referring to the climatic characteristics in that region through diverse thermodynamic relations (Lillesand et. al., 2008). As the result of its spatial, spectral, radiometric and temporal resolutions will influence the quality of remote sensing data (Jensen and Kiefer, 2007) (Figure 2-2).

• Spatial resolution

The size of a pixel that is duplicated in a raster image – typically pixels may related to square areas ranging in size length from 1 to 1,000 meters (3.3 to 3,300 ft.).

• Spectral resolution

The number of frequency bands recorded by the platform– usually, this pertains to the wavelength width of the different frequency bands recorded. Presently Landsat collection is that of eight bands including several in the infra-red spectrum, ranging from a spectral resolution of 0.07 to 2.1 m. The Hyperion sensor on earth can observe-1 separates 220 bands from 0.4 to 2.5 m, with one band has spectral resolution of 0.10 to 0.11 m radiometric resolution

The sensor can distinguish many of different intensities of emission. Essentially, this ranges from 8 to 14 bits, answered to 256 levels of the gray scale and up to 16,384 intensities or "shades" of color, in each band. It also relies on the instrument noise.

•Temporal resolution

The number of fly-pasts, the satellite or airplane, and is only pertinent in time-series studies or those need an averaged or mosaic photos the same as in deforesting monitoring. This was first utilized in the intelligence community where repeated coverage exposed changes in infrastructure, the stretching of units or the modification of apparatus. It is essential to repeat the collection of said location where the region is covered by cloud.
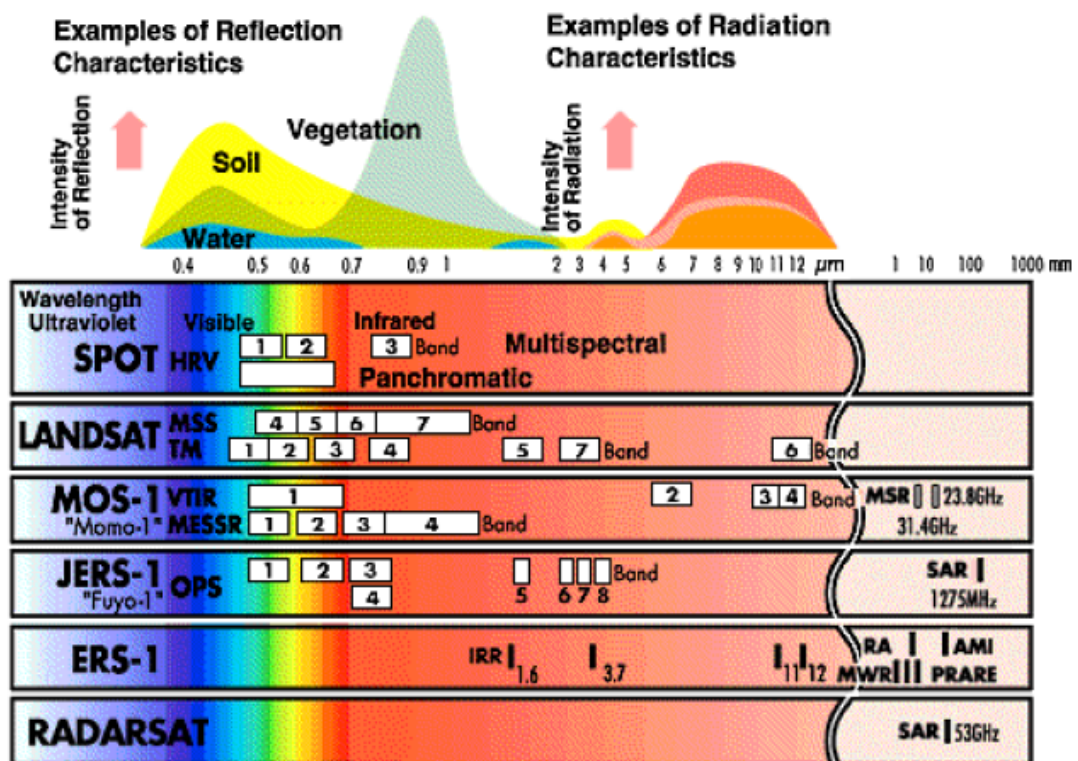
Figure 2-2 Radiometric resolution of satellites characteristics.

2.1.2 Geographic information system

2.1.2.1 Definition

Geographic information system (GIS) is new technology equipment, which is coming to be necessary tools for considering and obviously passing on knowledge about the earth. Definitions of geographic information system are numerous. For example, "a computer system, which has ability to capturing, saving, examining, and demonstrating geographically referenced information; that is, data recognized because of location is defined by the United States Geological Survey-USGS (2007). Entrepreneurs also identified a GIS as comprising "the algorithms, performing personnel, and spatial data that go into the system". Another meaning of geographic information system can be defined as "software systems with competency for key in, stock pile, administrate/analyze and output/display of geographic (spatial) data" is suggested by Briggs (2010). Nevertheless, Skrdla (2005) gave an explanation of the geographic information system as "a geographic component is managed into information and originally saved in vector form with associated characteristics."

2.1.2.2 Geographic information system techniques

The key index of GIS is spatial-temporal location as uneven for all other data. Just as many different tables using various common key index factors can be linked a connectional database including text or numbers, GIS can refer otherwise unassociated fact by using the key index variable as location. The key is the location and may be range in space-time.

GIS can quoted any variable that can be located spatially, and dramatically also secularly, Places or scopes in Earth space-time probably be reported as dates or times of happening, and longitude, latitude, and elevation representing as x, y, and z coordinates , respectively. There are many quantifiable systems of temporal-spatial reference could be acted for those GIS coordinates (for example, stream gauge station, geodesist benchmark, building address, water depth sounding , street intersection, film frame number, entrance gate, POS or CAD drawing origin/units). Units used to noted temporal-spatial data can alter broad (although when inputting precisely the identical information), but all location, which Earth-based spatial-temporal and reference extent should, theoretically, be associated to one another and eventually to a "genuine" physical location or range in space-time (Bettinger and Wing, 2004).

An unbelievable category of real-world and shown past or future facts can considered allied to precise spatial data, comprehensible and representative to simplify education and determination making. Open new methods of scientific inquiry were begun by the way of the key property of GIS into characteristics and patterns of previously analyzed unconnected real-world data.

2.1.2.3 Components of GIS database

 Clarke (2001) mentioned that there are two widely procedures customarily, used to keep information in a GIS for both kinds of concepts mapping references: Spatial data and Attribute data. In addition, spatial data is typically represented on maps as one of two type of spatial primitive: raster data and vector data expressed by Sutton et al. (2009)

Raster data are formed as a grid of values, or pixel or fixed size cells having digital charges, overspreading a definite area, furnished by satellite images, scanned maps and digital terrain modeling. Raster data exhibits continuous data across an area.

A series of x, y coordinate pairs is a stored form for vector data inside the computer's memory. Point's features represent as vector data, which act as spatial data showing at a single place, lines represent linear features and polygon features represent enclosed homogeneous areas or regions. A polygon is an enclosed area is created by a group of connected line segments.

Appearance data is an object's explanation which may be graphical, such as a symbol, point, line or polygon, or it could be try narrating specific nature of an object, i.e. number of inhabitants, production volume, and population density. The attribute data is stored in a relational database, with the spatial data saved in a standard hierarchical database (Clarke, 2001) (Figure 2-3).
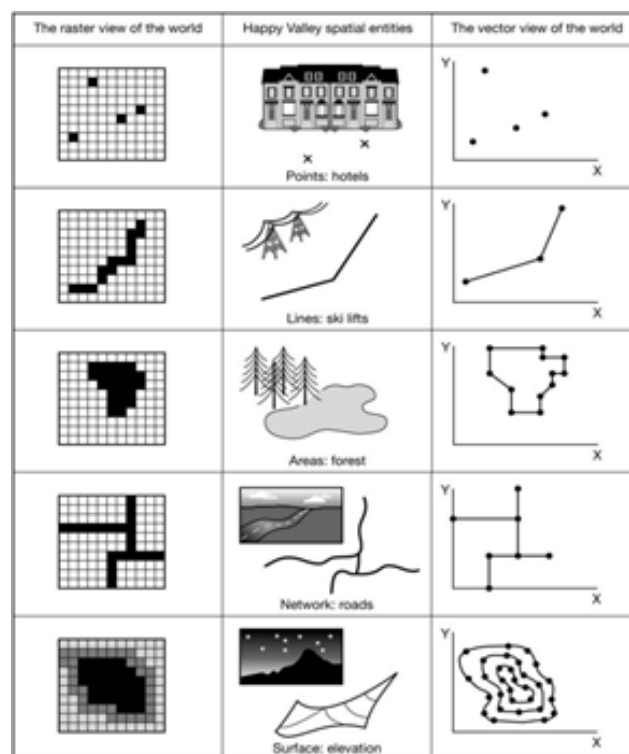
Figure 2-3 Spatial data in GIS database (Indiana University, 2005).

2.2 Geological evolution in the Sunda shelf and northern Thailand

Researchers (Tapponnier et al.,1982 ,1986; Daly et al., 1991 ; Dewey et al., 1989 ; Rangin et al., 1990 ; Lee and Lawver,1995 ; Hall , 1996 ; Packham, 1996; and Matthew et al., 1997) have accepted the result of tectonics event as Tertiary formation in the South East Asia was the Indian plate collided the Eurasian plate. The propagation extrusion model (Tapponnier et al., 1982) is accepted by many workers, which has a free boundary to the east and the west. The experiment of Tapponnier et al., 1982 indicated many similarities in their results, which seem similar to the geology features in the Southeast Asia. For instance, they suggest the Altya Tagh Fault as the F2 fault in the experiment and the F1 fault is the Red River fault. According to Molnar and Tapponnier (1975), the Himalayan Thrust Fold belt was plane between the conjugate fault of the sinistral Quetta Charman in the west and the dextral Sittang fault, Sagiang Fault in the east. NE-SW sinistral strike-slip fault and NW-SE dextral fault are numerous in this area (Ni and York, 1978).

The convergent plate, soft collision, Indian and Eurasia commenced in Late Paleocene to Middle Eocene(58-44Ma), while the hard collision was began in the Middle Eocene(44Ma) (Lee and Lawver, 1995). The tectonic evolution of this region in Cenozoic can be discussed in four stages, through the northern movement of the Indian plate relative to the Eurasian plate. The right corner of the Indian plate has penetrates into the Eurasian plate (Lacussin et al., 1997) and it has changed the stress pattern of this region through time. The opening of sedimentary basins in this area and South China Sea were controlled by the altered stress pattern as well as the movement of the major strike-slip fault (Huchon et al., 1994).

Srisuwan,2002 suggest that the Cenozoic tectonic evolution of this region can be discussed in four stages, stage I : Early Eocene to Early Oligocene (50-32 Ma): the South China Sea extensional border occurred before the collision of Indian-Eurasian and the presumed time of initiated of the Red River fault. Moreover, there are more rifting in the South china Sea and also included the first rifting in the West Natuna Basin for this stage. The opening of Mekong, Malay Delta and the part of the gulf of Thailand had been started at 40-35 Ma.

Stage II: Early Oligocene to Early Miocene (32-23 Ma): the left lateral Mae Ping Fault was end proximately 30 Ma. The widespread extension of the gulf of Thailand, Malay and West Tatuna sea basin had begun in the same time; Late Oligocene. The Mergui Basin and Andaman Sea are speculated to be formed during Late Oligocene and continued to early Miocene. The Mae Ping Fault and Three Pagoda fault changed to dextral movement, on the other hand the Mae Chan, Uttaradit and Phrae-Theon Fault became sinistral. In addition, the northern Thailand basin might be developed in this stage.

Stage III: Early to Middle Miocene (23-15 Ma): the rotation of the whole Sunda block and increase the rate of convergent along the Sunda arc. Northern Sumatra basin and Central of Thailand basin were still bearing extension. Malay Peninsula and Sumatra had rotated counter clockwise and the Southern Thailand were clockwise during 20 to 15 Ma. Reversion in the Malay, most of Cenozoic basin in the gulf of Thailand and onshore was experienced uplift and erosion that resembled to a pervasive Middle-Miocene unconformity.

Stage IV: Middle Miocene to recent (15 to 0 Ma): Borneo still continued counter-clockwise rotation when the Thai-Malay Peninsula and Sumatra discontinued and did not crease to the northern movement of Australia. North Sumatra had whirled counter-clockwise with South Malaya and the rotation progressed the orientation of the Sumatran border became less slanting to the Indian plate motion direction. This affected the dextral strike-slip system of Sumatra, and extension in the Andaman region. The gulf of Thailand happened to be expanded, while the Andaman Sea kept opening toward its existing range. In the Sunda area, dextral, was the main fault trend for all NW-trending strike-slip fault zones. The structural in the Cenozoic basins were slowed down from the reversion and uplift approximately 10 to 5 Ma, during this period regional subsidence occurred and was presumably induced by post-rift thermal re-equilibrium. This late stage sinking has proceeded to the present time.

2.3 Major tectonic elements in Southeast Asia

Concerning the Southeast Asia region, N-S trending extensional faults dominated the structural scope of Cenozoic basins in Thailand which related to the movement of the NW-SE and NE-SW trending strike-slip faults. There are major strike-slip faults such as the NW-SE Red river fault, Mae Ping, Three Pagoda and Sumatra faults when the Mae Tha, Rayong, Klong Marui and Nan-Uttaradit fault are the NE-SW trending conjugate strike-slip faults which are eliminated by the principal NW-SE strike-slip faults (Polachan, 1988)

Extension of the Mae Ping Fault and the Three Pagoda Fault are 450 and 250, respectively. They seemingly connected to the southeastward underneath the Chao Praya central plain and in the gulf of Thailand (Bunopas,1981; Tapponneir et al,1986 and Lacussin et al, 1997). These faults briefly are parallel to the Red River Fault Zones and trend NW-SE. Sagiang Fault Zone in Myanmar had shorten the Three Pagoda Fault and the Mae Ping Fault. The spray of Mae Ping Fault may be expanded southeastward to Chonburi province and the other probably extended to the Toule Sap depression in Cambodia. The farther southeast to the west of Mekong basin (Tapponneir et al, 1986; Lacussin et al, 1997). The Nan-Uttaradit Fault zone oriented in NE-SW is bounded to the east of Nakhon Thai Plate by which a belt of ultramafic and mafic rocks associated with basaltic to andesitic metavolcanics, blueshcist (Barr and Macdonald, 1987) and turbidites are situated. The Nan-Uttaradit Fault and this belt checked the suture zone of Shan-Thai block and the passive margin of the Kontum-Khorat block of the SE (Bunopas, 1981; Barr and Mcdonald, 1987).

Subduction and consequent collision probably occurs between the Upper Permian and Middle Triassic (Bunopas, 1981; Sengor and Hsu, 1984; Barr and Mcdonald, 1987; and Hutchinson, 1989). The Mae Tha Fault Zone (MTF) is roughly parallel to the Nan-Uttaradit Fault (NUF), but it has a sigmoidal shape, swinging N-S through the central to the southern part of Northern Thailand. A series of anastomosing strike-slip fault and dip-slip faults were an occurrence of this fault (Strogen, 1994). Both the NUF and MTF show sinistral movements based on earthquake fault plane solutions (Le Dain et al, 1984).

2.4 The Mae Ping fault zone

Hinthong (1995 and 1997) divides active faults into four classes based on degree of activeness as potentially active, historically and seismologically active, neotectonically active, and tentatively active. He regarded that the Mae Ping fault zone is historically and seismologically active.

Lacassin et al. (1997) found evidence of intense ductile left-lateral shear in the Lansang gneisses along the Wang Chao fault zone (also known as the Mae Ping fault zone). Dating by $^{40}Ar/^{39}Ar$ represent that deformation probably terminated nearly 30.5 Ma. Based on $^{40}Ar/^{39}Ar$ results suggest that magmatic belt suffered rapid cooling.

According to Charusiri et al. (2001), Thailand active faults were classified into five seismic belts (SABs), which were defined as linear or elongate zones of seismicity. These SABs were commonly classified based upon neotectonic movements and coincident with major tectonic structures. They are Northern, western-Northwestern, Central Peninsula, Southern Peninsula, and Eastern-Northeastern SABs. The Western-Northwestern SABs, Mae Ping Fault Zones was considered as the potentially active fault.

Preecha (2006) proposed characteristic of the Moei-Mae Ping fault zone that northwest-southeast trending, oblique-slip fault with total length about 230 kilometers. This fault zone is divided in 10 segments, ranging in length from 8 – 43 kilometers. Most of evidences indicated that the Mae Ping fault zone is still active until present.

 Morley (2007) investigated evolution of deformation styles of the Mae Ping fault zone. Based on published cooling age data with new apatite and zircon fission-track results indicated that the Miocene–Recent history of the Chainat duplex is one of minor sinistral and dextral displacements, related to a rapidly evolving stress field, influenced by the numerous tectonic reorganizations that affected SE Asia during that time.

2.5 Tectonicgeomorphology

2.5.1 General

According to interactions of tectonic and fluvial processes, continental landscapes of the earth are formalized in a large part, which are altered by the pervasive manipulation of late Quaternary climate changes. Tectonics is the study of crustal deformation. Mainly, this regards the evolution of geologic structures fluctuating from mostly transition zones: crustal plates to small faults and folds. The study of landscapes, also occurrences and the processes that are the result of their shape, what geomorphology is. Tectonic geomorphology consists in the area of both vertical and horizontal deformation in fluvial, coastal, glacial processes and the outcome landscapes.

The principal significance for this study is that how fluvial system reacts to tectonic deformation. The duty for us is using tectonic signals in the landscapes to try more thoroughly recognizing. Definite geologic structures are the consequences of earth deformation, which extremely influence landscape evolution and geomorphic processes. Reversely, evolution of landscape assemblages can be utilized to decrypt the kinematics of faults and folds. Tectonic inquiries are assisted through tectonic geomorphology with many temporal and spatial scales. Some researchers attempt to conceive how horizontal and vertical in land deformation influences the forms of hills and streams in a discovery to better understand long-term partition of stress along plate boundary-fault systems (Lettis and Hanson, 1991). Earthquake renewal intervals are studied by many scientists in virtue of landslides determination and to create maps portraying patterns of seismic shaking caused by prehistorical earthquakes. Landscape development studies spend many time spans. Topics such as the effects of rapid mountain-range erosion on crustal processes entail time spans more than 1 My.

2.5.2 Landscape responses to regional uplift

The strong buzz saw of stream-channel downcutting increases the streams cutting into ever deeper as bedrock. Functions of vertical tectonic displacement rates, excess unit stream power, and resistance of earth objects to degradation are amounts and rates of tectonically induced downcutting. A bedrock uplift rate of 0.1 m/ky may not be able to correspond with the downcutting, which are small brooks gushing over resistant welded tuff; such stretches to erode uninterruptedly. In the other hand, downcutting by imperishable streams flowing over soft rock easily keeps speed with bedrock uplift of 5 m/ky. However stream-channel downcutting happens only during suitable climatic and tectonic limitations.

The inclination of streams to cut down to the minimum slope needed to transport their sediment load has been a long standing underlying concept in fluvial geomorphology (Powell, 1875; Mackin, 1948; Leopold, Wolman, and Miller, 1964; Leopold and Bull, 1979; Bull, 1991). Advancement mountains with headwater reaches of rivers lean to stay on the degradational side of the starting point of critical power, but downstream reaches with their greater unit stream power, are more probably to achieve the base level of erosion by way of the process of tectonically induced downcutting. Leonard (2002) examined the larger dales drainpipe the eastern side of the Rocky Mountain. Tectonically induced downcutting occurs from the uplift, which raised isostatic uplift. He supposes that the base of the Ogallala formation was planar and slanted eastward. Leonard's modeling advises that the isostatic component of rock uplift accounts for 50% of the total rock uplift with the remnant being tectonic uplift. Greater uplift occurred about 540 m, C transects at the Arkansas River valley than at the valley of the South Platte River.

McMillan et al., (2002) proposed the fewer uplift amounts along the valley of the North Platte River, which estimated through Leonard's consequence. The bedrock-uplift concept updates the means in which we research tectonics of mountain ranges on active or passive plate margins. Geomorphology recently plays a crucial role in studies of earth history because of the need to comprehend prospect responses to uplift caused by either tectonic or isostatic uplift. Evaluation of sediment flux from continental landmasses to ocean basins differ from the local erosion and deposition by different time spans, areas, and geomorphic processes, which related with a single-rupture event fault scarp. Conceiving geomorphic models that resemble ideal for their formative study area and the information may come to be quite insubstantial when adapted to dissimilar spatial, tectonic, and climatic settings.

2.5.3 Geomorphic tools for describing relative uplift rates

Experiencing rapid tectonic deformation in areas can be recognized through some geomorphic directory files, which have been progressed (Keller, 1986; Keller and Pinter, 1996) Because of their equip a rapid assessment of large regions and can be obtained effortlessly from topographic maps or aerial photos, geomorphic indices are principally beneficial in tectonic studies (Strahler, 1952). Furthermore, in contemporary decades, the increasing utility of GIS software has created for more convenient to undertake instantaneous and elaborated processing of data. At present, in morphotectonic studies, morphometric analysis of landforms and geostatistical topographic have incorporated with analysis traditional geomorphic analysis. (Keller et al., 1982; Mayer, 1990; Cox, 1994; Merritts et al., 1994; Lupia Palmieri et al., 1995; Lupia Palmieri et al., 2001; Currado and Fredi, 2000; Pike, 2002; Della Seta, 2004; Della Seta et al., 2004).

2.5.3.1 Mountain-front sinuosity

Most faults or folds, which are straight or tenderly curving nature grants evaluation of the order of erosional adjustment of a structural landform. The linear nature of the front is sustained by the rapid uplift along a range-bounding fault. The Landscape evolution is dominated through erosion after discontinuance of uplift and builds a sinuous mountain–piedmont junction, particularly where lithologic resistance to erosion is feeble. Intermediate scenarios implicate the interaction of progressing uplift and prolonged fluvial degradation, which diverges exceedingly with climatic setting. The noticeable process that shapes the mountain-front landscape in tectonically inactive environment is stream flow.

Streams rapidly downcut to their base level of erosion by displacing small amounts of rock, and then gradually broaden their vale floors by taking away large amounts of debris drew from hill slopes. Maximum concentrations of stream dynamism mouths result in erosional embayments that spread up the larger valleys. The effect is extremely snaky mountain–piedmont intersection. Comparatively, fluvial erosion is governing over uplift but sluggish uplift may be proceeding. Advancement of embayments derived from erosion in sections of a mountain front between the principal watersheds at a much slower rate and also lessens. Map mountain–piedmont junctions can utilize as a category of topographic information sources. If the mountain–piedmont junction is viewed on images larger than 1:60,000, replication measurements will be accurate. SRTM radar images can be ideal, in the contrast, Landsat is borders.

2.5.3.2 Valley floor width to valley height ratio

The valley floor width–valley height ratio is another responsive index to current and progressing uplift, valley-floor widths extent with watershed size, erodibility of rock type, and with decline of uplift rate. Valley heights reduce with the passage of time after discontinuance of uplift, but not approximately as fast as valleys widen. The valley floor width–valley height ratio is exceptionally sensitive to late Quaternary tectonic base-level falls because diminishing of a valley floor is achieved fast by the downcutting action of streams. Great Discovery in signifying differences (at the 0.99 confidence level) by Bull and McFadden (1977) in the means of Vf ratios of tectonically active and inactive mountain fronts. Choosing sites need the carefulness to measure valley floor width– valley height ratios. Vf values are more likely to be delegate of the relative degree of tectonic base-level fall if ascertained in similar rock types and at the same basin-position coordinate for a suite of similar size drainage basins along a given mountain front.

Annual unit stream power to deal with the work of erosion enlarges downstream, but rock resistance to erosion may not alter. Consequently, part of the difference in valley-floor width is a function of drainage-basin size. A circumscribed range of drainage-basin sizes is desired because stream discharge increases in a nonlinear manner in the downstream direction, especially for streams of humid areas (Wolman and Gerson, 1978). Measuring valley floor widths can be complicated. Preferably they should be the represent value of several measurements made in the field. High quality topographic maps achieve quite well. If meager resolution combines valley floor and footslope relief, digital sources grant inconsistent consequences, hence failing to notice unexpected margins ordinary to many valley floors.

Vf ratios are more susceptive to fluvial base level controls than V ratios because variations in the widths of valley floors happen much more speedily than hill slope relief is reduced. Valleys may be engraved in less than 10 ky in reaction to a base-level fall. Valley floor tapering naturally is more than the simultaneous enlarge of valley cross-section relief. After that valley floor width may two times in 100 ky, but >1 My may be required to decrease valley height by half at the unchanged position in a drainage basin. Exceedingly active mountain fronts regularly have Vf ratios between 0.5 and 0.05. If downcutting does not break in proceedings (times of accomplishment of the base level of erosion), stretch terraces will miss in such narrow canyons. The miniscule widths of such valley floors, relative to the adjacent watershed ridge crest heights, result in Vf ratios that obviously describe situations where tectonically induced downcutting sustains the mode of stream operation far to the degradational side to the threshold of critical power.

2.6.3.3 Stream length-gradient index

The Stream Length–Gradient Index (SL Index) is one of the quantitative geomorphic parameters incorporated in morphotectonic analysis (Hack, 1973). The SL Index can be a valuable tool to identify tectonic displacements in tectonically active areas, and/or at the regional scale of investigation, (Keller and Pinter, 1996; Chen et al., 2003 and references therein; Zovoili et al., 2004). Nonetheless, the effectiveness of the parameter in detecting local active structures has not been assured for small drainage basins and/or in regions where tectonic activity is not more strong(Chen et al., 2003; Verrios et al., 2004). Anomalous values of the SL Index likely cannot be discriminate from the tectonic activity in small stream basins, according to the contribution of the lithological effect.

CHAPTER III

METHODOLOGY

The sources of input data and the steps in analysis used remote sensing are comprehensively explained hereafter indicate that as the data entry and production are the most complicated and time consuming steps of any kinds of GIS and remote sensing techniques. The thematic data used in this research are prepared and processed below. Meanwhile, geomorphic indices and tectonic interpretation by GIS techniques are reviewed. However, the detailed of each geomorphic index and tectonic interpretation will be explained in the following chapter.

3.1 Phases of morphotectonic analysis in remote sensing and GIS techniques

The following phases can be distinguished in the process of a morphotectonic analysis using GIS (Biswas and Grasemann, 2005; Bhatt et al., 2007). They are listed in logical order or sequence though sometimes they may be overlapping as follow:

- Preliminary phase:

    Phase 1: Defining of objective and the methods of study which will be applied.

- Data collection phases:

    Phase 2: Collection of existing data (collection of existing maps and reports with relevant data)

    Phase 3: Lineament interpretation (interpretation of lineaments and creation of new input maps)

    Phase 4: Geomorphic indices (calculated geomorphic indices from digital elevation data)

    Phase 5: Fieldwork (to verify the geomorphic indices)

    Phase 6: Tectonic interpretation

- GIS work:

    Phase 7: Data entry (digitizing of maps and attribute data)

    Phase 8: Data validation (validation of the entered data)

    Phase 9: Data computation (computation and transformation of the raw
    data in an index which can be used in the analysis)

    Phase 10: Data analysis and interpretation (analysis of data for preparation
    of morphotectonic maps)

    Phase 11: Presentation of output maps (final production of morphotectonic
    maps and adjacent report)

The pattern GIS for morphotectonic analysis combines conventional GIS procedures with digital elevation processing capabilities and a relational data base. Map overlaying, and integration with satellite images are required, thus a raster system is preferred. The program should be able to perform spatial analysis on multiple-input maps and connected attribute data tables for map overlay, calculation, and various other spatial functions.

3.2 Thematic data preparation from GIS and remote sensing techniques

Remote sensing data can be merged with other sources of geo-coded information as a GIS. This allows the overlapping of several layers of information with the remotely sensing data, and the application of a virtually unlimited number of forms of data analysis. The input data used for morphotectonic analysis in this thesis consists of several spatial data categories from the available resources (as shown in Table 3-1), being digitized from available maps and prepared from lineaments interpretation, and from field investigation data.

These input data will be further used to analyze the morphotectonic and tectonic activities. The brief techniques and thematic maps of the input data produced in this thesis, namely, digital elevation, topography, stream line, and geologic data are consequently presented as below.

Table 3-1 Overview of the important input data themes that were pre-processed and calculated in this thesis.

Themes	Data types	Data preparation methodology
Digital elevation data	Raster	Download from http://.gdem.aster.ersdac.or.jp: resolution 30 m
Satellite image	Raster	Download from http:// earthexploler.usgs.gov: resolution 30 m
Contour line	Vector	Generated from digital elevation data: contour interval 20 m
Stream line	Vector	Generated from digital elevation data: 1:50,000 map scale
Geologic data	Vector	Derived from Department of mineral resources: 1:50,000 map scale

3.2.1 Digital elevation data

The Digital Elevation Model is only representing height information without any further definition about the surface. Other definitions equalize the terms DEM, which is also representing other morphological elements. In some definitions can be found which define the DEM as a digital regularly spaced GRID. All datasets which are captured with satellites, airplanes or other flying platforms are originally DEM (like SRTM or the ASTER GDEM).

A DEM can be represented as a raster (a grid of squares, also known as a height map when representing elevation) or as a vector-based triangular irregular network (TIN). A much higher quality DEM from the Advanced Space borne Thermal Emission and Reflection Radiometer (ASTER) instrument of the Terra satellite is also freely available for 99% of the world, and represents elevation at a 30 meter resolution. The study area consists of them that range between -23 to 2,138 meters (Figure 3-1).
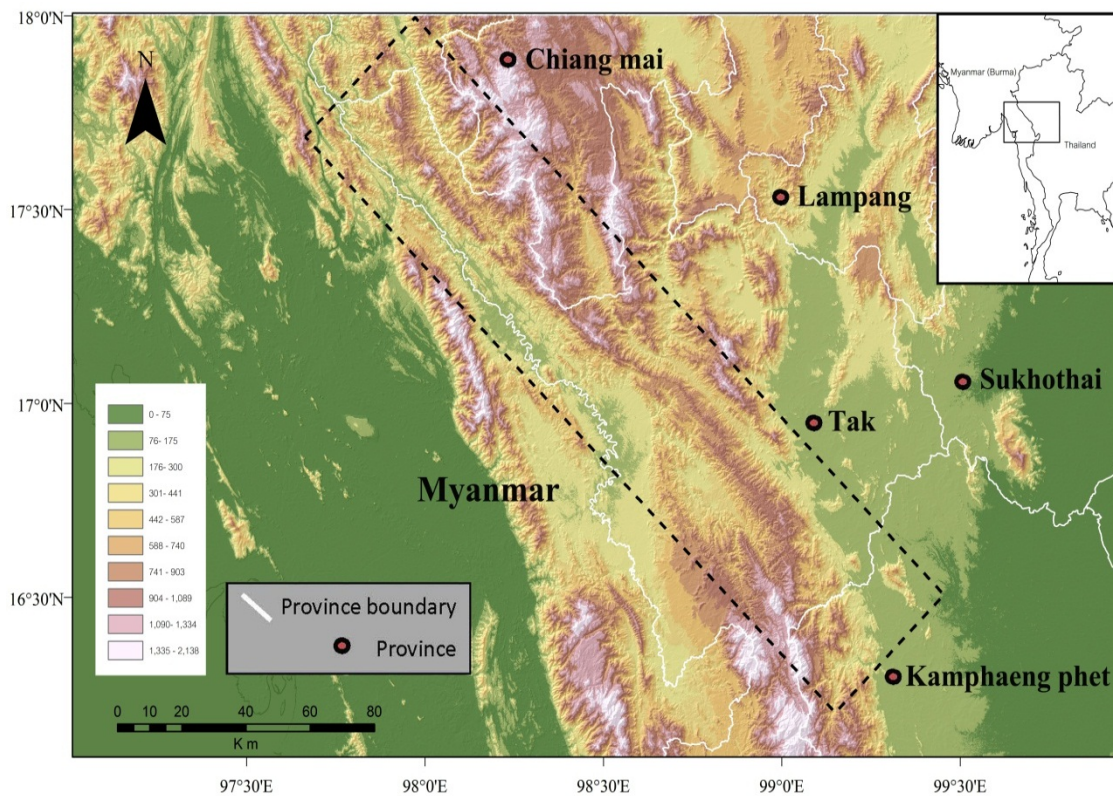
Figure 3-1 Digital elevation map of the study area.

3.2.2 Satellite image

A study of lineaments interpretation in this study area was carried out using remotely sensed data. Landsat 7 ETM+ path/row 130-131/48-49 acquired on 23th December 2002, 5th April 2004, 12th April 2004, and 4th March 2006 respectively which are selected as primary remotely sensed data is a false-color composite, band 4, 5, and 7 represented in red, green, and blue in order (Figure 3-2).
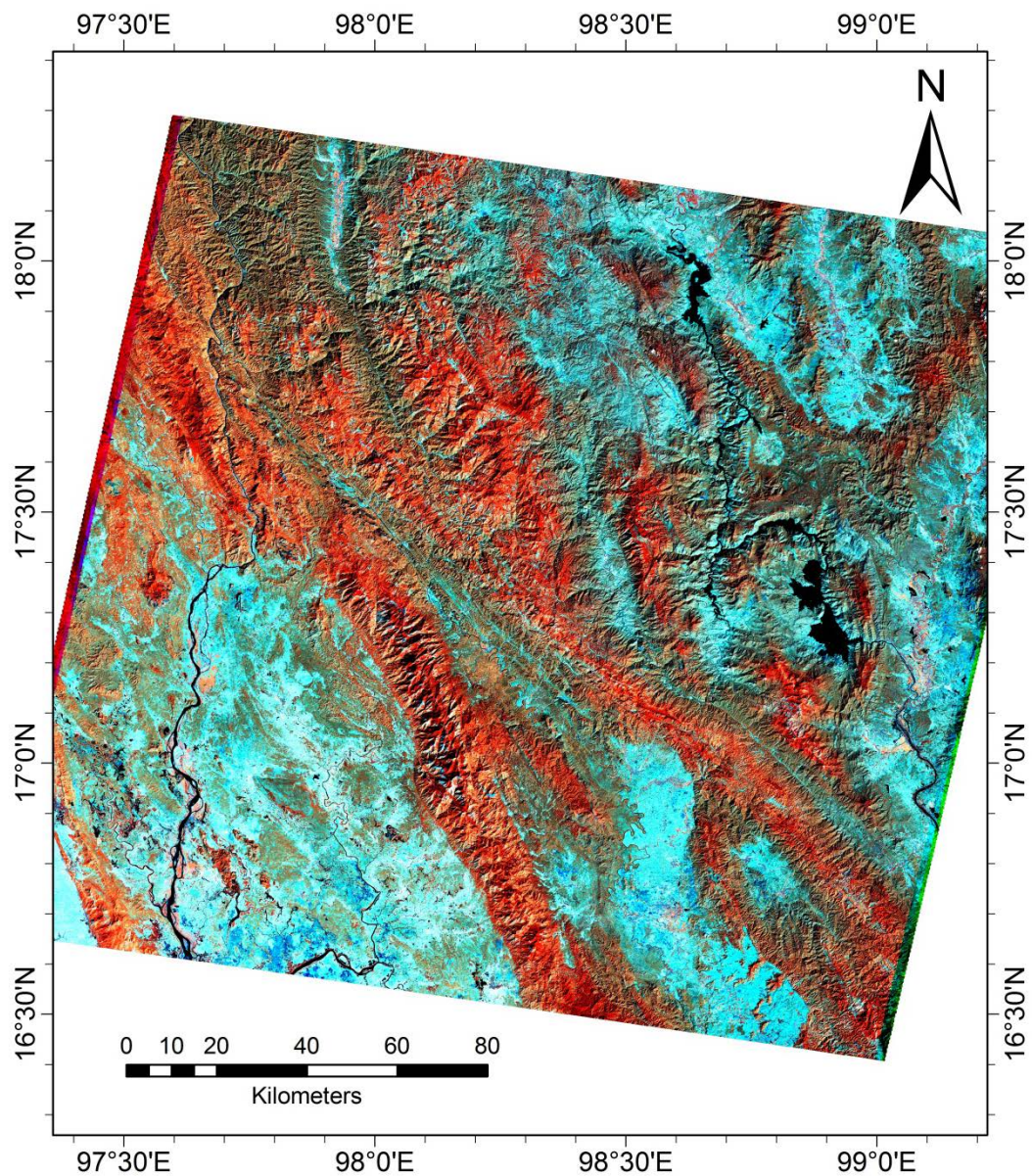
Figure 3-2 Landsat 7 ETM+ (R=4, G=5, B=7) satellite image map of the study area.

3.2.3 Contour lines

Contour lines are curved or straight lines on a map representing the intersection of a real or hypothetical surface with one or more horizontal planes. The configuration of these contours that generated from digital elevation data. Contour interval of this study area is 20 meters (Figure 3-3).
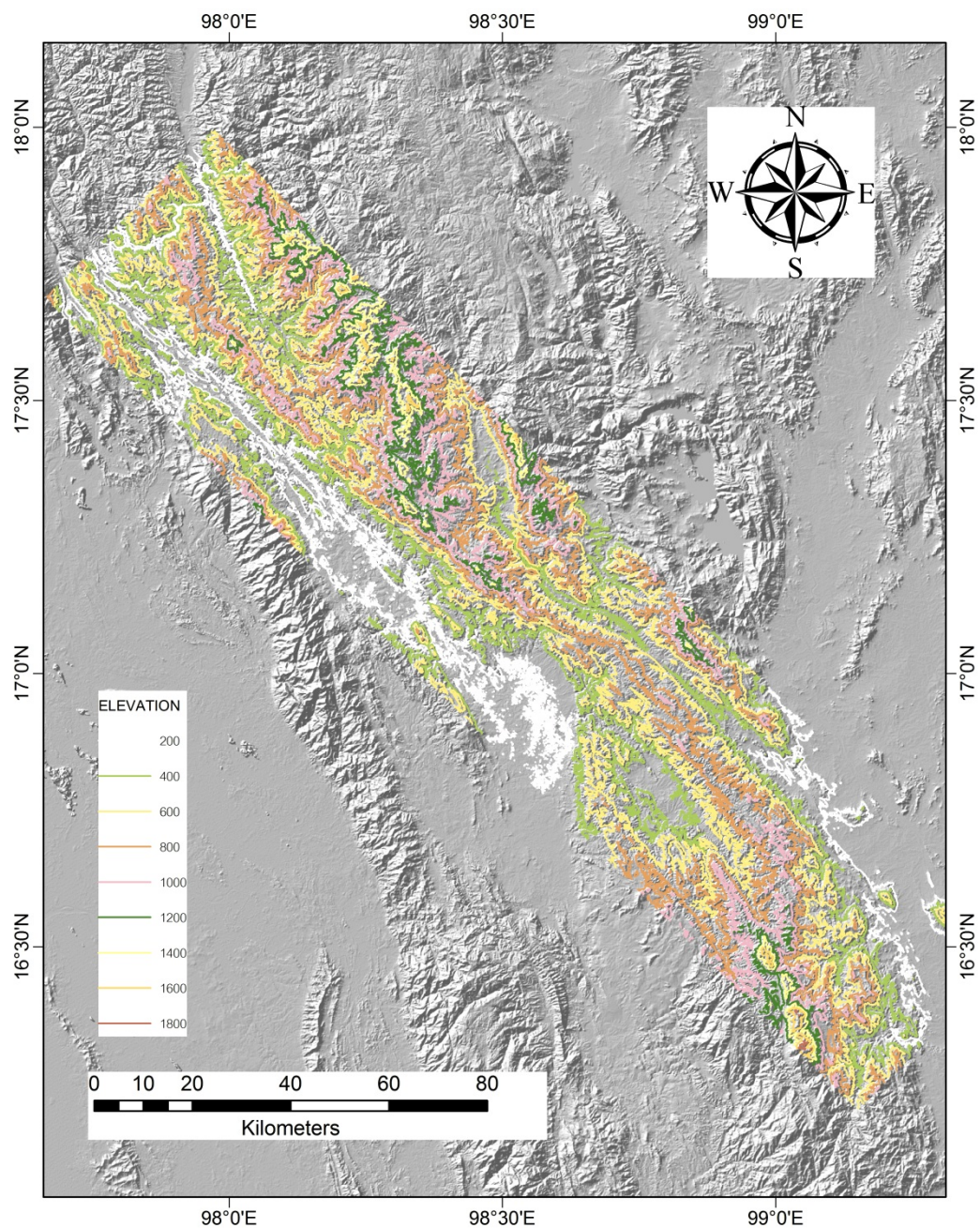
Figure 3-3 Contour lines map of the study area.

3.2.4 Stream lines

Stream networks geometry can provide clues to understanding geologic processes and geomorphic history of and area. The stream lines are generated from digital elevation data. This study area are consists of 21,257 stream lines (Figure 3-4).
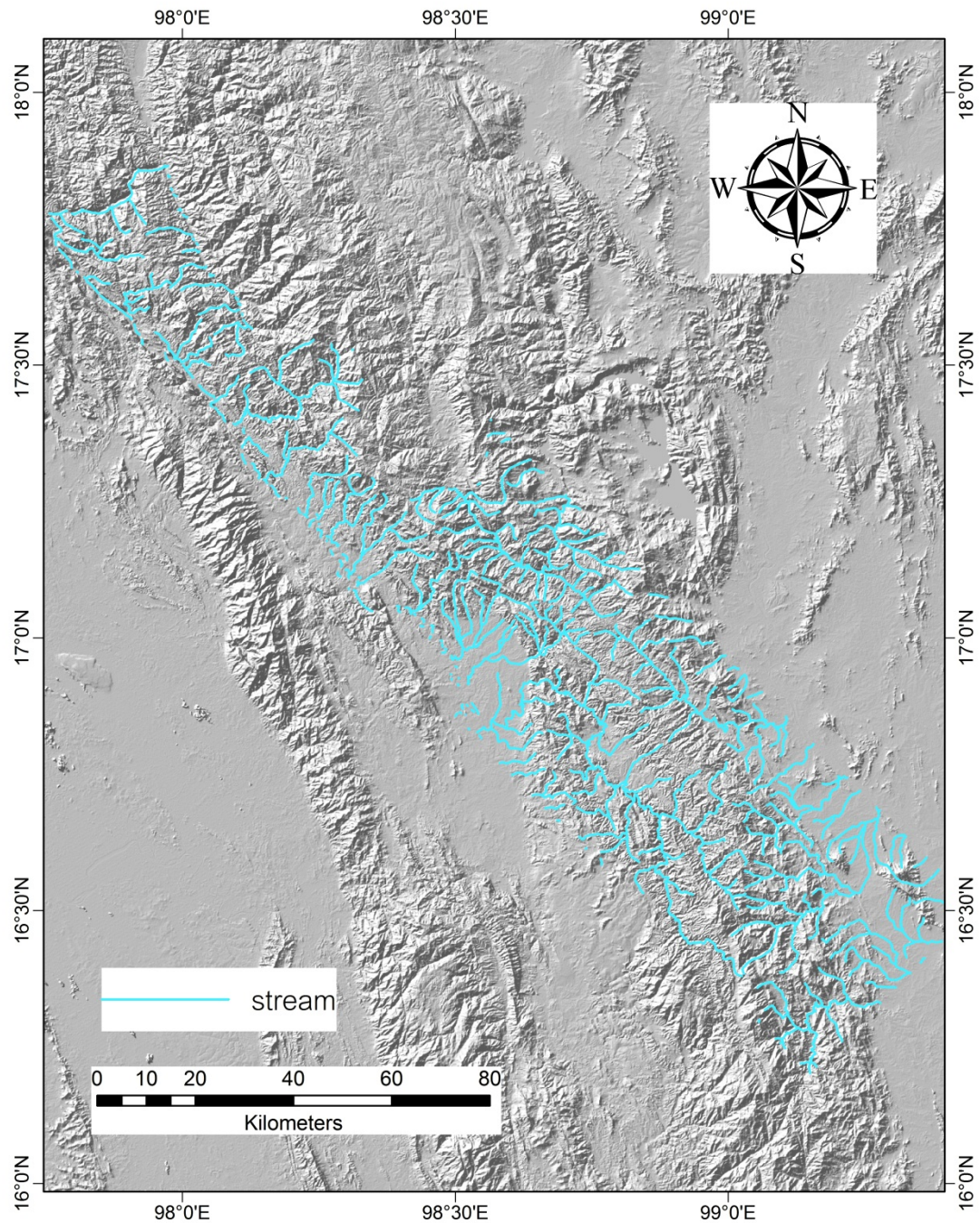
Figure 3-4 Stream lines map of the study area.

3.2.5 Geologic data

A geologic map shows the distribution of geologic features, including different types of rocks and faults. The geology is represented by colors, lines, and special symbols unique to geologic maps (Figure 3-5).
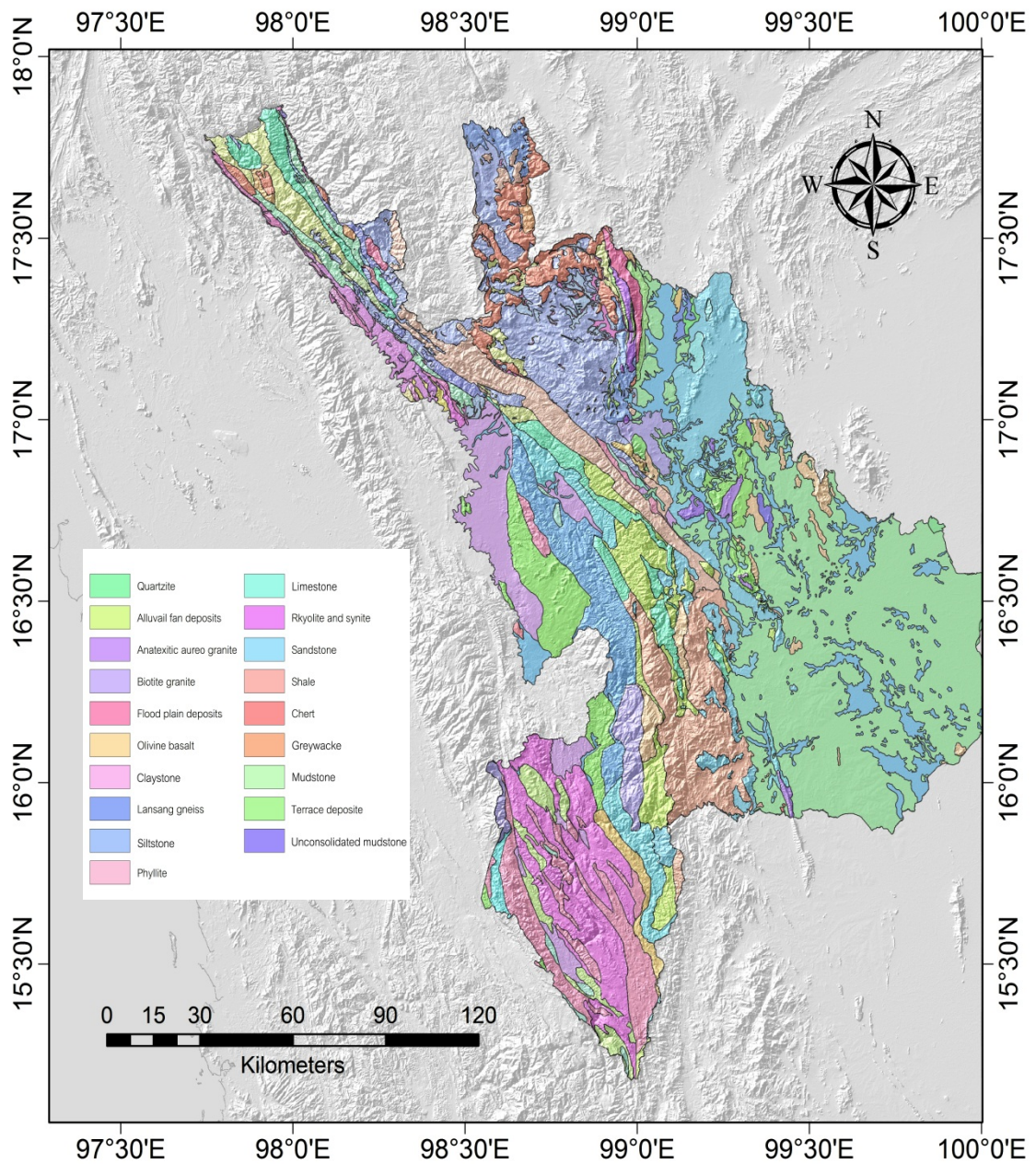
Figure 3-5 Geologic map of the study area (Department of Mineral Resource, 2006)

3.3 Lineaments interpretation

Lineaments are mention to linear feature appear on the earth's surface. This feature takes at least few kilometers, which can be described on maps or on aerial or satellite images (O'Leary et al., 1978). On the surface, there are many weathering and erosional areas include morphologic and geologic features which are separated by lineaments (O'Leary and Simpson, 1977). Generally, lineaments have been found with straight or curve streams and valleys, topographic alignment, boundary between area and slope, and both lithologic change or break. These surfaces break lines more often to found relation with tectonic activities (Strandberg, 1967). By geomorphological, lineaments are also referring to significant lines of landform which show the hidden structure of the rock basement (Hobbs, 1972). Fault or fault zone, associated with structures build up the surface expression which is real lineaments from tectonic activity (Park et al., 1994). The identification of individual lineaments based on continuity, character, and orientation. There are many geomorphological features related to lineament termination i.e. restraining bends, branch and cross-cutting structures, and change in sense of movement. Satellite images and remote sensing data, which provided data in regional scale that, important in lineament analysis of morphotectonic and structural investigation (Charusiri et al., 1996). Identification of lineaments was achieved by visual image interpretation; traceable lines are layout on digital map info by using remote sensing (DEM and Landsat-7 ETM+) and GIS program (Kitti, 2007).

A systematic study of visual image interpretation usually concerns several basic characteristics of features shown on a satellite image. The elements of visual image interpretation are tone, color, size, shape, texture, pattern, site, height and association (Table 3-2). These are regularly order used when interpreting a satellite images as shown in figure 3-6 (Jensen and Kiefer, 2007). This study used satellite images Landsat 7 ETM+ in the years 2002, 2004, and 2006 representing the geological land forms and morphological features.

Table 3-2 Elements of image interpretation (Jensen and Kiefer, 2007).

No.	Interpretation elements	General characteristics
1	tone/ color	Relative brightness of black and white image and hue for colored pictures
2	size	Relative dimension of different objects
3	shape	Form also height of an object (in 3D)
4	texture	Relates to the frequency of tonal change and is expressed as coarse, fine, smooth or rough, even or uneven, etc
5	pattern	Spatial arrangement of objects and implies characteristic repetition of certain forms or relationship. It can be described as concentric, radial, check board, etc
6	site	Occurrence of an object to a particular easily identifiable feature
7	height	z-elevation, slop, aspect, volume
8	association	Close relationship/links of different or combination of objects.
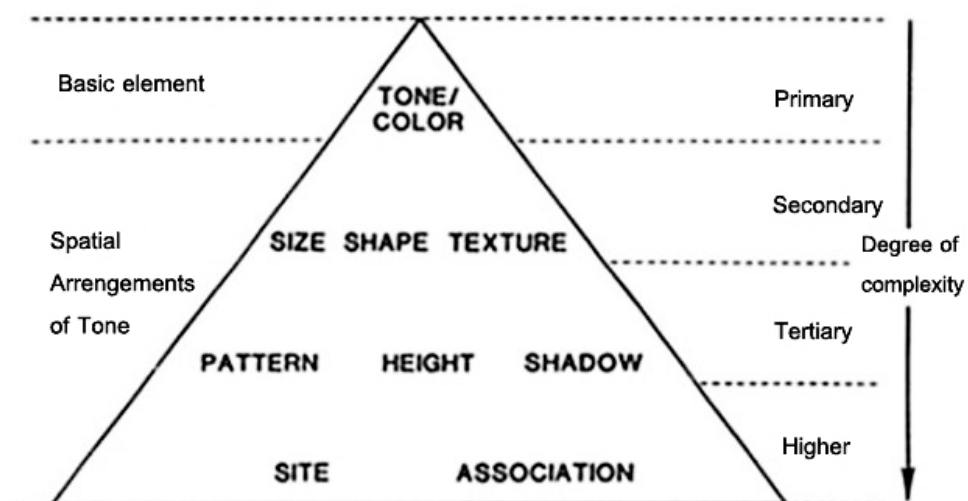
Figure 3-6 Primary ordering of image elements fundamental to the analysis process (Jensen and Kiefer, 2007).

3.4 Geomorphic indices

The quantitative measurement of landform is based on the calculation of geomorphic indices using topographic maps, digital elevation data and field work. The results of several indices can be combined in order to explain tectonic activity and to provide an assessment of a relative degree of tectonic activity in an area (Keller and Pinter, 1996). Geomorphic indices calculated included the mountain front sinuosity (Smf index), the valley floor width to valley height ratio (Vf index), and the stream length gradient index (Sl index). Each of geomorphic indices will be described as below.

3.4.1 Mountain front sinuosity index

The straight or slightly curving nature of most faults or folds allows evaluation of the variation of erosional modification of a structural landform. Rapid uplift along a range-bounding fault generates the linear nature of the front. Erosion dominates landscape evolution after discontinuous of uplift and creates a sinuous mountain front, especially where rock resistance to erosion is weak (Bull, 2007). An index for this equation is simply defined as below (Bull and McFadden, 1977).

$$Smf = \frac{Lmf}{Ls}$$
(Equation 3-1)

Where Smf is mountain front sinuosity index, Ls is the straight line distance along contour line, and Lmf is the true distance along the same contour line. In this study, Smf was calculated from the DEM data generated contours. Contours were derived with help of Global Mapper Software and were calculated in the GIS software after careful comparison with the topographic map. This mountain front sinuosity index is show in figure 3-7
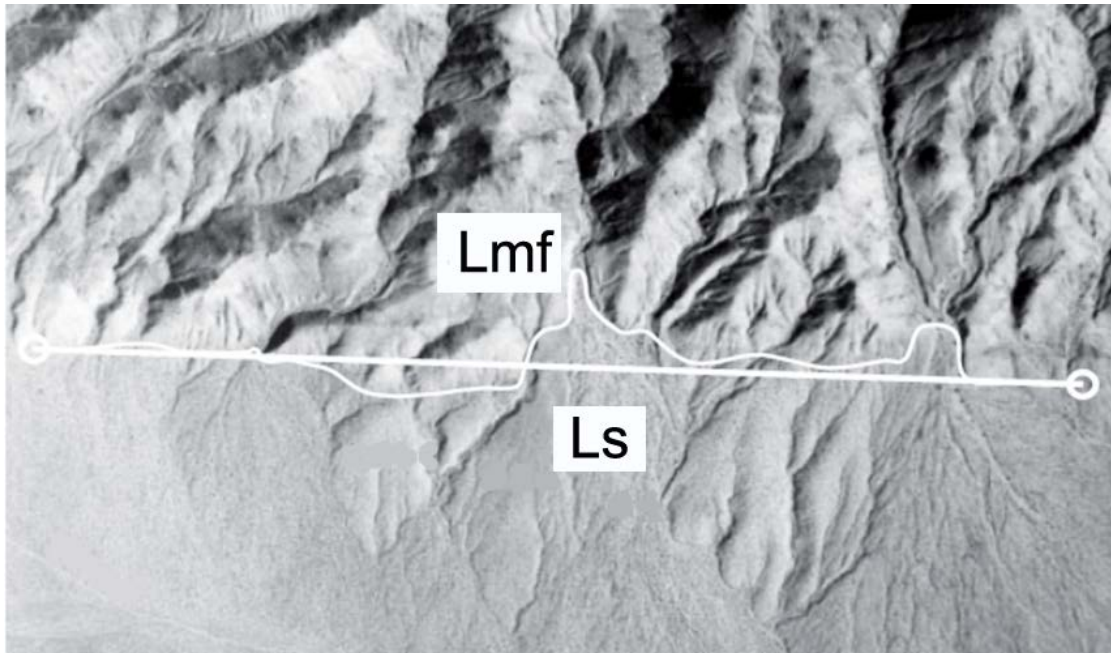
Figure 3-7 The length of the straight white line Ls, is the length of the range bounding fault. The sinuous white line Lmf, is along the mountain front (Bull, 2007).

Values of Smf approach 1.0 on the most tectonically active mountain fronts, whereas Smf increases if the rate of uplift is reduced and erosional processes begin to construct a mountain front that becomes more irregular. Smf values lower than 1.4 indicates tectonically active mountain fronts (Rockwell et al., 1984, Keller, 1986). Smf values between 1.4 to 3.0 indicate slightly active mountain fronts while higher Smf values more than 3.0 are commonly associated with inactive fronts in which the initial range–front fault may be more than 1 Km away from the present erosional front (Bull and McFadden, 1977).

3.4.2 Valley floor width to valley height ratio

This index helps in identifying the areas of tectonic inactive and areas that have been recently uplifted (Rhea, 1993). Relation of the floor width of a valley to the height provides an index suggesting whether stream is actively down cutting or primarily eroding laterally into the adjacent hill slopes. This index is defined by Bull and Mc Fadden (1977) as

$$Vf = \frac{2Vwf}{(Eld-Esc)+(Erd-Esc)}$$
(Equation 3-2)

Where, Vf is the valley floor width to valley height ratios, Vwf is the width of valley floor, Eld and Erd are elevations of the left and right valley divides (looking downstream), and Esc is the elevation of the valley floor. High values of Vf are commonly related to low tectonic activities on the other hand low values are associate with active areas of abruptly uplift and valley incision. This valley floor width to valley height ratios is show in figure 3-8
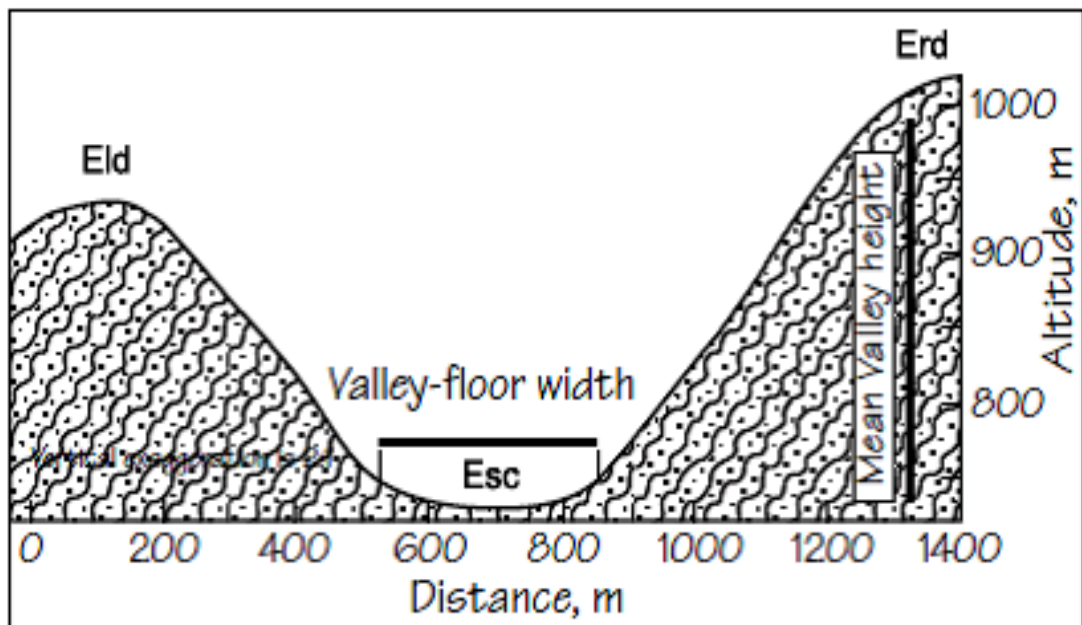
Figure 3-8 Measurement of Valley floor width to height ratio along the triangular facet (Bull, 2007).

3.4.3 Stream length-gradient index

According to the stream networks that are in balance with uplift, erosion and deposition to be steady concave longitudinal profiles with a downstream reducing slope. Changes from this stream profile can result from many factors such as rock resistance, and tectonic activities (Peters and Balen, 2007). Stream power variation which is equivalent to the gradient shifts of the river. An increase in stream power might be the results of an increase in gradient and inclining of the slope. In order to present gradient changes the stream length-gradient index (SL) was developed by Hack (1973).The SL index is defined the channel slope at a point and the channel length to the upstream as equation below

$$SL = \left(\frac{\Delta H}{\Delta L}\right) \times L \qquad \text{(Equation 3-3)}$$

Where, ΔH is the difference elevation between the ends of segment, ΔL is the length of segment, L is the total length from upstream to the point of interest. This index is responsive to the channel incline and relates with the stream energy, which is detect areas of anomaly uplift in a landform. This stream length-gradient index is show in figure 3-9.
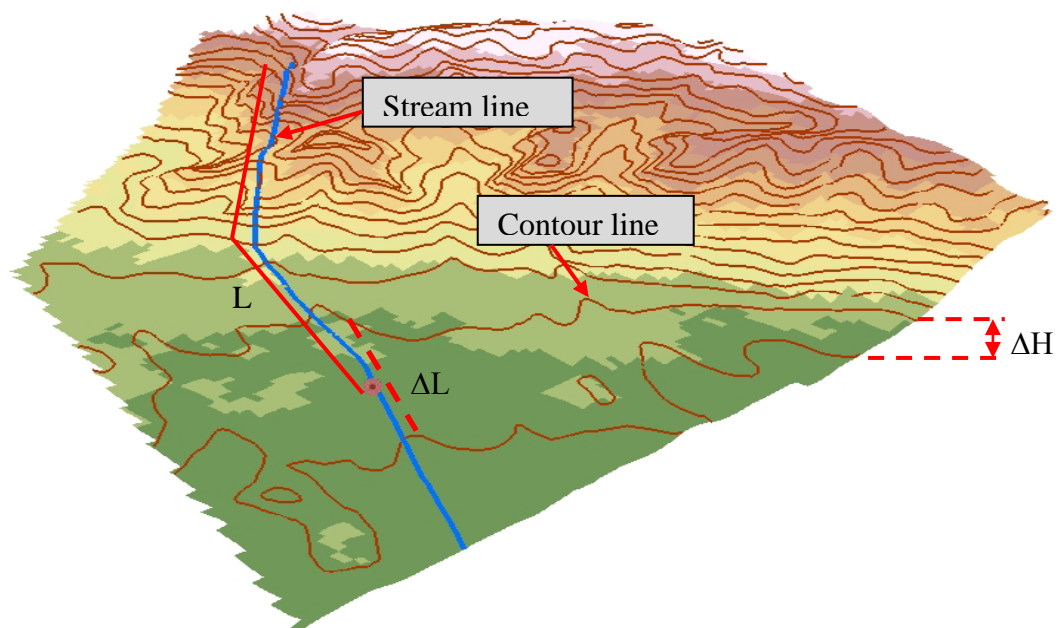
Figure 3-9 Measurement of SL indexes along the stream line (Hack, 1973).
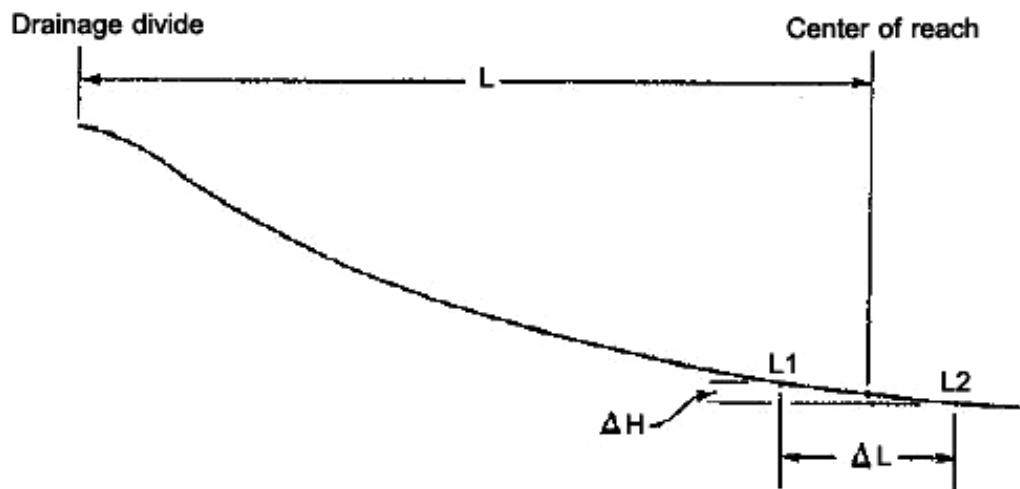
Figure 3-10 Measurement of stream length-gradient Indexes longitudinal section of
the stream line (Hack,1973).

3.5 Field investigation

The field investigation was related from the result of geomorphic indices. First of all, review the general geology of each section in these study areas. Then, investigated the field evidence of the morphotectonic features such as, offset streams, triangular facets, shutter ridges, and fault scarps or structural land form along the fault segment. Lastly, description field survey in each area, including filed investigation data and results from morphotectic analysis.

CHAPTER IV

ANALYSIS AND RESULTS

The satellite images, DEM, and Geomorphic indices were used in this research to analyze tectonic geomorphology of the Mae Ping fault zone. The final results show lineaments pattern, mountain front sinuosity, valley floor width to height ratio, stream length gradient index, stream longitudinal profile and field investigation in the Mae Ping fault zone.

4.1 Lineament patterns

Lineament patterns in an area are clearly seen on satellite images (Figure 4-1). The study area covers about 10,000 km^2, hence this research area is divided into three section based on difference geomorphology. The Mae Ping fault zone display mountain topography in most of area and lineaments were identified by fault pattern and their continuity. The first one is extended from the south of Amphoe Sop Moei, Changwat Mae Hong Son to the east of Amphoe Tha Song Yang, Changwat Tak (N17°48'47"– 17°12'40" and E97°42'32''– 98°18'29'') and shows dominant lineaments azimuth direction of NW-SE. The second expands from the south of Amphoe Tha Song Yang to the east of Amphoe Mae Ramat (N17°18'05"– 16°50'25" and E97°42'28''– 98°57'30'') and shows lineaments direction of NW-SE nearly to W-E. This zone exhibits the complicate of lineaments which are releasing bend and short cross-cut by geomorphological change. The third is the eastern part of the study area reach from Amphoe Muang, Changwat Tak to Amphoe Khlong Lan, Changwat Kamphaeng Phet (N16°58'06"– 16°20'57" and E98°50'09''– 99°20'54''), which shows lineaments direction of NW-SE (Figure 4-2).
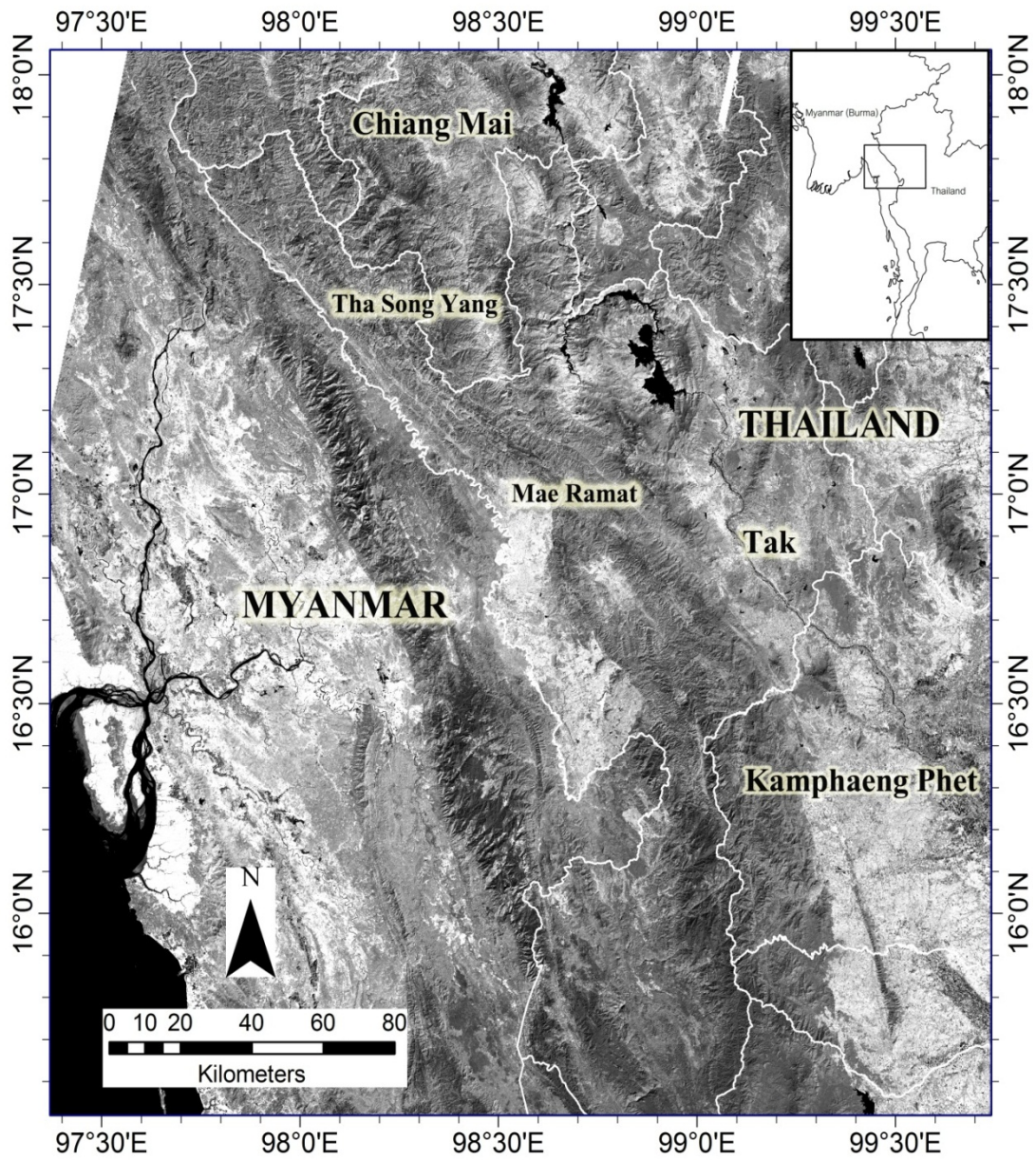
Figure 4-1 Enhanced Landsat 7 ETM+ ((R=7, G=7, B=7)) taken on March 4, 2006

showing physiographic features of the study area (Interpreted result shows in figure 4-2)
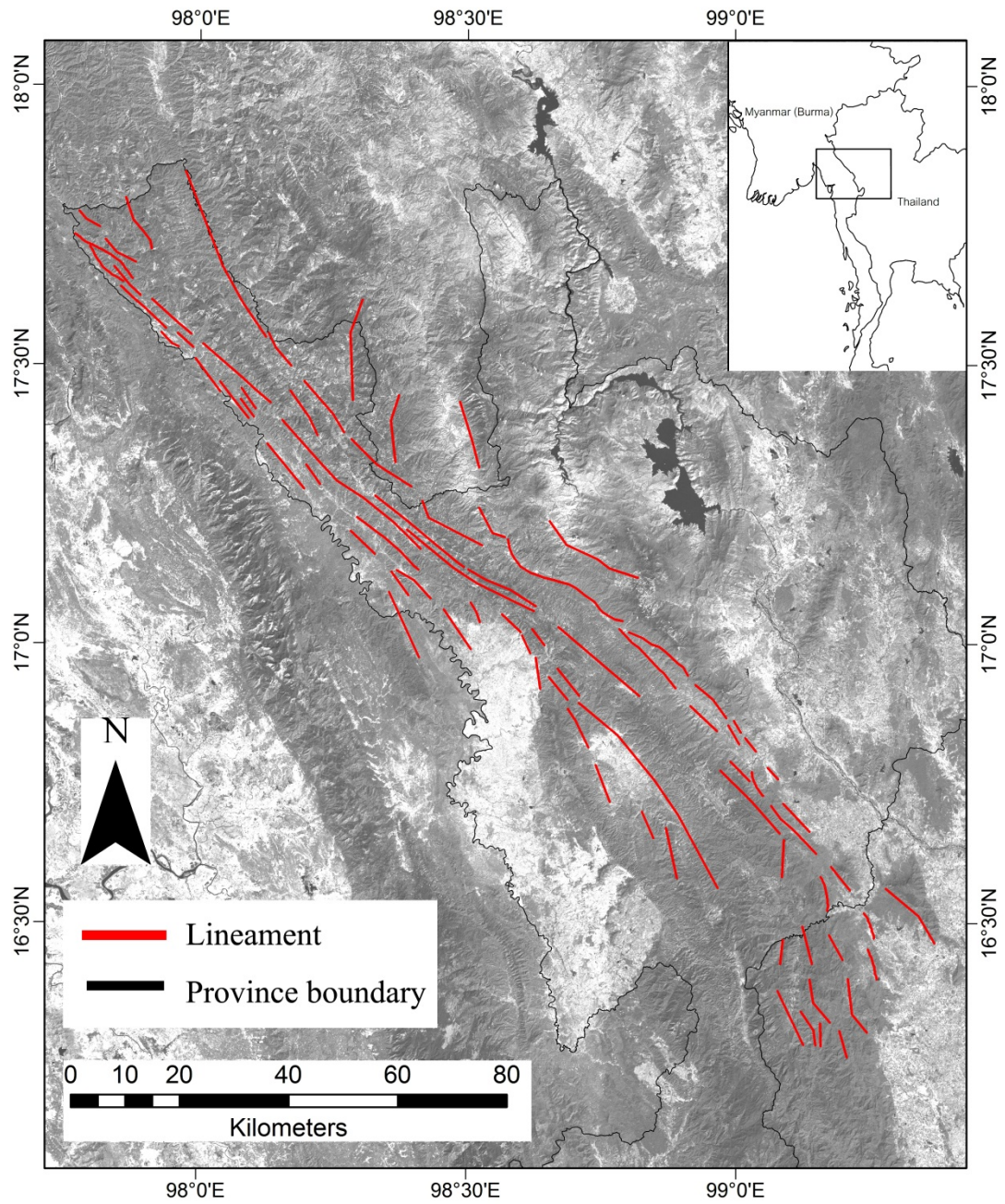
Figure 4-2 Lineament map of the study area showing lineaments pattern interpreted

using enhanced Landsat 7 ETM+ (R=7, G=7, B=7) images (figure 4-1)
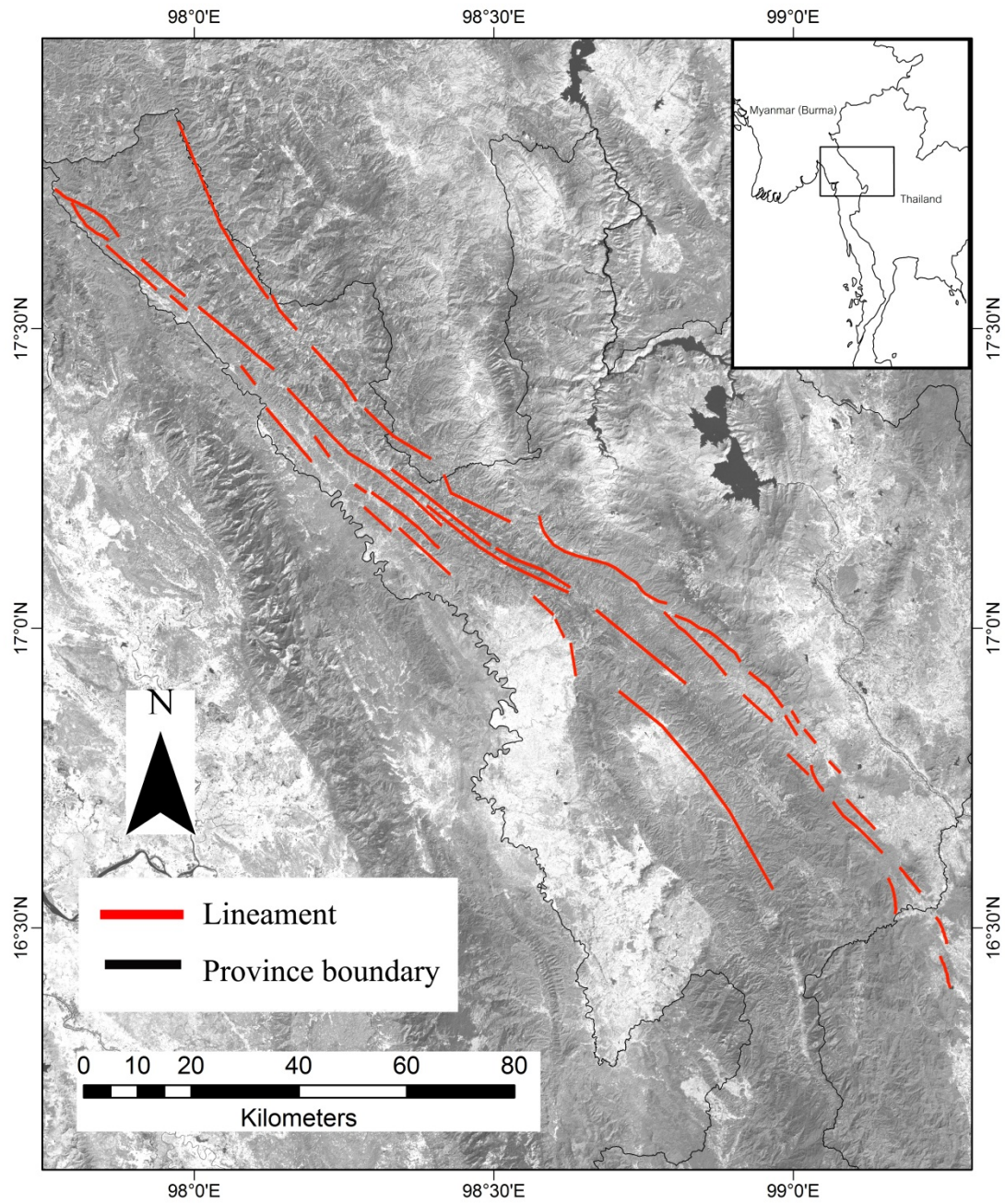
Figure 4-3 Lineament map of the study area which are selected by geomorphological features and geomorphic indices.

4.2 Geomorphic indices

4.2.1 Mountain front sinuosity index

The calculated data reveal that Smf represents low values (1.04 to 1.77) in the study areas where the Mae Ping fault zone has most horizontal and/or vertical movement (Figure 4-3). This mountain front sinuosity map shows low values in the zone 1 of the study area (1.07 < Smf < 1.73) are associated with high tectonics activities (Figure 4-4). In zone 2 Smf increase show maximum values (Smf = 1.77) that imply lower tectonic activities than zone 1 (Figure 4-5). Low Smf values in zone 3 (1.04 < Smf < 1.66) indicate the highest tectonic activities in this area (Figure 4-6). Different uplift rates (for a given climate and lithology) have characteristic ranges of sinuosity. Sinuosity of high tectonic activities, mountain fronts generally range from 1.0 to 1.3, moderately activities fronts range from 1.3 to 3, and low activities fronts from 3 to more than 10. Developments in mountain front sinuosity typically take long time spans, because geomorphic processes change mountain slopes slowly.

In relationship between different lithology and mountain front sinuosity, the result shows that clastic sedimentary rocks display higher values than metamorphic rocks in same lineament segment; because of metamorphic rock has more resistance than clastic sedimentary rock. In some part of low tectonic activities zone, metamorphic rock show low value of mountain front sinuosity index. Moreover, carbonate sedimentary rock display very low values because of it weathering characteristic i.e. Karst topography. For this reason, only one index cannot indicate tectonic activities in an area.
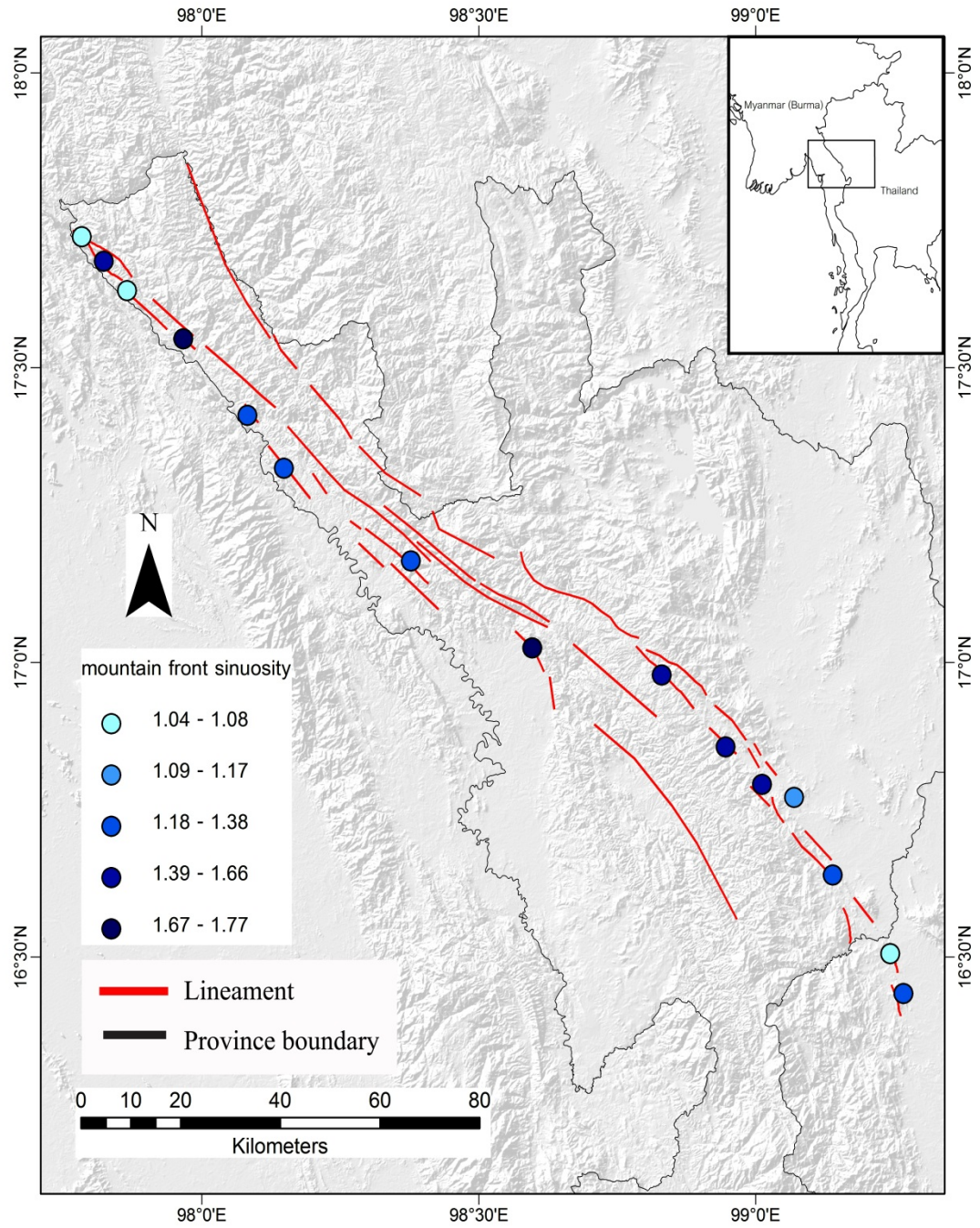
Figure 4-4 Mountain front sinuosity index map of the study area
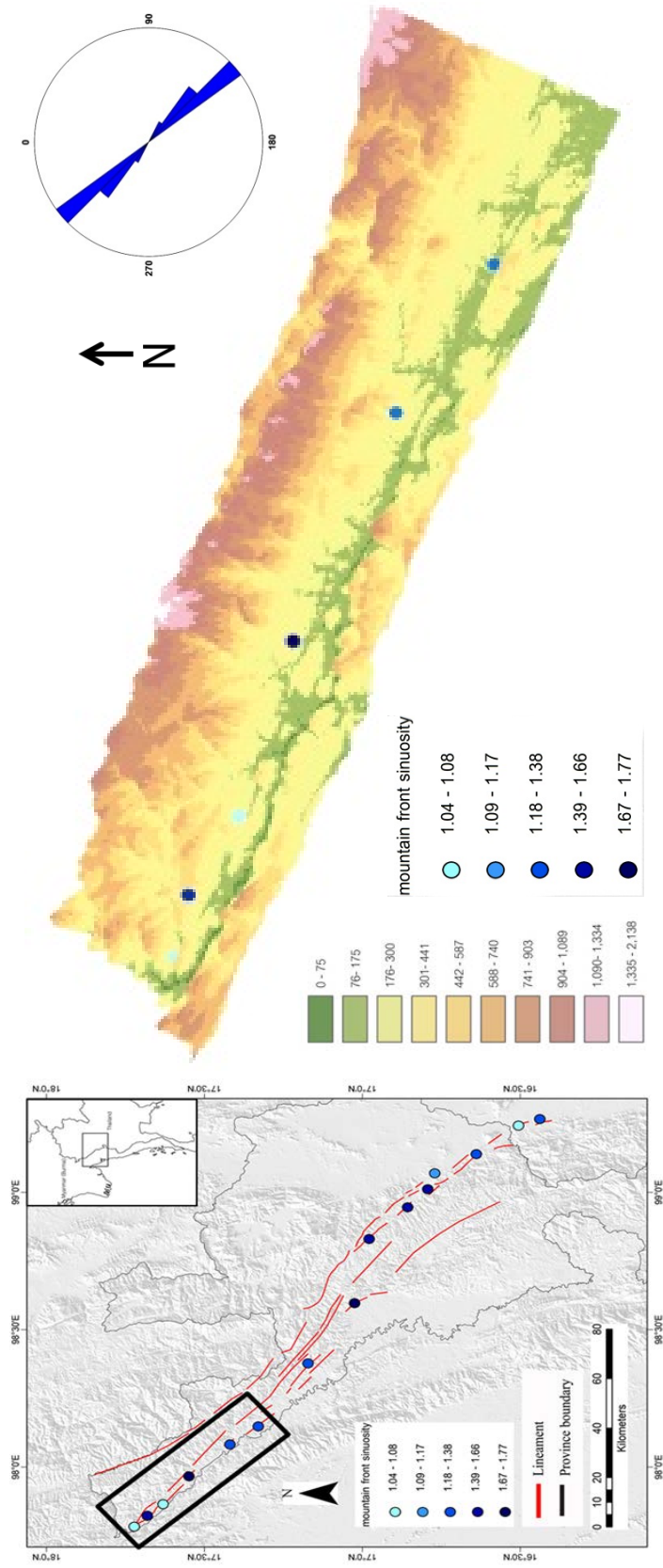
Figure 4-5 Mountain front sinuosity index 3D map in zone 1 with lineament orientation plot in rose diagram
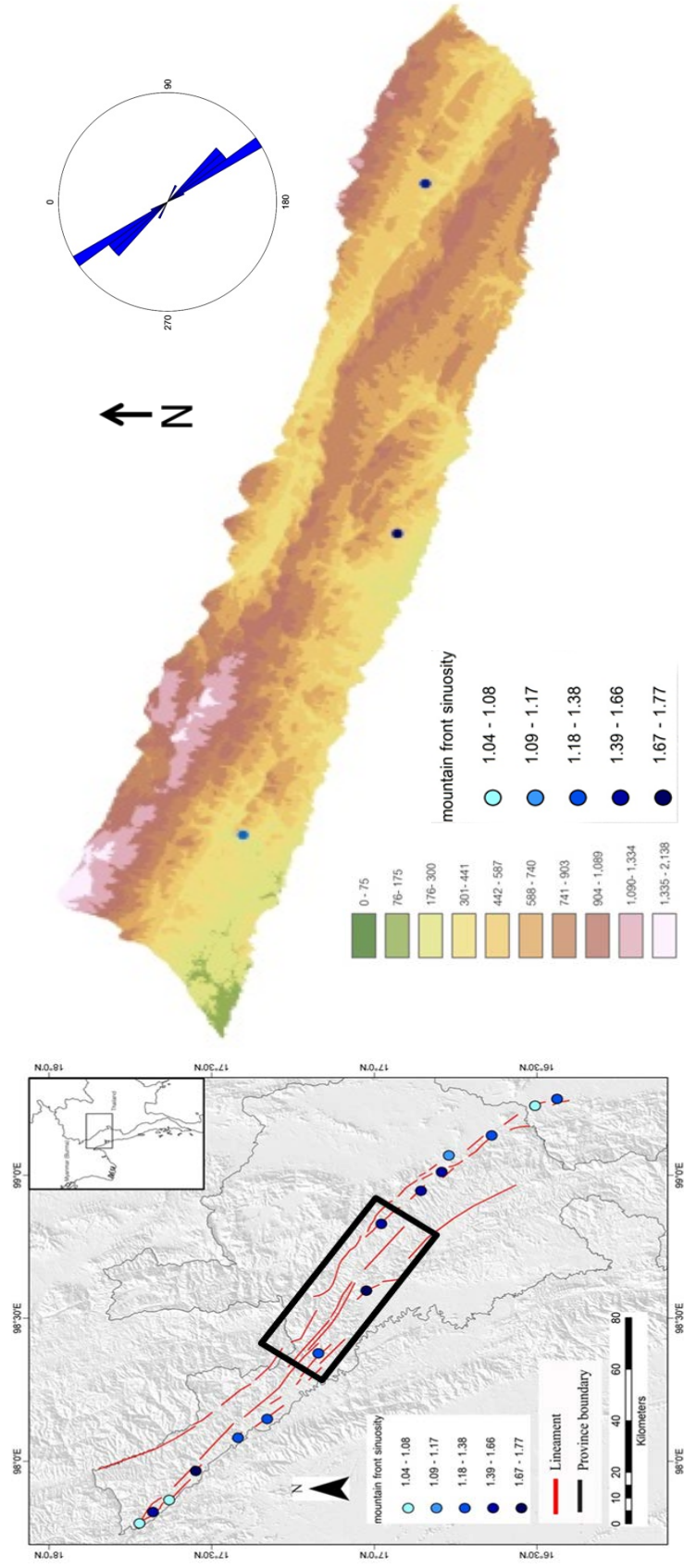
Figure 4-6 Mountain front sinuosity index 3D map in zone 2 with lineament orientation plot in rose diagram
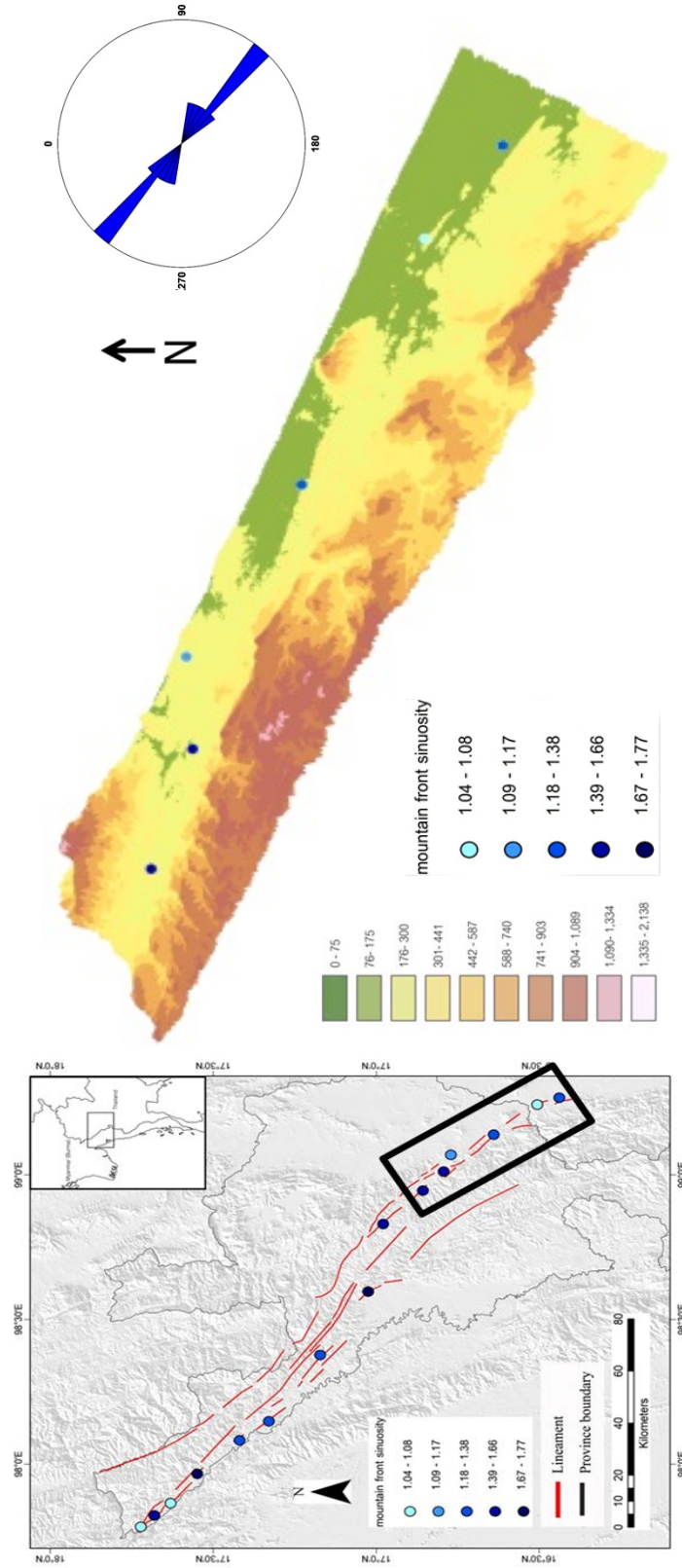
Figure 4-7 Mountain front sinuosity index 3D map in zone 3 with lineament orientation plot in rose diagram

4.2.2 Valley floor width to height ratio

All variable values were measured along the different valley profile. The parameters were calculated from the DEM and contour line data using ArcGIS 9.3 and Google earth software. In this case, we selected valley profiles at a distance of 200 m – 1 km northward from active mountain front (Figure 4-7). In the northern part of the study area valley profile shows low values (Vf = 2.66). On the other hand, another valley profile in zone 1 shows values from 0.30 - 2.66 (Figure 4-8). Vf values range from 0.37 to 1.33 in zone 2. In the middle part show high values indicated that tectonics activities lower than northern part. (Figure 4-9). Valley profiles in zone 3 give Vf values from 0.31 to 2.23. In the southern part shows low values which imply to higher tectonic activities than the other parts (Figure 4-10). Apparently, variable Vf values in the northern part of the study area indicated more variety of rock, where the lineament cut through.

Determined in similar rock types at the mountain front in the same basin, Vf values are more likely to be typical of the relative degree of tectonic activities. Rock resistance to erosion may not change, even annual unit stream erosion power increases downstream. Therefore, part of the variation in valley-floor width is a function of drainage-basin size. A limited range of drainage-basin sizes is preferred because stream discharge increases in a nonlinear style in the downstream direction, particularly for streams of humid regions (Wolman and Gerson, 1978). Moderately to slightly tectonic activities valleys have flights of strath terraces that record pauses in stream channel downcutting. Very low tectonic activities valleys may lack strath terraces, but only if they remain at the base level of erosion.
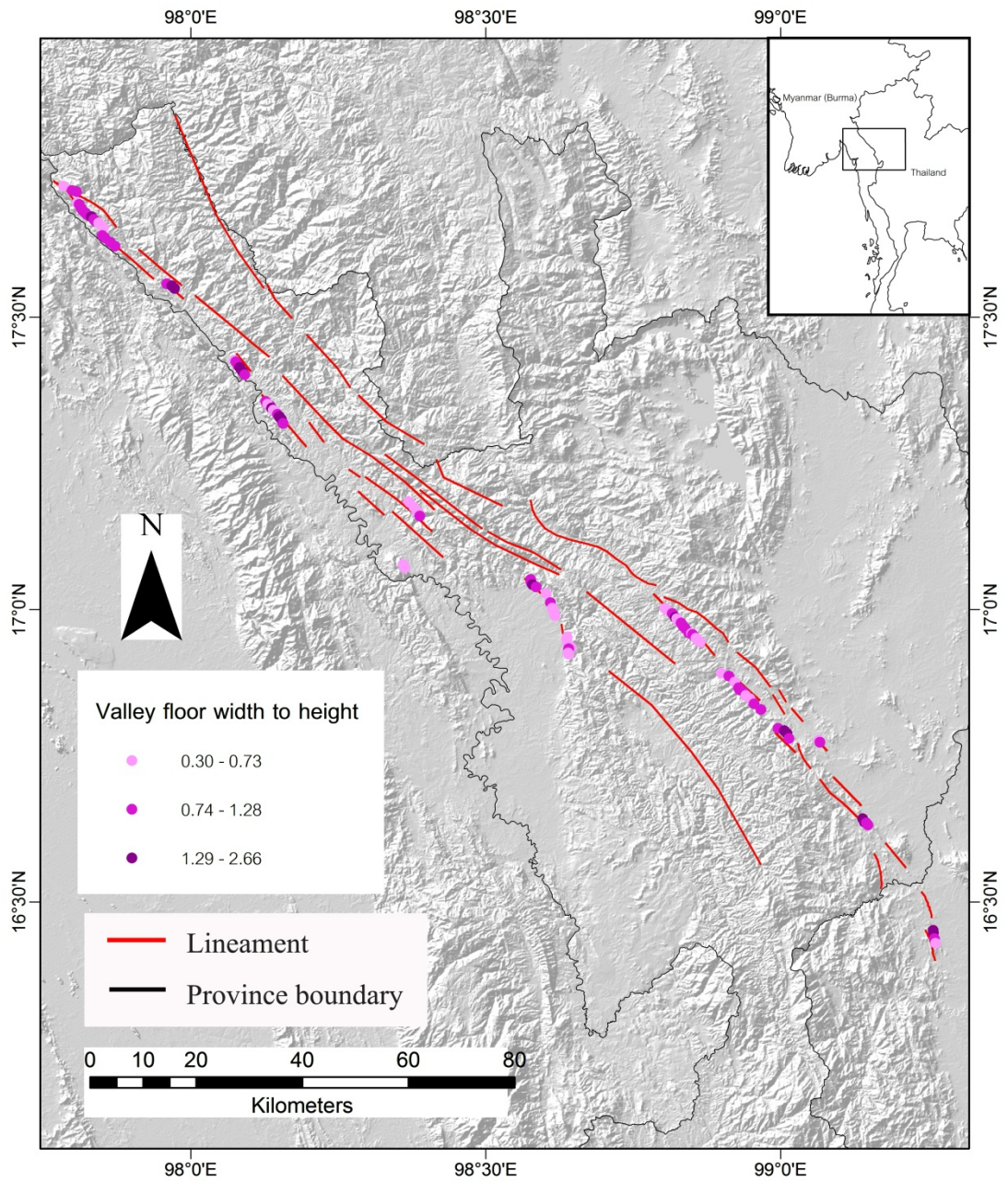
Figure 4-8 Valley floor width to height ratio map of the study area
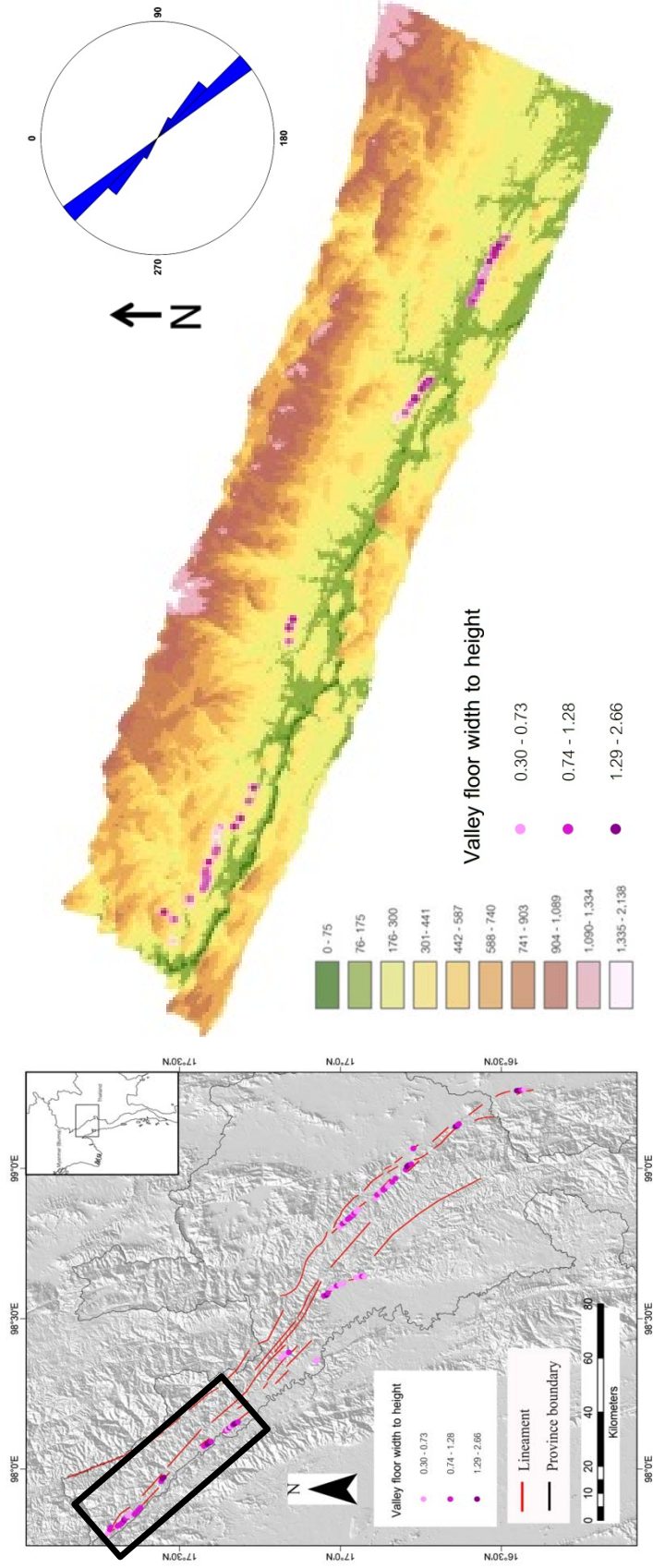
Figure 4-9 Valley floor width to height ratio 3D map in zone 1 with lineament orientation plot in rose diagram
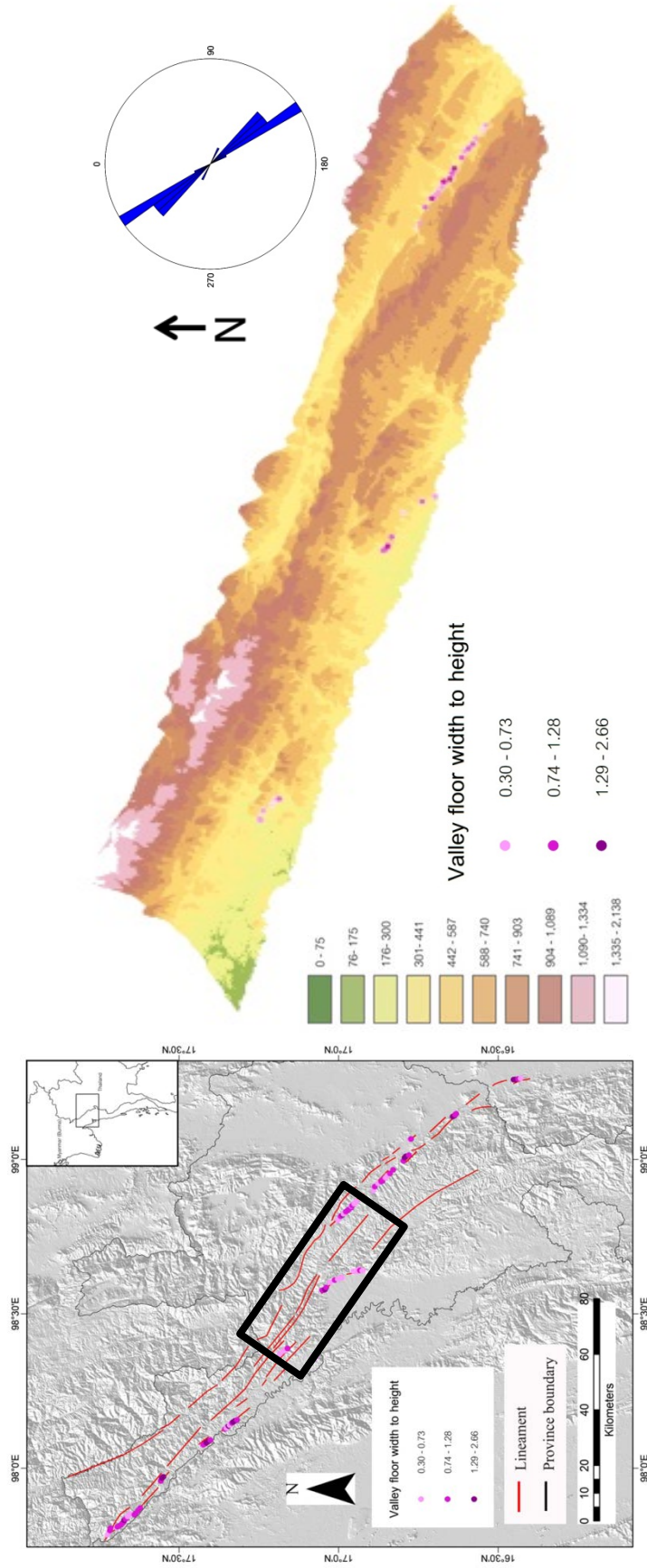
Figure 4-10 Valley floor width to height ratio 3D map in zone 2 with lineament orientation plot in rose diagram
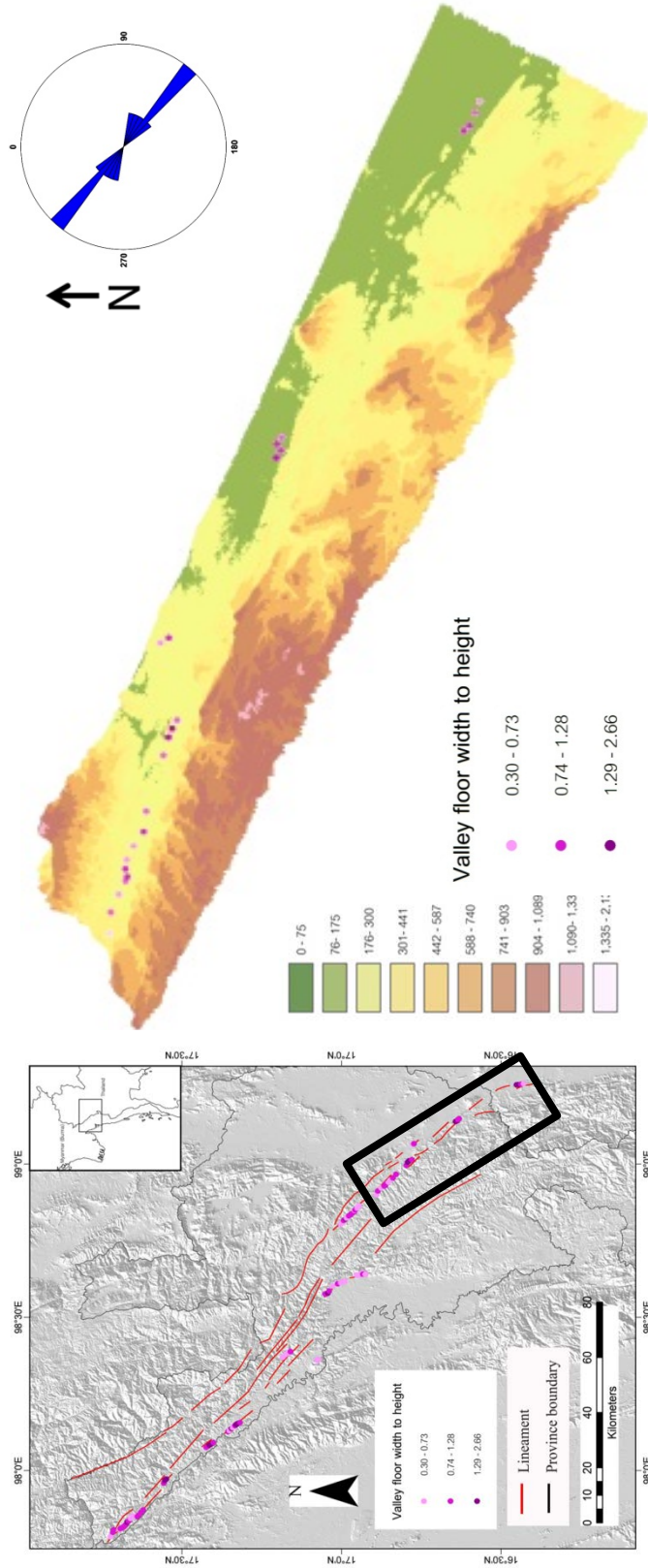
Figure 4-11 Valley floor width to height ratio 3D map in zone 3 with lineament orientation plot in rose diagram

4.2.3 Stream length gradient index

Stream length gradient index have been calculated for five order streams that across the lineaments in the study area. The stream length gradient index values range from 0 to 171630512 (Figure. 4-11). In the stream length gradient index map the values are grouped in 5 classes. Two classes of stream length gradient index values (20137366–45464462 and 45464462–171630512) widely occur within the northern part of the study area (Figure. 4-12). In middle part display values as same as the northern part (Figure. 4-13). Nevertheless, the southern part show stream length gradient values that trend away from these two classes, reaching the lowest values (Figure. 4-14).

In detail, the highest value is located across the lineament, where the stream length gradient index reaches the maximum value of 171630512 in correspondence with sharp fault scarps, which are typical indicator of normal faulting. Anomalous high values are coinciding with the occurrence of a northwest–southeast trending lineaments. The stream length gradient index reaches the lowest value, about 0 at the downstream. To the south of the study area high anomalies can be found with a general NW–SE trend coinciding with the lineaments.

The stream length gradient values are anomaly high in northern and middle part of the study area and for some rivers in the eastern part. Normally, all rivers at the east of study area show low values which is compatible with flat topography. The northern and middle parts of the study area are high tectonic activities correspond with high values of stream length gradient index.
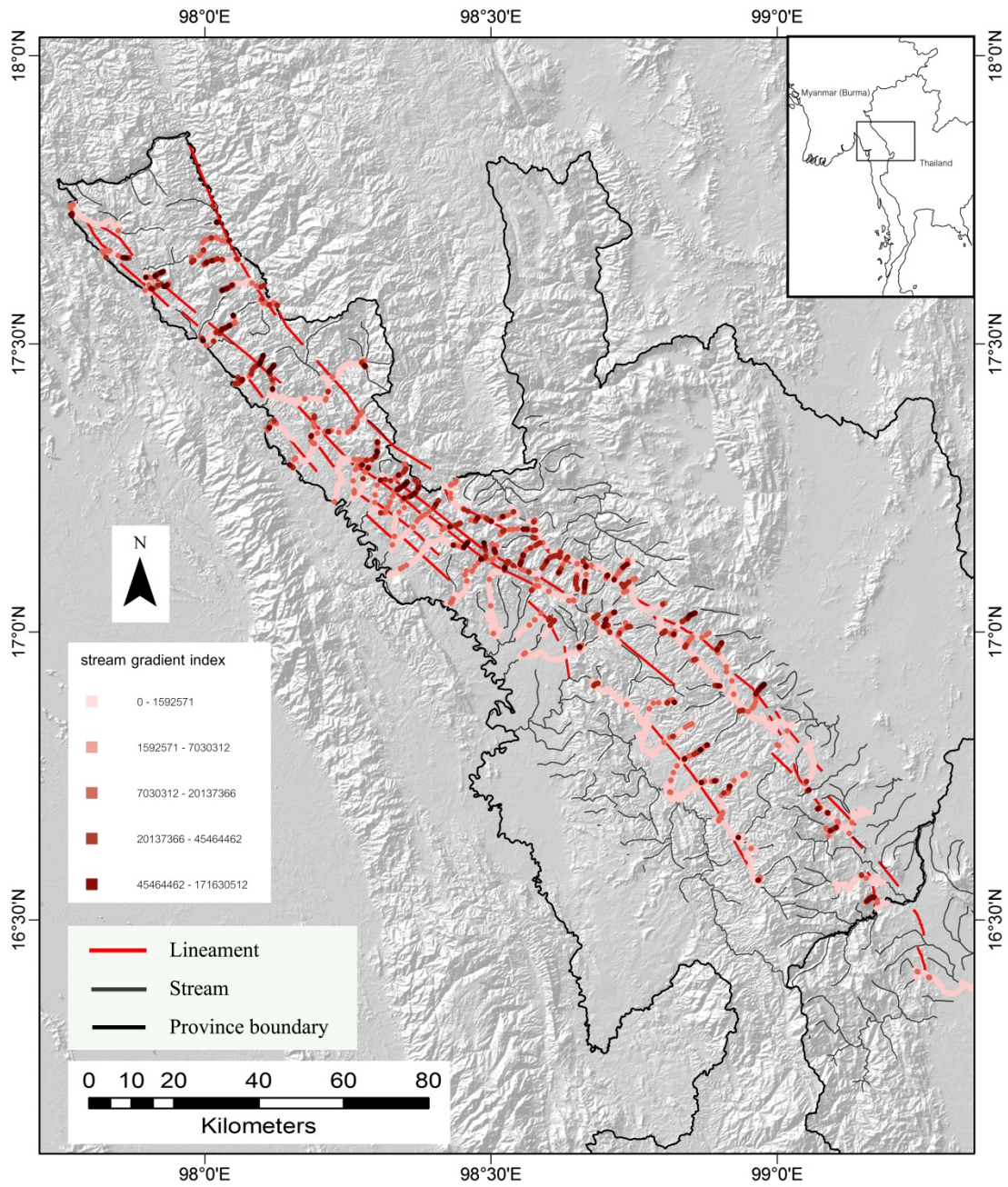
Figure 4-12 Stream length gradient index map of the study area
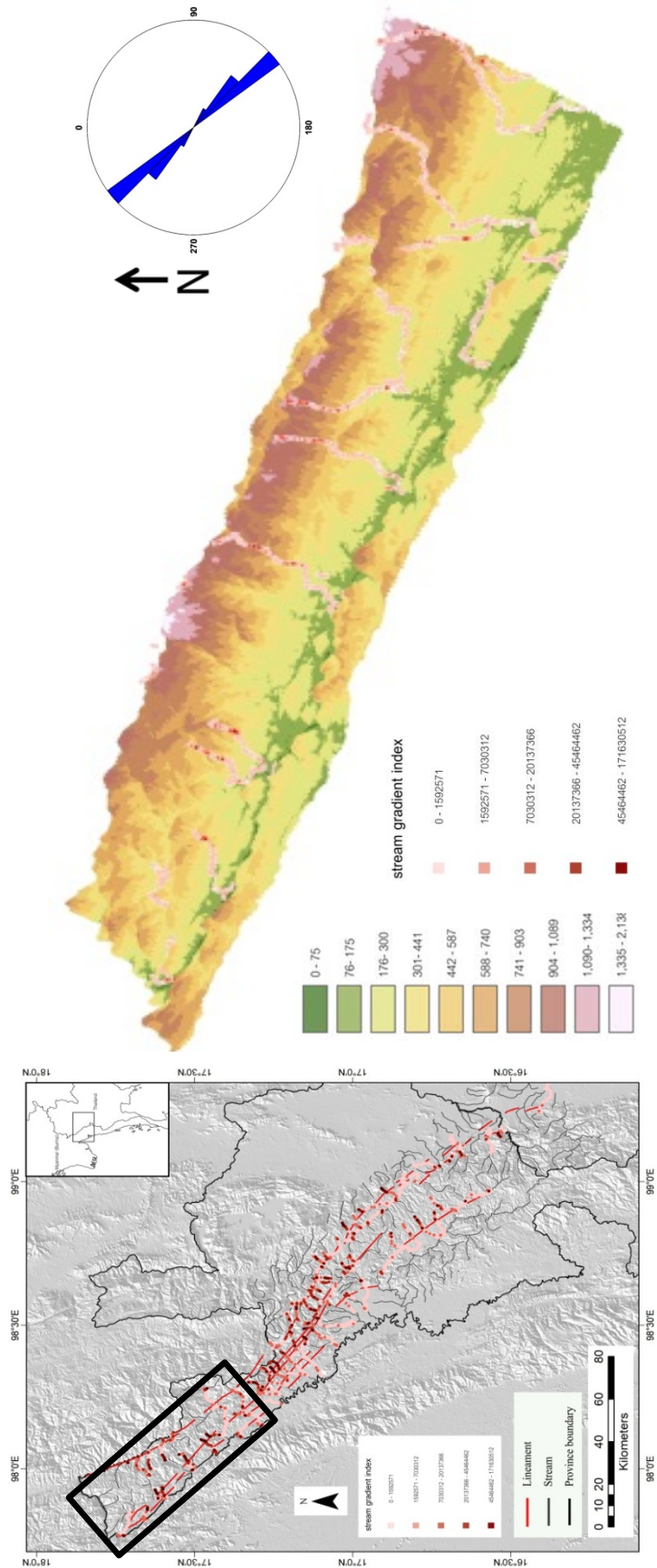
Figure 4-13 Stream length gradient index 3D map in zone 1 with lineament orientation plot in rose diagram
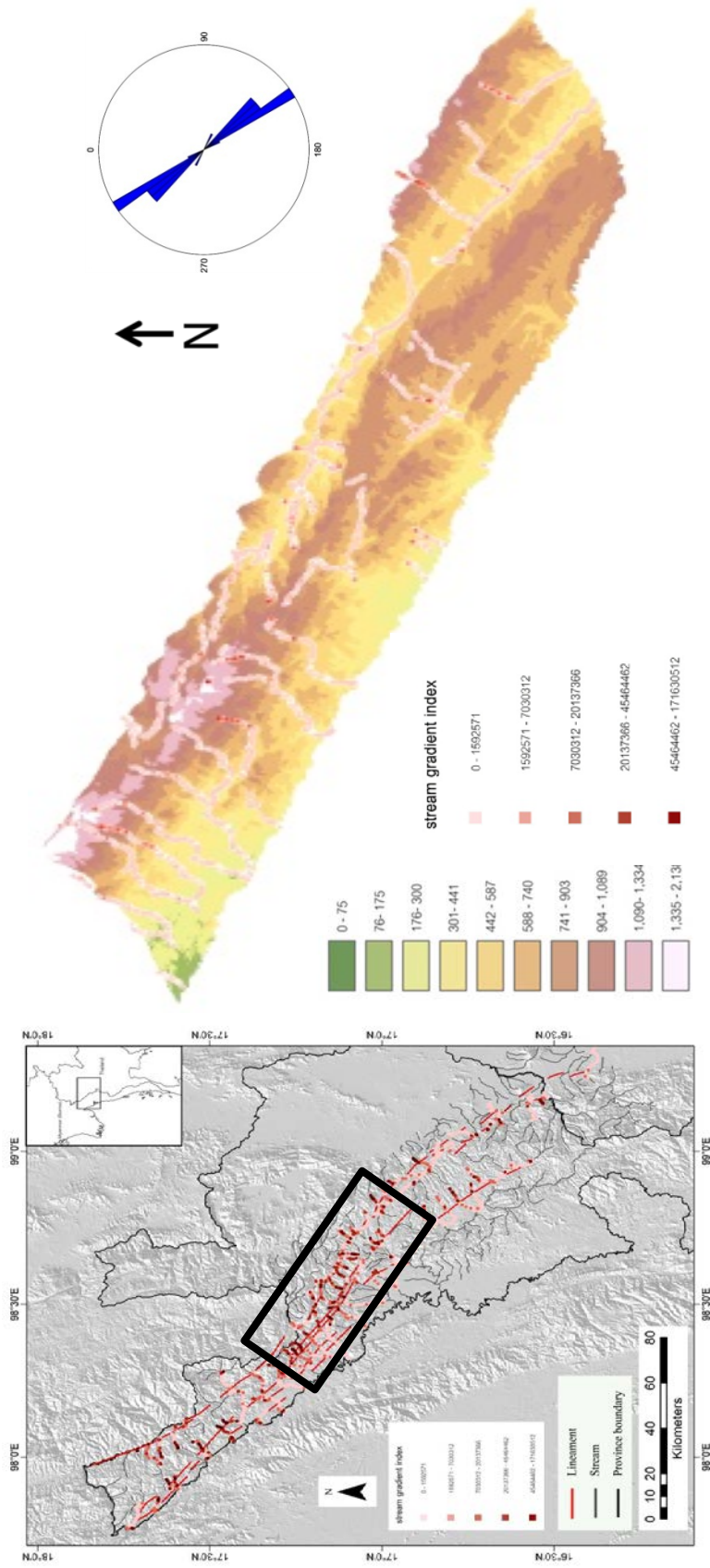
Figure 4-14 Stream length gradient index 3D map in zone 2 with lineament orientation plot in rose diagram
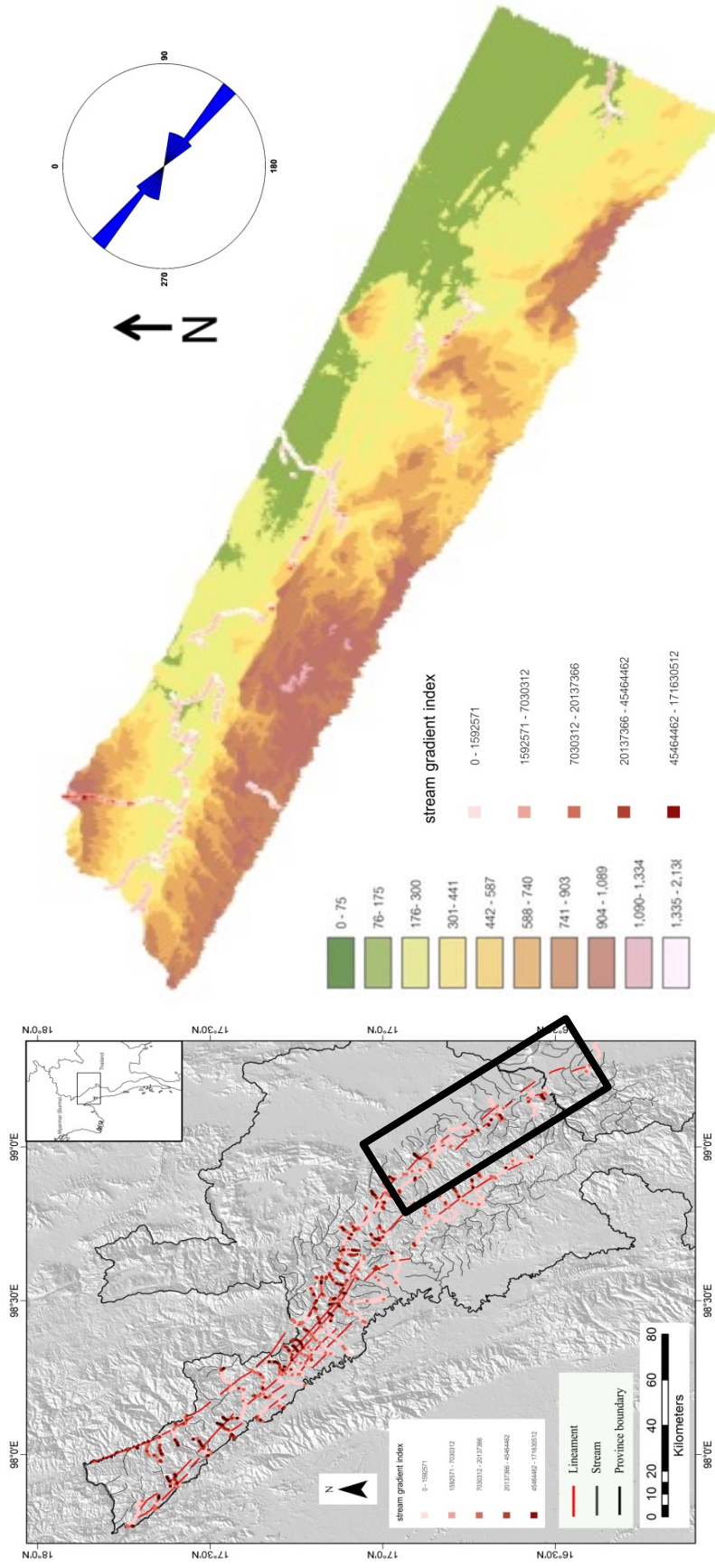
Figure 4-15 Stream length gradient index 3D map in zone 3 with lineament orientation plot in rose diagram

4.3 Stream longitudinal profile

Modification from a concave-up shape of stream longitudinal profiles may indicate a disequilibrium state of channels due to tectonic, climatic or lithology perturbations (Mackin, 1948; Molin and Fubelli, 2005). Normally, the longitudinal profiles of streams are high gradients and straight which are low gradients and form smooth curve in downstream. Stream longitudinal profile could be changed by difference ground substrate and sediment input from turbidities current or variation of waters.

Especially, convex segments can be explored to evaluate tectonic perturbation at different scales, from the whole chain to local structures (Seeber and Gornitz, 1983). The longitudinal profiles of the present thalweg of stream in study area. In case, stream longitudinal profile abruptly change pass through many streams suggest that influence by tectonic process (Biswas and Graseman, 2005). Rejuvenation heads on each stream profile are associated with geomorphic indices to support effect from tectonic activity. In this study show 6 stream longitudinal profiles along the study area (Figure 4-15).

A steep profile, broke off by a knickpoint, about 0.2 km away from the divide, characterizes the head sector of the river. This knickpoint conforms well to the boundary between sedimentary rocks and metamorphic rocks. Another knickpoint occurs conforming well with a lineament at the study area.
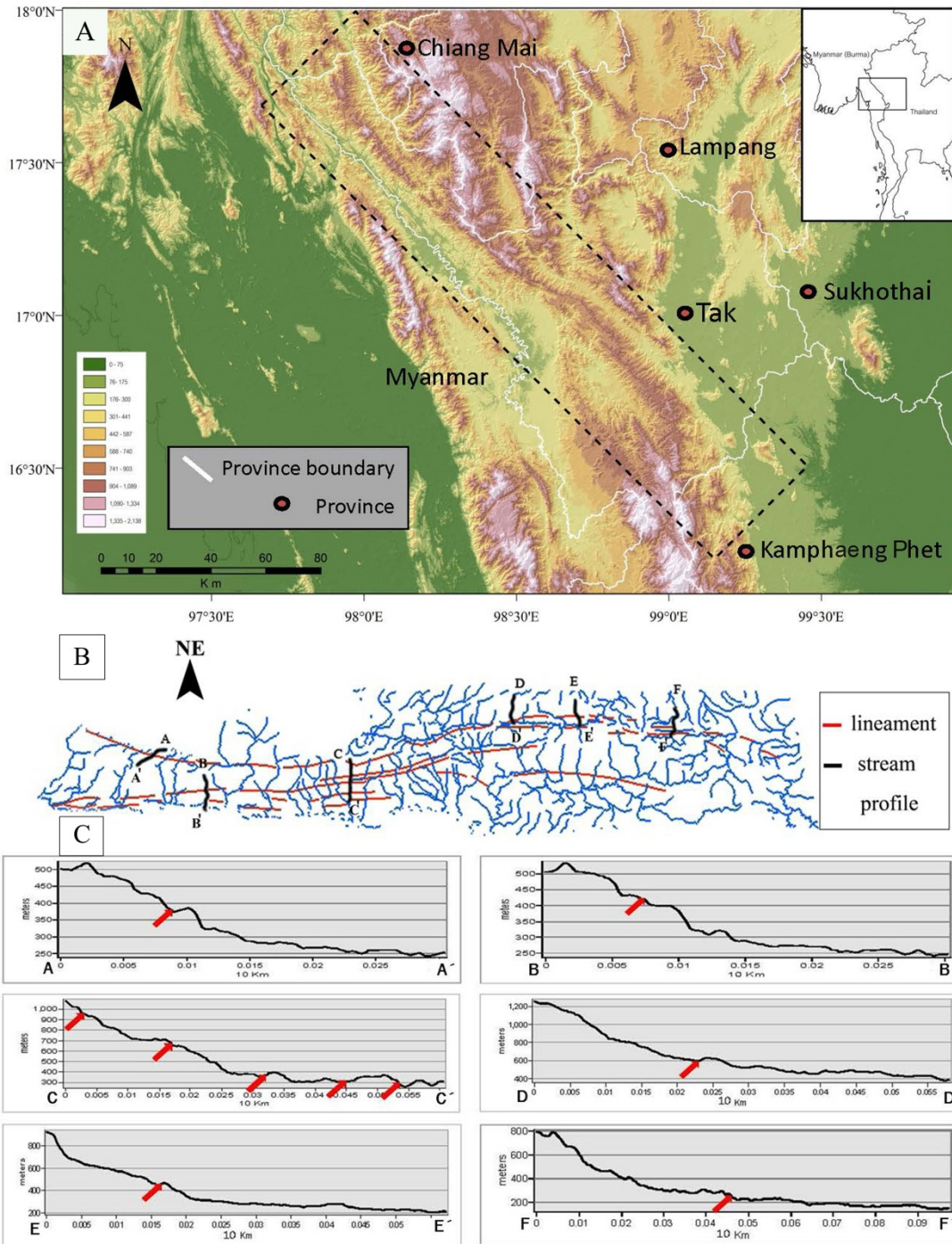
Figure 4-16 Map showing structural features and longitudinal stream profile for few selective rivers. A) Interpreted lineaments in Digital Elevation Model. B) Stream and boundary of the studied area. C) Longitudinal stream profile (positions are marked on B), knickpoints of corresponding lineaments are marked by arrows.

4.4 Field investigation

In order to verify evidences from morphotectonic features as infer from result of remote sensing interpretation, morphotectonic features or landforms as investigated in the field along related lineament segments. The following is the description of that evidence.
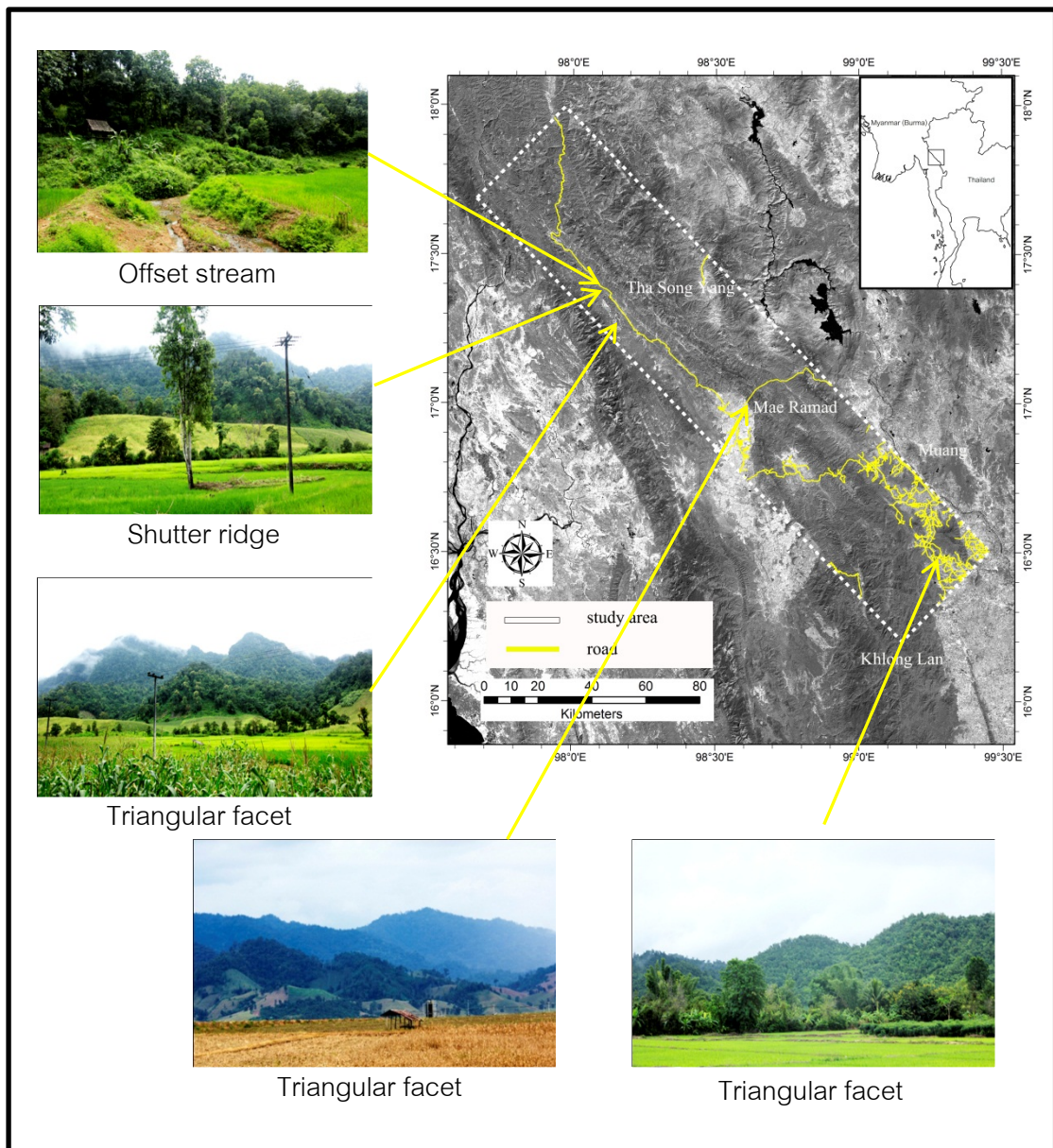
Figure 4-17 Field investigation located in the Mae Ping fault zone

Most of the field investigation was a set of intensive 4 ground survey points to localize different landform and morphology in order to refine visual image interpretation.

4.4.1 Ban Mae Ou Su, Amphoe Tha Song Yang, Changwat Tak

The Ban Mae Ou Su is located near the valley of Huai Mae Ou Su, about 20 kilometers from Amphoe Tha Song Yang. Most of hills cover by dense forest and some agriculture fields. Based on geologic map scale 1:50,000, this area and adjacent area consist of limestone, shale, sandstone, mudstone, and siltstone of Paleozoic, Mesozoic, and Cenozoic succession. The recent Quaternary sediments deposits on Amphoe Tha Song Yang were supplied by Mae Nam Moei which composes of gravel, sand, silt, and clay.

The result from field survey indicated the morphotectonic evidences of offset stream along Huai Chicago which offset about 200 meters. The set of triangular facets as observed along the highway no 105 (Amphoe Tha Song Yang to Ban Mae Ou Su) consist of five facets. About 10 Kilometers of average base width and about 100 meters average height from the base. This facets showing linear valley parallel to the main fault and directly flowing down to Mae Nam Moei. The result of field investigation analysis reveals several features of morphotectonic evidences are recognized such as offset stream, shutter ridge, and set of triangular facets, which are generated by normal and strike-slip faulting.
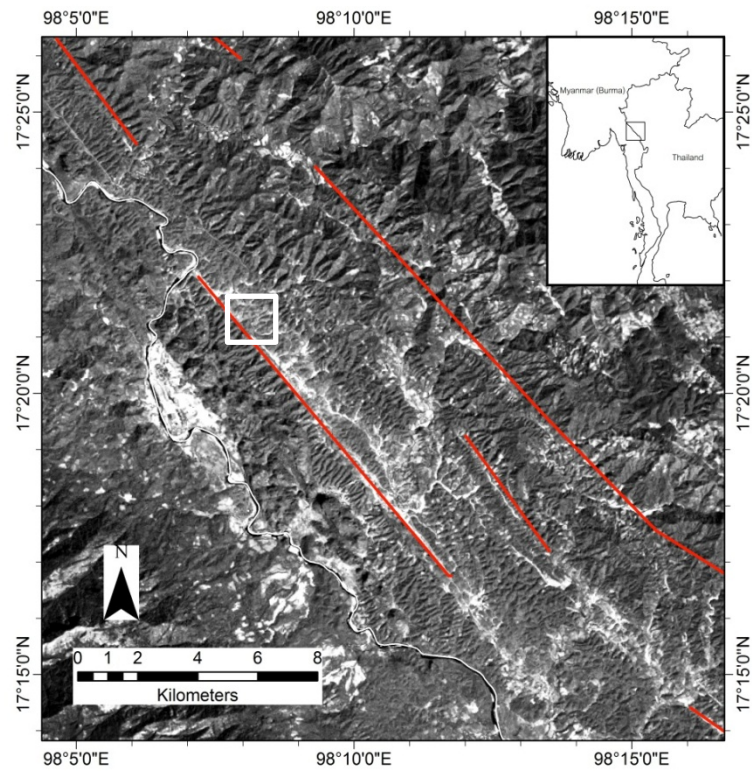
Figure 4-18 Landsat 7 ETM+ (R=7, G=7, B=7) satellite image of Amphoe Tha Song

Yang showing location of lineament segment. Note that the rectangular

represent the area of field investigation
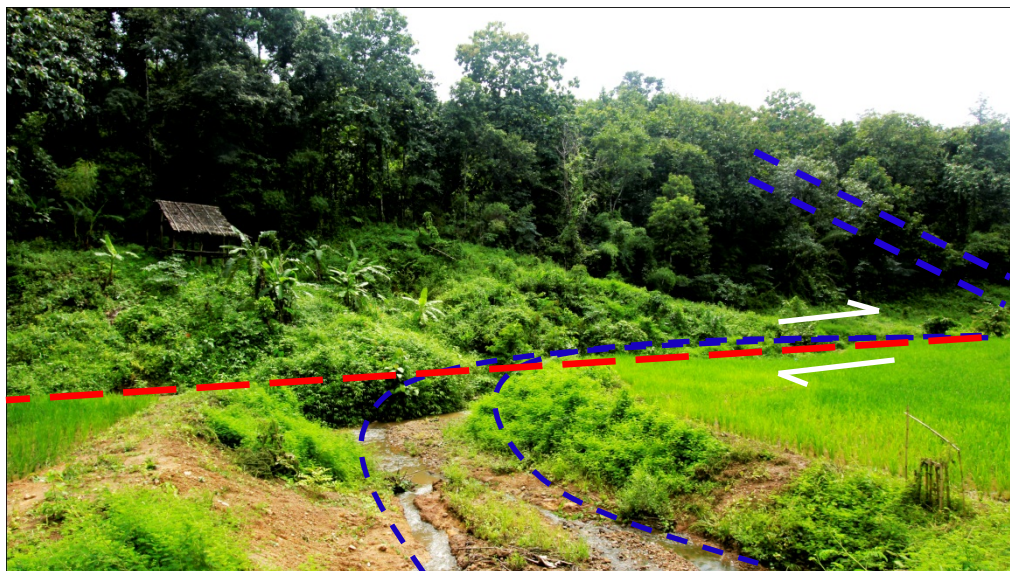
Figure 4-19 Photographs showing the NE-trending offset stream observed along

Ban Mae Ou Su, Amphoe Tha Song Yang, Changwat Tak (17°20'N/98°8'E)

Figure 4-20 Photograph showing the shutter ridge observed along Ban Mae Ou Su,

Amphoe Tha Song Yang, Changwat Tak (17°20'N/98°8'E)

Figure 4-21 Photograph showing the set of triangular facets observed along

Ban Mae Ou Su, Amphoe Tha Song Yang, Changwat Tak (17°20'N/98°8'E)

4.4.2 Ban Mae Ramat, Amphoe Mae Ramat, Changwat Tak

The Ban Mae Ramat lies in the hilly terrain, about 9 kilometers from Amphoe Mae Ramat. Most of areas cover by agriculture fields and population community set up near the rivers. There is Mae Ka Sa hot spring in this area. Based on geologic map 1:50,000 this area and adjacent area are located on Paleogene rocks, which are composed of semi-consolidated clastic sedimentary rocks, including oil shale and peat. NW-SE trending lineament segments with gradually change closely to N-S direction are major structural control boundary of this area.

In an area of the Ban Mae Ramat the lineament segments consist of three discontinuous sub segments, one is trending towards northwest with a length of 5 kilometers, two is trending towards northwest with a length of 4 kilometers, and the other is trending closely to the north with a length of 6 kilometers. Field investigation indicates a set of large triangular facets occurring clearly in sandstone. The facets strikes northwest and dips southwest, suggesting the orientation of the Mae Ping fault zone. Along the northwest lineament segment in this area, there exists a few beheaded stream developed in response to the sudden change of relief and slopes. A hot spring is also found nearby indicating the tectonic active area at Ban Mae Ka Sa. In an area several features of morphotectonic evidences are recognized as a result of ground truth survey, such as triangular facets, shutter ridges, and offset streams that are commonly indicator of strike-slip faulting.
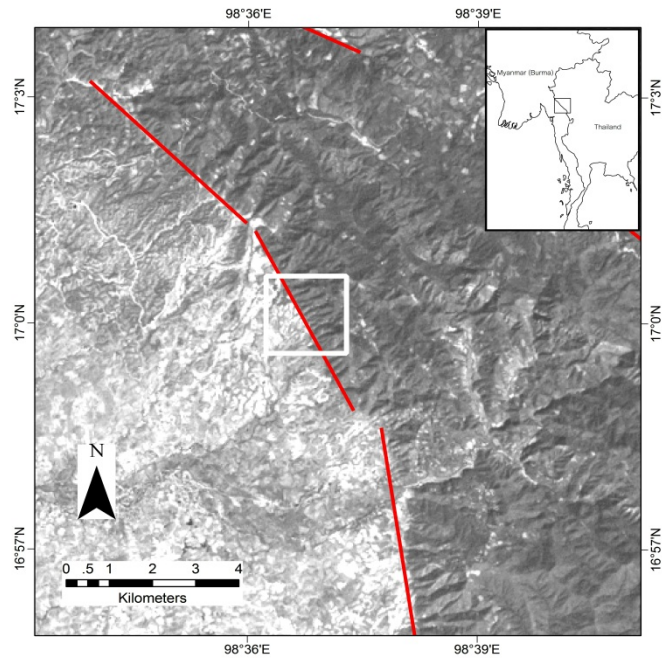
Figure 4-22 Landsat 7 ETM+ (R=7, G=7, B=7) satellite image of Amphoe Mae Ramat

showing location of lineament segment. Note that the rectangular

represent the area of field investigation

Figure 4-23 Photograph showing the set of triangular facets observed along

Ban Mae Ramat, Amphoe Mae Ramat, Changwat Tak (17°0'N/98°36'E)

4.4.3 Ban Na Bot, Amphoe Muang, Changwat Tak

Part of this area, located in the Lan Sang National Park, is jungle and highly mountain area. Some part is underlain that flat land using for agriculture and farm field. Based on geologic map 1:50,000 this area and adjacent area consist of Pre-Cambrian gneiss, schist, calc-silicate and marble in mountain area and Quaternary deposits in the low land. The Permian is composed of limestone, sandstone, and conglomerate which are fault boundaries with the older rocks. The Paleogene rocks, located over undulated terrains are composed of semi-consolidated sedimentary rocks. The recent sediments including gravel, sand, and silt are also deposited. The northern parts of this area represent the Triassic granite pluton.

The result from ground truth survey in the Ban Na Bot area illustrated that the lineament segment is almost continuous and has a length of 13 kilometers. Triangular facets trend towards a northwest-southeast direction. The triangular facet feature show five facets of about 5 kilometers base width and of about 120 meters average height from the base and it faces to the northeast direction. Field data observed reveal the exposure of colluvial deposits, a small shutter ridges, and offset streams. This offset is caused by a dextral strike-slip movement with the total displacement of about 100 meters. In an area several features of morphotectonic evidences are recognized as a result of ground truth survey, such as triangular facets, shutter ridges, and offset streams that are controlled by oblique strike-slip faulting.
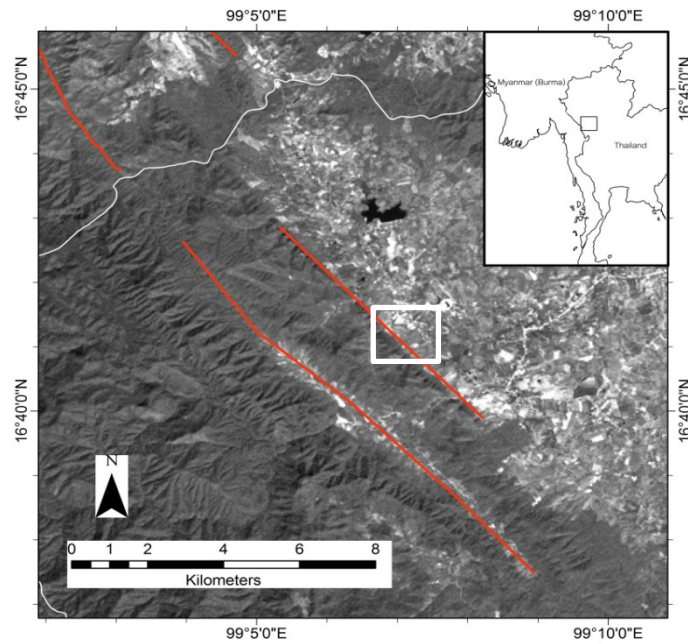
Figure 4-24 Landsat 7 ETM+ (R=7, G=7, B=7) satellite image of Amphoe Muang

showing location of lineament segment. Note that the rectangular

represent the area of field investigation

Figure 4-25 Photograph showing the set of triangular facets observed along

Ban Na Bot, Amphoe Muang, Changwat Tak (16°41'N/99°7'E)

4.4.4 Ban Na Bo Kham, Amphoe Muang, Changwat Kamphaeng Phet

Part of this area, located in the Khong Lan National Park, is the forest area and highlands. This area extends continuously from the area Ban Na Bot therefore; its geology is similar to that of the area Ban Na Bot.

The field reconnaissance survey in Ban Na Bo Kham reveal that the triangular facet shows three facets with average base width 3 kilometers and average high 80 meters above the base with dip to the WE direction. Result of the field investigation in Ban Na Bo Kham indicates morphotectonic landforms, including triangular facets and a few offset streams that generated by strike-slip faulting.
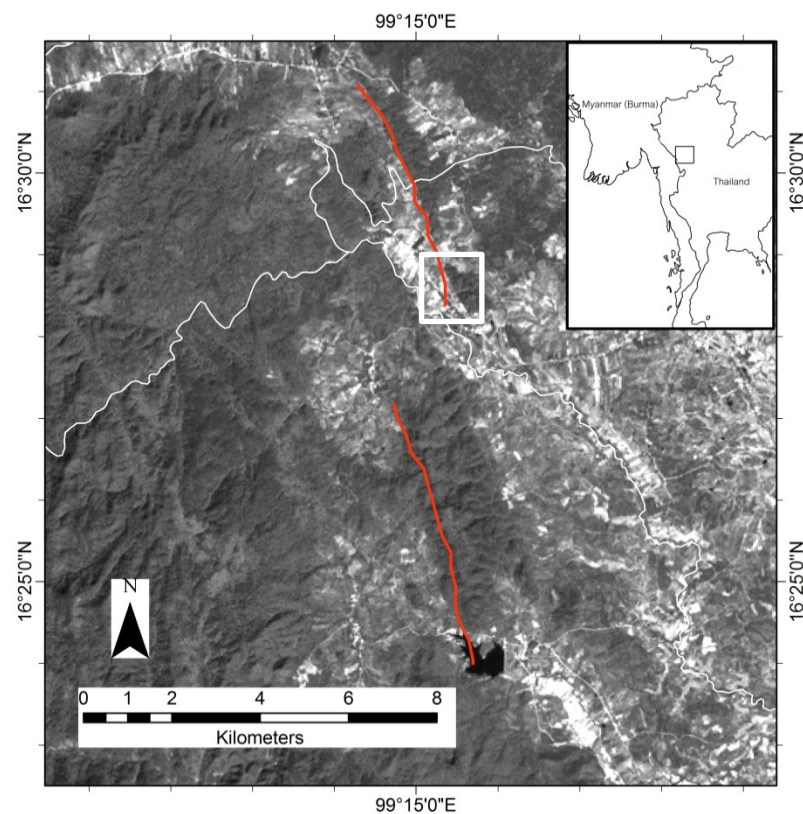
Figure 4-26 Landsat 7 ETM+ (R=7, G=7, B=7) satellite image of Amphoe Muang

Changwat Khamphaeng Phet showing location of lineament segment.

Note that the box represents the area of field investigation.

Figure 4-27 Photograph showing the set of triangular facets observed along

Ban Na Bo Kham, Amphoe Muang, Changwat Kamphaeng Phet (16°28'N/99°15'E)

CHAPTER V

DISCUSSIONS

5.1 Discussions

In this part, the results by the study methods as previously mentioned are discussed in to four categories. First of all, lineaments pattern interpretation result are proposed and discussed. Secondly, interpretation of geomorphic indices is discussed. Thirdly, tectonic activities of the Mae Ping fault zone based on geomorphic indices are discussed. Finally, the problems and recommendations in this study are discussed.

5.1.1 Lineament patterns interpretation

In this research, the author applied remote-sensing data for evaluating and interpreting lineaments in a regional scale using Landsat 7 ETM+ and DEM. Satellite images is useful tool to understand regional characteristics and patterns of geological lineaments in the study area. Preecha (2006) stated that the results from enhanced Landsat 5 TM images for neotectonic evidences along the Mae Ping fault zone. The false-colored composite are added to the image data of band 4, 5, and 7 respectively. The result shows the appearance of various neotectonic features consist of fault scarps, triangular facets, offset streams, and shutter ridges. Lineaments can be traced from eastern belt Myanmar to the border zone of northwestern Thailand. The major trend of lineaments along the Mae Ping fault zone in the northwest-southeast direction, and its branches probably extend to the Mae Hong Son area. Three other minor trends of lineament lay in northeast-southwest, east-west, and north-south direction.

Morley (2007) proposed that the results from satellite images interpretation the Mae Ping fault zone trend significant in northwest-southeast directions but display important north-south trending in fault segments. The Mae Ping fault zone has sinistral strike-slip movement where the north-south segments would have perform as restraining bends within the overall northwest-southeast trend.

Remote-sensing data for morphotectonic investigation in this research are integrated data from Landsat 7 ETM+ and DEM data. The Landsat 7 ETM+ images with scale 1:50,000 is a false-colored composite, band 4, 5, and 7 represented in red, green, and blue respectively. In addition, DEM data were used for creating a hill shade image which is used to assist in delineating large scale geomorphological features and to define orientations and directions of investigated lineaments. This study shows the same results in the major trend lineament and segment as prior work. The major trend of lineament is northwest-southeast and display the same northwest-southeast in segments. However, north-south trend is out of study area thus it doesn't exist in this study. Lineaments in this study were selected by geomorphological features and geomorphic indices. Geological lineaments were constructed by tectonic processes which display high intensities in active region. In some part of study area are cover by dense forests or lower exposures, Identification of lineaments via visual image interpretation may be obscure or impossible. The significant influencing parameters involved in the lineaments interpretation are images quality, visual image interpretation, dense vegetation, and poor exposure.

5.1.2 Interpretation of geomorphic indices

Remote sensing data (e.g. Digital elevation model (DEM), Satellite image) is a utility tool for quantitative study lineaments in regional scale. DEM and satellite image are source for calculated geomorphic indices which use to explain tectonic activities in the Mae Ping fault zone where dense of high mountains and logistic problem. The result from the satellite images interpretations show that high tectonic activities in the study area and all geomorphic indices associate with lineament patterns. Low values of mountain front sinuosity, valley floor width to valley height, and high values of stream length gradient are according with high tectonic activities. Consequently, the idea that the erosional processes are control the study area is not sustain by geomorphic indices. The variation of rocks in the Mae Ping fault zone such as exhumation of metamorphic rocks, sedimentary rocks, and granite intrusion, may take effect on values of mountain front sinuosity index because of difference rock resistance on each types (Figure 5-1).
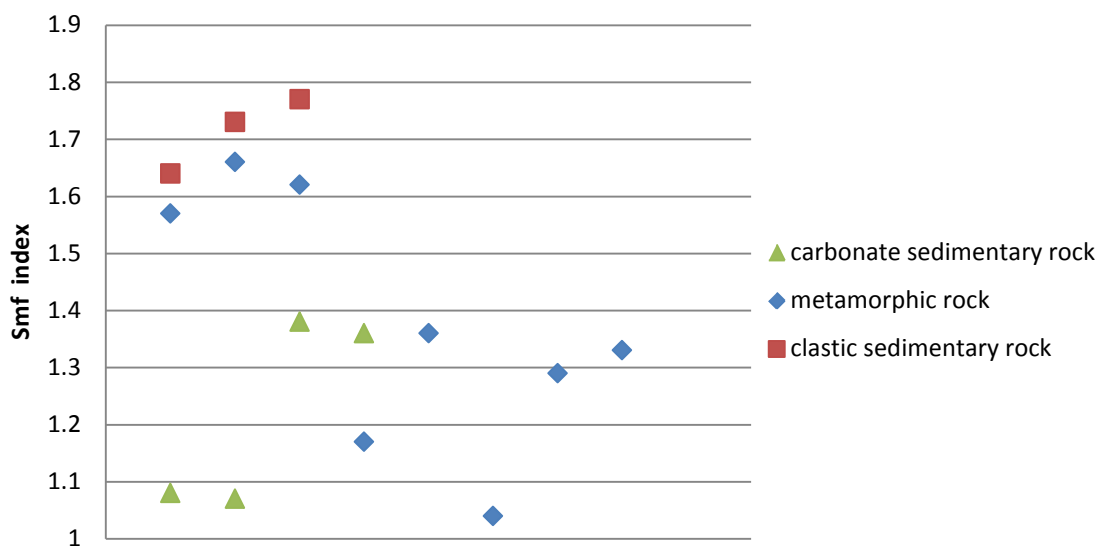
Figure 5-1 Relationship between mountain front sinuosity and lithology

Based on geologic map 1:50,000, the study area and adjacent area are consisting of four groups of rock types. The first group is carbonate sedimentary rocks which are given Smf values from 1.07 to 1.38, and average Vf values from 0.60 to 1.18. The second group is clastic sedimentary rocks which are given Smf values from 1.64 to 1.77, and average Vf values from 0.53 to 0.78. The third group is semi-consolidated sedimentary rocks which are given Smf values 1.73 and average Vf values 1.18. The last group is gneiss and meta-sedimentary rocks which are given Smf values from 1.04 to 1.66, and average Vf values from 0.55 to 1.52 (Table 5.1). The values of geomorphic indices probably variation by difference degree of weathering and climate that give the various weathering and erosion rate in each region.

From the trend of all geomorphic indices we propose that the geomorphological features in this study area are not only produces by erosional processes. Higher values of SL index indicate higher stream line gradient change that generated from normal fault activities. The northern part of the Mae Ping fault zone in this study area display highly mountain topography. The erosional processes can generate rugged shape landform and wine-glass canyon along the mountain. The mountain lay down on NW direction and range of elevation is 220-2,138 meters above mean sea level. Geomorphic features from tectonic activities in this part are triangular facets which are produced from normal fault. Hence, shutter ridges and offset streams which are generated from strike-slip fault. The middle part is limited by Mae Ramad basin. The eastern part is stop expanded by Mae Nam Ping. The southern part is reach to Amphoe Khlong Lan and the end of this fault zone is uncertain.

Table 5.1 Values of geomorphic indices from the study area

No.	Location	Lithology	Front length (km)	Smf	Average Vf
I	Tha Song Yang	Ordovician carbonate sedimentary rocks	14.3	1.08	0.89±0.27
II	Tha Song Yang	Triassic clastic sedimentary rocks	9.8	1.64	0.53±0.24
III	Tha Song Yang	Ordovician carbonate sedimentary rocks	12.3	1.07	0.98±0.27
IV	Tha Song Yang	Tertiary semi-consolidated sedimentary rocks	4.2	1.73	1.18±0.43
V	Tha Song Yang	Triassic carbonate sedimentary rocks	4.7	1.38	1.18±0.52
VI	Tha Song Yang	Triassic carbonate sedimentary rocks	8.0	1.36	0.60±0.17
VII	Tha Song Yang	Permo-Caboniferous meta-sedimentary rocks	15.6	1.33	0.66±0.28
VIII	Mae Ramat	Tertiary clastic sedimentary rocks	9.3	1.77	0.78±0.30
IX	Mae Ramat	Pre-Cambrian gniess	13.5	1.57	0.79±0.29
X	Muang	Pre-Cambrian gniess	11.5	1.66	0.82±0.29
XI	Muang	Pre-Cambrian gniess	4.5	1.62	0.55±0.17
XII	Muang	Pre-Cambrian gniess	3.0	1.17	1.52±0.55
XIII	Wang Chao	Pre-Cambrian gniess	13.0	1.36	0.78±0.12
XIV	Khong Lan	Pre-Cambrian gniess	5.4	1.04	1.51±0.49
XV	Khong Lan	Pre-Cambrian gniess	6.3	1.29	1.14±0.47

5.1.3 Tectonic activities of the Mae Ping fault zone based on geomorphic indices

The conjunction of mountain front sinuosity and valley floor width to height ratio values have been used to estimate tectonic activities of the Mae Ping fault zone. From three main activities classes of active mountain front which are describe as low values of Smf index (Smf<1.4) and Vf values lower than 0.5 are attribute to straight mountain front, high uplift rate is define as active front (Class 1). Moderately active front that show Smf in range from 1.4 to 3 and Vf values higher than 0.5 is determine class 2. Sinuous mountain front and broad valley show high values of Smf (Smf>3) and Vf is define as inactive setting (Class 3) (Bull and McFadden, 1977; Silva et al., 2003).

The plot of Smf and Vf values from mountain front in the study area. A batch of data expanded in three difference group considered by Smf values. These difference groups are set up to the tectonic activities class 1, 2, and 3 depend on values gap of Smf which may indicated erosional change and uplift rate (Figure 5-2).
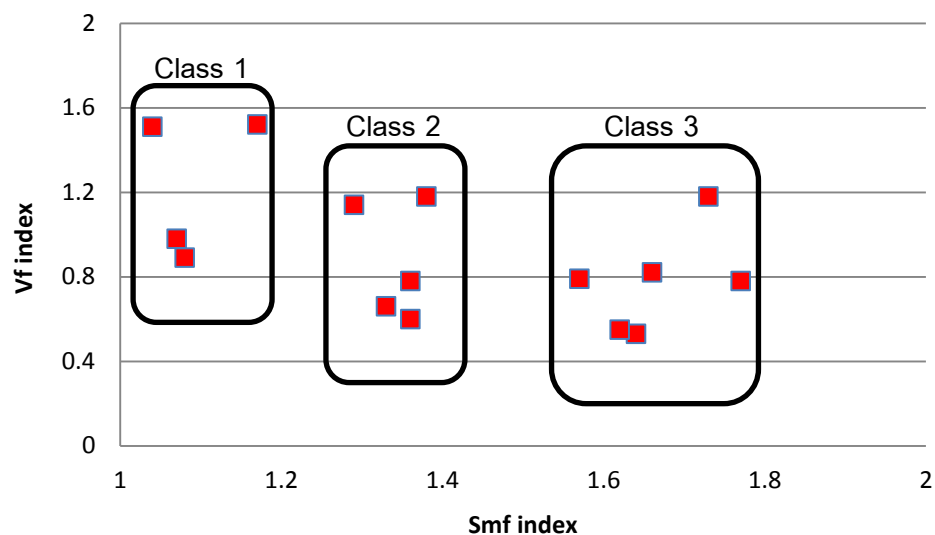
Figure 5-2 Plot of Smf and Vf for the Mae Ping fault zone showing their group of tectonic activities class based on Bull and McFadden (1977) and Silva (2003)

First of all, class 1 group consist of Smf values in range from 1.04 to 1.17 and mean Vf values in these group range between 0.89 and 1.52. From data of these group indicated that mountain front and valley shape control by normal faulting, the offset stream in the study area is developed by strike slip faulting in this region. Secondly, class 2 groups on Smf values ranging from 1.29 to 1.38 and average Vf values between 0.60 and 1.18. In this class has a lower tectonic activity than class 1 that has the same faulting style (normal and strike-slip fault) of five mountain front. Finally, class 3 group show an enlarge range of Smf values from 1.57 to 1.77 with mean Vf values between 0.53 and 1.18. All of mountain front in this group were controlled by normal and strike-slip fault as same as two other group.

Comparing the morphotectonic analysis and previous tectonic studies of the Mae Ping fault zone it can be infer that the Mae Ping fault zone first developed from collision of the Burma Block with the western margin of Sundaland (Morley, 2004). This research is associate with class 1 activities are located near collision plate boundary which has high tectonic activities and uplift rate. Moreover, a group of class 1 is located on the southern part of the study area where toward to center of plate boundary that because the results of transpression at the exiting bend of the Khlong Lhan restraining bend, with evolution from a thrust-dominated to strike-slip dominated type (Morley, 2007). Moderately active are characteristic of class 2 activities which are stage between class 1 and class 3 are located on middle part of the study area where exposure of the mid-crustal levels of deformation associated with the 5–6 km. wide mylonitic to ultramylonitic shear zone in the Lan Sang national park (Lacassin et al. 1993, 1997). Inactive setting is defined as class 3. In contrast, class 3 activities for this study are equivalent to class 2 of Bull and McFadden, 1977. A group of class 3 data located on whole part of the study area. All of three activities class that show on figure 5-3.
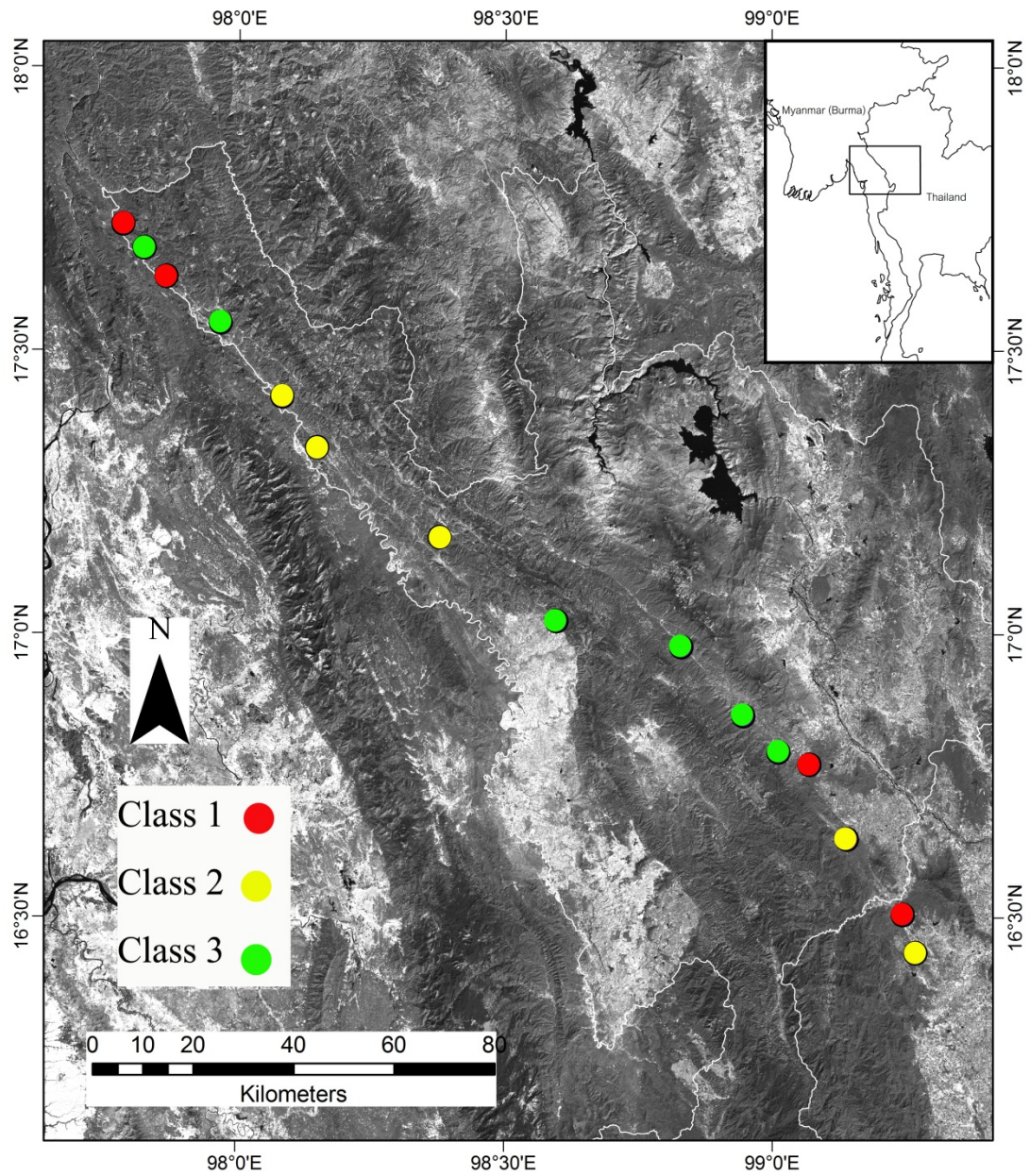
Figure 5-3 Located map of three tectonic activities class for the study area

5.2 Problems and recommendations

There are some problems in this study. Using Landsat 7 and DEM with 30 m. resolution reveal more accuracy results than using only Landsat 5. However, the results from this study can be used as basic data to estimated tectonic activities in the Mae Ping fault zone that can be used to help urban planning and earthquake hazard management in the area. It can be noticed that the highest tectonic activities area in this fault zone.

For the research to be more basically applied, more fault data related such as slip rate, structural data, and earthquake magnitude that are not available in whole part of the study area as well as the advance will be needed to be used in detail for more accurate results in the future.

CHAPTER VI

CONCLUSIONS

According to, the results of remote sensing analysis (Landsat 7 ETM+ and digital elevation data 30-m resolution) combine with geomorphic indices and ground-truth investigation of the Mae Ping fault zone in Changwat Tak and Changwat Kamphaeng Phet, northwestern Thailand, the conclusions can be describe as the following;

1) These study prove the utility of remote sensing in delineating structural features and quantitative morphotectonic parameters in GIS environment. Lineaments mainly trend in northwest-southeast directions

2) Geomorphic indices show low values of mountain front sinuosity, valley floor width to height ratio, and high values of stream length gradient index including with geomorphological features like offset streams, triangular facets, and shutter ridges which are discovered along the Mae Ping fault zone which are imply that tectonic activities in the study area control by strike-slip fault and normal fault.

3) Tectonic activities in zone 1 where located near the collision plate boundary are higher than zone 2 that toward to the intraplate environment. Tectonic activities in zone 3 where transpression at the exiting bend of the Khlong Lhan restraining bend is the highest activities in three zone.

REFERENCES

Allen, C. R., Armand, F., Richter, C.F., and Nordquist, J. M. (1965). Relationship between Seismicity and Geology Structure in the Southern California Region. Bulletin of the Seismological Society of America 55(4): 753-797.

Barr, S.M., and MacDonald, A. S. (1987). Nan River Suture Zone, Northern Thailand. Geology 15: 907-910.

Bell, W. T. (1979). Thermo luminescence dating: Radiation dose-rate data. Archaeometry 21: 243-245.

Bettinger, P., and Wing, M.G. (2004). Geographic Information System: Application in Forestry and Natural Resources Management. New York: McGraw-Hill.

Bhatt, C.M., Chopra, R., and Sharma, P.K. (2007).   Morphotectonic analysis in Anandpur Sahib area, Punjab (India) using remote sensing and GIS approach. Journal of the Indian Society of Remote Sensing 35(2): 129-139.

Biswas, S., and Grasemann, B. (2005). Quantitative morphotectonics of the southern Shillong Plateau (Bangladesh/India). Austrian Journal of Earth Sciences 97: 82-93.

Briggs, R. (2010). Geographic information system Fundamentals [Online]. Available from: http://www.utdallas.edu/~briggs/gisc6381.html[2010, October 29]

Bull, W.B. (1977). Tectonic Geomorphology of the Mojave Desert. In U.S. Geological Survey Contract Report 14-08-001-G-394. Melano Park, CA: Office of Earthquakes, Volcanoes, and Engineering.

Bull, W.B. (1991). Geomorphic responses to climatic change. New York: Oxford University Press.

Bull, W.B., and MC. Fadden, L.M. (1977). Tectonic geomorphology north and south of the Garlock Fault, California. Journal of Geomorphology 1: 15-32.

Bunopas, S. (1981). Paleogeographic History of Western Thailand and Adjacent part of Southeast Asia. A plate tectonic interpretation. Doctoral dissertation. Victoria University of Wellington.

Charusiri, P., Daorerk, V., and Supajanya, T. (1996). Application of Remote-Sensing Techniques to Geological Structures Related to Earthquakes and Earthquake-Prone Areas in Thailand and Neighbouring Areas. A Preliminary Study. Journal of Scientific Research Chulalongkorn University 21(1): 14-38.

Charusiri, P., Daorerk, V., Choowoing, M., Archibald, D., Hisada, K., and Ampaiwan T. (2002). Geotectonic Evolution of Thailand: A New Synthesis. Journal of the Geological Society of Thailand 1: 1-20.

Charusiri, P., Kosuwan, S., Fenton, C. H., Tahashima, T., Won-in, K., and Udchachon, M. (2001). Thailand Active Fault Zones and Earthquake Analysis: A Preliminary Synthesis. The Journal of Asian Earth Sciences (submitted for publication).

Clarke, K. C. (2001). Getting started with geographic information system. London: Prentice Hall.

Cooper, M. A., Herbert, R., and Hill, G. S. (1989). The Structural Evolution of Triassic Intermontane Basins in Northeastern Thailand. In International Symposium on Intermontane Basins: Geology and Resources, 231-240. Chiang Mai University.

Daly, M. C., Cooper, M. A., Wilson, I., Smith, D. G., and Hooper, B. G. D. (1991). Cenozoic Plate Tectonic and Basin Evolution in Indonesia. Marine and Petroleum Geology 8: 2-21.

Deway, J. F., Cande, S., and Pitman, W. (1989). Tectonic Evolution of the India/Eurasia Collision Zone. Eclogae Geologicae Helvetiae 82: 717-734.

Hack, J.T. (1973). Stream-Profile analysis and stream-gradient index. U.S. Geological Survey Journal of Research 1: 421-429.

Hall, R. (1996). Reconstructing Cenozoic SE Asia. In: Hall, R., and Blundell, D., eds. Tectonic Evolution of Southeast Asia. Geological Society of London Special Publication 106: 153-184.

Hinthong, C. (1995). The Study of active Faults in Thailand. In Proceeding of the Tectonical Conference on the Progression and Vision of Mineral Resources Development, 129-140. Bangkok : Department of Mineral Resources.

Hinthong, C. (1997). The Study of Active Faults in Thailand. Report of EANHMP. An Approach to Natural Hazards in the Eastern Asia, 17-22. Geological Survey of Japan.

Hobbs, W. H. (1972). Earth Features and Their Meaning. New York: Macmillan.

Huchon, P., LePichon, X., and Rangin, C. (1994). Indochina Peninsula and the collision of India and Eurasia. Geology 22: 27-30.

Hutchison, C. S. (1989). Geological evolution of south-east Asia. New York: Oxford University Press.

Jensen, J.R., and Kiefer, R.W. (2007). Remote sensing of the environment. 2nd edition. Pearson Prentice Hall.

Keller, E.A., and Pinter, N. (1996).   Active Tectonics: Earthquake, Uplift, and Landscape. Upper Saddle River, NJ.: Prentice Hall.

Keller, E.A., and Rockwell, T.K. (1984). Tectonic geomorphology, Quaternary chronology and Paleoseismology. In J.E. Costa and P.J. Fleisher, editors, Developments and Applications of Geomorphology, pp. 203–239. Berlin: Springer-Verlag.

Khaowiset, K. (2007). Neotectonics along the Pua Fault in Changwat Nan, northern Thailand : evidence from remote sensing and thermoluminescence dating. Master's thesis. Department of Geology, Chulalongkorn University, 218 pp.

Lacassin, R., Leloup, P. H., and Tapponnier, P. (1993). Bounds on strain in large Tertiary shear zones of SE Asia from boudinage restoration. Journal of Structural Geology 15: 677–692.

Lacassin, R., Hinthong, C., Siribhakdi, K., Chauviroj, S., Charoenravat, A., Maluski, H., Leloup, P.H., Tapponnier, P., (1997). Tertiary diachronic extrusion and deformation of western Indochina: Structural and 40Ar/39Ar evidence from NW Thailand. Journal of Geophysical Research 102: 10,013-10,037.

Le Dain, A. Y., Tapponnier, P., and Molnar, P. (1984).   Active faulting and tectonics of Burma and surrounding regions. Journal of Geophysical Research 89: 453–472.

Lee, T. Y., and Lawver, L. A. (1995). Cenozoic plate reconstructions of Southeast Asia. Tectonophysics 251: 85-138.

Leloup, P. H., Arnaud, N., Lacassin, R., Kienast, J.R., Harrison, T.M., Trong, T.T.P., Replumaz, A., Tapponnier, P., (2001). New constraints on the structure, thermochronology and timing of the Ailao Shan–Red River shear zone, SE Asia. Journal of Geophysical Research 106: 6683–6732.

Leonard, E. M., (2002). Geomorphic and thermal forcing of late Cenozoic warping of the Colorado Piedmont. Geology 34: 595-598.

Leopold, L. B., Wolman, M.G., and Miller, J.P. (1964). Fluvial processes in geomorphology. San Francisco: W.H. Freeman.

Leopold, L. B., and Bull, W.B. (1979). Base level, aggradation, and grade. Proceedings of American Philosophical Society 123: 168-202.

Lillesand, T. M., Kiefer, R. W., and Chipman, J. W. (2008). Remote Sensing and Image Interpretation. Hoboken, N.J: John Wiley & Sons.

Littis, W. R., and Hanson, K. L. (1991). Crustal strain partitioning; implications for seismic-hazard assessment in western California: Geology 19: 559-562.

Mackin, J.H., (1948). Concept of the graded river. Geological Society of America Bulletin 59: 463-512.

Matthews, S. J., Fraser, A. J., Lowe, S., Todd, S. P., and Peel, F. J. (1997). Structure, Stratigraphy and Petroleum Geology of the SE Nam Con Son Basin, Offshore Vietnam. In: Fraser, A., Matthews, S., Murphy, R., eds., Petroleum Geology of Southeast Asia. Geological Society of London Special Publication 126: 89-106.

McMillan, M. E., Angevine, C. L., and Heller, P.L. (2002), Postdepositional tilt of the Miocene-Pliocene Ogallala Group on the western Great Plains: Evidence of late Cenozoic uplift of the Rocky Mountains. Geology 30: 63–66.

Morley, C. K. (2002). A tectonic model for the Tertiary evolution of strike-slip faults and rift basins in SE Asia. Tectonophysics 347: 189–215.

Morley, C.K., Smith, M., Carter, A., Charusiri, P., and Chantraprasert, S. (2007). Evolution of deformation styles at a major restraining bend, constraints from cooling histories, Mae Ping fault zone, western Thailand. <u>Geological Society of London Special Publications</u> 290; 325-349.

Morley, C. K. (2004). Nested strike-slip duplexes, and other evidence for Late Cretaceous–Palaeogene transpressional tectonics before and during India–Eurasia collision, in Thailand, Myanmar and Malaysia. <u>Journal of the Geological Society of London</u> 161: 799–812.

Ni, J., and York, J. E. (1978). Late Cenozoic Tectonics of the Tibetan Plateau. <u>Journal of Geophysical Research</u> 83: 5377-5384.

O' Leary, D. W., and Simpson, S. L. (1977). Remote Sensing Application to Tectonism and Seismicity in the Northern Part of the Mississippi Embayment. <u>Geophysics</u> 42 (3): 542-548.

Park, R. G., and Jaroszewski, W. (1994). Craton Tectonic, Stress and Seismicity. In Hancock, P. L. (ed.), <u>Continental Deformation</u>, pp. 200-222. Pergomon Press: Oxford.

Peters, G., Van Balen, R.T. (2007). Tectonic geomorphology of the northern Upper Rhine Graben. <u>Germany Global and Planetary Change</u> 58: 310–334

Rangin, C., Jolivert, L., and Pubellier, M. (1990). A Simple Model for the tectonic Evolution of Southeast Asia and Indonesia Region for the past 43 m.y. <u>Bulletin de la Societe geologique de France</u> 8: 889-905.

Rhea, S. (1993). Geomorphic observations of rivers in the Oregon Coast Range from a regional reconnaissance perspective. <u>Geomorphology</u> 6: 135–150.

Rockwell, T.K., Keller, E. A., Clark, M. N., and Johnson D. L. (1984). Chronology and rates of faulting of Ventura River terraces, California. <u>Geological Society of America Bulletin</u> 95: 1466–1474.

Saithong, P. (2006). <u>Characteristics of the Moei-Maeping Fault Zone, Changwat Tak, Northwestern Thailand</u>. Master's thesis. Department of Geology, Chulalongkorn University, 218 pp.

Sengor, A. M. C., and Hsu, K. J. (1984). The Cimmerides of Eastern Asia, History of the Eastern End of the Paleo-Tethys. Memoire de la societe geologique de France 147: 139-167.

Silva, P.G., Goy, J.L., Zazo, C., and Bardaji, T. (2003). Fault-generated mountain fronts in southeast Spain: geomorphologic assessment of tectonic and seismic activity. Geomorphology 50: 203–225.

Skrdla, M. P. (2005). Introduction to GIS. Nebraska, USA: Lincoln.

Srisuwan, P. (2002). Structural and Sedimentological Evolution of the Phrae Basin, Northern, Thailand. Doctoral dissertation. Department of Geology, Royal Holloway University of London.

Strahler, A.N. (1952), Dynamic basis of geomorphology. Geological Society of America Bulletin 63: 923–938.

Strandberg, C. H. (1967). Aerial Discovery Manual. New York: John Wiley & Son.

Strogen, D. M. (1994). The Chiang Muan Basin, a Tertiary Sedimentary Basin of Northern Thailand. Doctoral dissertation. Department of Geology, Royal Holloway and Bedford New College, University of London.

Sutton, T., Dassau O., and Sutton, M. (2009). A Gentle Introduction to GIS. Eastern Cape:Department of land Affairs [Online]. Available from: http://download.osgeo.org/qgis/doc/manual/qgis-1.0.0_a-gentle-gis-introduction_en.pdf[2010, October 29]

Tapponnier, P., Peltzer, G., Armijo, R., Le Dain, A., and Coobbold, P. (1982). Propagating Extrusion Tectonics in Asia: New insights from simple experiments with plasticine. Geology 10: 611-616.

Tapponnier, P., Peltzer, G., Armijo, R. (1986). On the Mechanics of Collision between India and Asia. In Coward, M. P., and Ries, A. C. eds., Collision Tectonics. Journal of the Geological Society of London, Special Publication 19: 115-157.

Wolman, M.G., and Gerson, R. (1978). Relative scales of time and effectiveness of climate in watershed geomorphology. Earth Surface Processes 3: 189–208.

APPENDICES

APPENDIX A

Results of Mountain front sinuosity index

Parameter values of mountain front sinuosity index

Number	Latitude	Longitude	Lmf	Ls	Smf
1	16.4380	99.2670	14.64	8.27	1.77
2	16.5058	99.2431	3.68	3.43	1.07
3	16.6395	99.1393	9.79	7.18	1.36
4	16.7711	99.0695	5.41	5.01	1.08
5	16.7931	99.0117	14.11	8.60	1.64
6	16.8569	98.9459	4.08	3.81	1.07
7	16.9786	98.8302	5.19	3.91	1.33
8	17.0244	98.5968	5.93	4.31	1.38
9	17.1720	98.3774	5.05	2.92	1.73
10	17.3296	98.1480	6.01	4.66	1.29
11	17.4194	98.0822	3.97	3.80	1.04
12	17.5490	97.9665	7.51	5.52	1.36
13	17.6308	97.8647	3.34	2.87	1.17
14	17.6807	97.8229	17.09	10.32	1.66
15	17.7226	97.7830	7.23	4.47	1.62

APPENDIX B

Results of Valley floor width to height ratio

Parameter values of valley floor width to height ratio

Number	Latitude	Longitude	Vwf	Eld	Erd	Esc	Vf
1	17.7241	97.7840	76	360	340	180	0.45
2	17.7167	97.7985	104	340	360	220	0.80
3	17.7147	97.8062	123	340	320	220	1.12
4	17.6957	97.8071	76	360	360	200	0.48
5	17.6930	97.8104	94	320	320	200	0.78
6	17.6874	97.8136	102	300	320	200	0.93
7	17.6828	97.8162	115	340	360	220	0.88
8	17.6801	97.8189	92	380	360	260	0.84
9	17.6783	97.8210	122	380	340	240	1.02
10	17.6758	97.8233	127	320	300	180	0.98
11	17.6740	97.8257	119	300	320	180	0.92
12	17.6718	97.8310	137	320	300	220	1.52
13	17.6677	97.8353	101	380	340	240	0.84
14	17.6646	97.8379	94	360	360	240	0.78
15	17.6613	97.8434	84	500	460	200	0.30
16	17.6563	97.8493	142	420	500	180	0.51
17	17.6536	97.8520	141	400	360	160	0.64
18	17.6399	97.8496	80	320	340	260	1.14
19	17.6356	97.8540	75	300	300	240	1.25
20	17.6281	97.8635	81	300	240	180	0.90
21	17.6219	97.8712	71	240	240	180	1.18
22	17.5572	97.9587	93	340	320	220	0.85

Number	Latitude	Longitude	Vwf	Eld	Erd	Esc	Vf
23	17.5539	97.9677	139	300	320	220	1.54
24	17.5493	97.9721	135	320	320	220	1.35
25	17.4267	98.0739	65	360	380	180	0.34
26	17.4238	98.0763	132	360	320	180	0.83
27	17.4177	98.0796	71	260	240	180	1.01
28	17.4142	98.0826	89	220	240	180	1.78
29	17.4077	98.0869	67	200	220	160	1.34
30	17.4048	98.0895	77	180	200	140	1.54
31	17.4018	98.0911	56	200	180	140	1.12
32	17.3561	98.1266	69	240	220	160	0.99
33	17.3532	98.1287	75	220	220	160	1.25
34	17.3489	98.1338	65	240	220	160	0.93
35	17.3502	98.1313	84	280	240	180	1.05
36	17.3516	98.1300	51	220	240	160	0.73
37	17.3448	98.1368	95	280	220	180	1.36
38	17.3416	98.1397	84	300	280	160	0.65
39	17.3390	98.1434	78	280	280	160	0.65
40	17.3343	98.1466	114	280	280	180	1.14
41	17.3306	98.1497	106	260	260	180	1.33
42	17.3280	98.1517	91	260	260	200	1.52
43	17.3247	98.1536	133	240	220	180	2.66
44	17.3188	98.1564	73	300	260	200	0.91
45	17.1849	98.3689	116	440	480	280	0.64

Number	Latitude	Longitude	Vwf	Eld	Erd	Esc	Vf
46	17.1829	98.3706	68	380	380	280	0.68
47	17.1756	98.3780	132	540	580	320	0.55
48	17.1682	98.3825	101	600	580	320	0.37
49	17.1636	98.3873	100	580	500	320	0.45
50	17.1602	98.3882	103	440	440	320	0.86
51	17.0771	98.3598	89	480	420	260	0.47
52	17.0720	98.3630	73	460	380	260	0.46
53	17.0517	98.5763	120	440	460	340	1.09
54	17.0473	98.5767	131	420	440	300	1.01
55	17.0428	98.5790	106	440	440	360	1.33
56	17.0390	98.5854	91	520	480	400	0.91
57	17.0277	98.6022	54	480	540	400	0.49
58	17.0120	98.6094	87	460	480	360	0.79
59	17.0026	98.6125	76	420	420	300	0.63
60	16.9986	98.6142	50	400	420	300	0.45
61	16.9932	98.6160	60	400	400	300	0.60
62	16.9897	98.6173	66	380	380	280	0.66
63	16.9534	98.6377	114	540	480	320	0.60
64	16.9502	98.6369	80	480	540	320	0.42
65	16.9446	98.6381	90	540	560	320	0.39
66	16.9405	98.6401	102	580	520	320	0.44
67	16.9360	98.6447	68	520	480	320	0.38
68	16.9333	98.6402	80	380	400	300	0.89

Number	Latitude	Longitude	Vwf	Eld	Erd	Esc	Vf
69	16.9263	98.6396	87	400	380	240	0.58
70	16.9241	98.6404	77	380	360	240	0.59
71	17.0023	98.8034	72	700	600	420	0.31
72	17.0000	98.8066	70	580	520	420	0.54
73	16.9935	98.8162	75	560	540	460	0.83
74	16.9871	98.8211	128	520	500	420	1.42
75	16.9847	98.8235	67	560	520	420	0.56
76	16.9831	98.8253	67	560	500	420	0.61
77	16.9788	98.8275	85	600	560	460	0.71
78	16.9772	98.8310	81	480	500	420	1.16
79	16.9747	98.8328	122	540	480	400	1.11
80	16.9709	98.8356	88	540	540	440	0.88
81	16.9678	98.8382	102	560	520	460	1.28
82	16.9607	98.8441	138	600	540	400	0.81
83	16.9599	98.8485	59	500	520	400	0.54
84	16.9576	98.8505	85	460	480	380	0.94
85	16.9548	98.8528	85	560	460	400	0.77
86	16.9514	98.8560	80	500	540	400	0.67
87	16.9473	98.8608	61	520	520	400	0.51
88	16.9447	98.8638	84	520	500	380	0.65
89	16.8913	98.8994	113	600	540	300	0.42
90	16.8866	98.9123	179	560	500	300	0.78
91	16.8764	98.9219	157	500	560	300	0.68

Number	Latitude	Longitude	Vwf	Eld	Erd	Esc	Vf
92	16.8662	98.9286	148	400	500	300	0.99
93	16.8627	98.9308	185	500	400	300	1.23
94	16.8605	98.9358	163	440	440	300	1.16
95	16.8535	98.9407	125	580	440	300	0.60
96	16.8482	98.9480	147	540	580	300	0.57
97	16.8390	98.9549	200	480	460	300	1.18
98	16.8291	98.9664	207	500	500	300	1.04
99	16.7972	98.9955	153	480	400	300	1.09
100	16.7933	99.0059	141	340	340	260	1.76
101	16.7886	99.0104	153	340	320	260	2.19
102	16.7800	99.0137	139	400	480	280	0.87
103	16.7768	99.0645	28	280	280	240	0.70
104	16.7733	99.0666	48	280	280	240	1.20
105	16.6424	99.1390	178	320	320	240	2.23
106	16.6372	99.1415	113	320	360	260	1.41
107	16.6355	99.1452	107	360	340	260	1.19
108	16.6319	99.1477	90	360	380	260	0.82
109	16.4517	99.2582	114	240	260	180	1.63
110	16.4472	99.2588	115	260	240	180	1.64
111	16.4376	99.2605	148	380	300	180	0.93
112	16.4299	99.2622	100	320	380	200	0.67

APPENDIX C

Results of Stream length gradient index

Parameter values of stream length gradient index

Number	Latitude	Longitude	SL index
1	17.7072	97.8241	2.9013
2	17.7122	97.8285	3.0000
3	17.7103	97.8266	3.0359
4	17.7072	97.8246	3.5079
5	17.7122	97.8299	4.1612
6	17.7122	97.8293	6.0000
7	17.7103	97.8502	10.1954
8	17.7100	97.8502	10.6601
9	17.7122	97.8288	12.0722
10	17.7033	97.8449	16.2891
11	17.7072	97.8243	16.5247
12	17.7072	97.8227	16.7100
13	17.7128	97.8302	19.0342
14	17.7122	97.8296	20.0360
15	17.7033	97.8446	22.0633
16	17.7072	97.8232	22.3475
17	17.7030	97.8430	94.1010
18	17.7083	97.8155	95.3629
19	17.7133	97.8357	98.7972
20	17.7080	97.8163	101.5836
21	17.7086	97.8143	101.7288
22	17.7078	97.8174	104.0569
23	17.7136	97.8316	104.5271
24	17.7075	97.8196	104.8778
25	17.7075	97.8191	107.4037

Number	Latitude	Longitude	SL index
26	17.7089	97.8127	109.7777
27	17.7136	97.8313	110.6005
28	17.7025	97.8441	113.6078
29	17.7044	97.8457	115.0630
30	17.7086	97.8141	115.4596
31	17.7086	97.8132	119.2455
32	17.7028	97.8432	898.5804
33	17.7069	97.8482	940.6013
34	17.7136	97.7982	988.2392
35	17.7041	97.8455	1022.6587
36	17.7125	97.8366	1030.6303
37	17.7122	97.8366	1039.4138
38	17.7061	97.8399	1052.8972
39	16.4663	98.7029	1079.9180
40	16.3123	99.6719	1097.8318
41	16.3123	99.6722	1097.9637
42	16.3117	99.6722	1124.2025
43	16.3131	99.6716	1137.0500
44	17.7089	97.8382	1173.7549
45	16.3125	99.6719	1180.9027
46	16.3120	99.6722	1183.5508
47	17.7022	97.8441	1207.0847
48	16.4377	99.7204	9984.1312
49	17.1523	98.6718	9984.8759
50	17.1510	98.6718	9990.7293
51	16.7850	99.1863	9993.2069
52	17.1765	98.6913	9997.3061

Number	Latitude	Longitude	SL index
53	17.1598	98.6743	10005.6438
54	16.4377	99.7207	10018.1783
55	17.1604	98.6752	10020.8705
56	17.1512	98.6718	10021.1257
57	17.1582	98.6735	10022.4386
58	17.1562	98.6724	10025.7411
59	17.1821	98.6846	99982.9068
60	17.1810	98.6854	99988.6465
61	17.1826	98.6843	99996.2170
62	17.1623	98.6807	100002.6069
63	17.1551	98.6721	100003.4789
64	17.1626	98.6807	100009.2459
65	17.1685	98.6874	100019.4620
66	17.1790	98.6879	100022.5128
67	17.1548	98.6718	100026.6273
68	17.1793	98.6879	100033.6343
69	17.1585	98.6740	100038.3047
70	17.1565	98.6727	499677.9504
71	17.1640	98.6854	499735.6459
72	17.1629	98.6840	499737.0742
73	17.1876	98.6829	499757.4774
74	17.1632	98.6846	499779.9337
75	17.1787	98.6888	499782.9042
76	17.1557	98.6724	499848.8902
77	17.1629	98.6838	499882.5884
78	17.1573	98.6729	499944.6740
79	17.1560	98.6724	500004.0153

Number	Latitude	Longitude	SL index
80	17.1640	98.6852	500016.9860
81	16.2719	99.8440	799240.3418
82	17.1654	98.6865	799406.2966
83	17.1660	98.6868	799497.4214
84	17.1710	98.6882	799525.7895
85	17.1687	98.6874	799576.1481
86	17.1982	98.6821	799655.2479
87	17.1607	98.6760	799745.4021
88	17.1679	98.6874	799800.4437
89	17.1687	98.6877	799846.1141
90	17.1701	98.6879	799967.0553
91	17.1718	98.6885	800000.0000
92	17.7072	97.8491	800016.7957
93	16.8231	99.1433	999901.8899
94	17.1721	98.6888	999913.7951
95	17.1660	98.6865	999934.0925
96	17.1551	98.6718	999951.1902
97	17.1565	98.6724	999966.8609
98	17.1515	98.6718	999981.7901
99	17.1785	98.6888	1000021.1990
100	17.1698	98.6879	1000034.0400
101	17.2040	98.6852	1000036.5390
102	17.1779	98.6904	1000038.3200
103	17.1103	99.0883	1000041.1330
104	17.1787	98.6882	59262858.9600
105	17.1105	99.0886	59262886.1100
106	17.1754	98.6904	59263137.1400

Number	Latitude	Longitude	SL index
107	17.1105	99.0883	59263834.6300
108	16.2699	99.8432	59264933.4300
109	17.1785	98.6890	59265614.2200
110	16.2696	99.8429	59291612.6600
111	17.1116	99.0894	59303426.8900
112	17.1105	99.0892	59327230.0300
113	17.1843	98.6838	59565755.4100
114	17.1122	99.0894	60714285.7100
115	16.2766	99.8496	60714319.7100
116	17.1119	99.0894	60714336.7100
117	17.2315	98.6927	78601155.2400
118	17.1568	98.6727	78622903.7700
119	17.1612	98.6774	78639475.9600
120	17.1757	98.6907	78660121.8300
121	17.1579	98.6732	78673107.4300
122	17.1796	98.6871	78699765.8300
123	17.1762	98.6910	81487941.9400
124	16.2585	99.8090	81488155.1000
125	17.1879	98.6827	81497704.3600
126	17.1618	98.6788	82143144.9000
127	17.1573	98.6732	82143306.0800
128	16.2588	99.8110	82224584.2600
129	17.1593	98.6743	82237031.2000
130	17.1860	98.6832	85185510.4200
131	16.2585	99.8085	85185852.7000
132	17.1532	98.6718	85186654.1900
133	17.1621	98.6793	85193471.0200

Number	Latitude	Longitude	SL index
134	17.1760	98.6907	85295445.8700
135	17.7069	97.8396	85360436.9000
136	17.1629	98.6846	85714796.6700
137	17.1743	98.6896	85715040.9400
138	17.1618	98.6782	85718164.4900
139	17.1621	98.6799	96297274.5700
140	17.1654	98.6863	96428624.4700
141	17.1621	98.6790	96428689.6500
142	17.1571	98.6729	96428761.4900
143	17.1637	98.6849	96429157.6200
144	17.1643	98.6857	96429274.8800
145	16.2918	99.9965	96429328.8800
146	17.1612	98.6768	96430037.1400
147	17.4071	98.6802	96430051.1000
148	16.2932	99.9926	96432194.4600
149	17.1114	99.0894	96453934.4800
150	16.2913	99.9979	96463924.8100
151	16.2932	99.9910	96537395.2500
152	16.2915	99.9971	98489939.6700
153	16.2927	99.9943	100000472.0000
154	16.2932	99.9915	100000909.1000
155	16.2932	99.9932	103704339.2000
156	16.2957	99.9837	107143017.7000
157	16.2932	99.9921	107220816.2000
158	17.1585	98.6738	107415108.5000
159	16.3004	99.9818	110721058.4000
160	16.2918	99.9962	110814172.5000

Number	Latitude	Longitude	SL index
161	16.2999	99.9821	114286387.7000
162	17.1926	98.6810	114343054.6000
163	17.1083	99.0817	114347984.4000
164	16.3002	99.9818	117857142.9000
165	16.2918	99.9971	117857929.9000
166	17.1108	99.0892	117868779.8000
167	17.1280	99.1006	117996010.1000
168	16.3007	99.9818	118658197.0000
169	17.1280	99.1008	121433097.3000

BIOGRAPHY

Acting Sub Lt. Phuriwat Jiratantipat was born in Bangkok, Thailand on September 10, 1984. In 2007 he received a Bachelor of Science degree in Marine Science from Department of Marine Science, Faculty of Science, Chulalongkorn University. In 2009 he entered the Earth Sciences program, Department of Geology, Faculty of Science, Chulalongkorn University for a Master of Science degree study.